

Synthesis and Characterization of Highly Functional Substituted Stilbene Copolymers and Semi-crystalline Poly(aryl ether sulfone)s

Min Mao

Dissertation submitted to the Faculty of Virginia Polytechnic Institute and State University in partial fulfillment of the requirements for the degree of

Doctor of Philosophy

In

Chemistry

Dr. S. Richard Turner, Chair
Dr. Timothy E. Long
Dr. Alan R. Esker
Dr. John G. Dillard
Dr. Richey Davis

September 5th, 2007
Blacksburg, Virginia

Keywords: stilbene, alternating copolymerization, rod-coil block copolymer, polyampholyte, birefringence, poly(aryl ether sulfone)

Copyright 2007, Min Mao

Synthesis and Characterization of Highly Functional Substituted Stilbene Copolymers and Semi-crystalline Poly(aryl ether sulfone)s

Min Mao

(ABSTRACT)

Novel, highly functional rod-like copolymers have been synthesized by alternating copolymerization of N, N, N', N'-tetraalkyl-4, 4'-diaminostilbenes (TDAS) with maleic anhydride. Dynamic light scattering, ^2H solid state NMR and persistence length measurement reveal high chain rigidity of the polymer backbone. Double quantum heteronuclear local field solid state NMR spectroscopy (2Q-HLF Solid State NMR) has been employed to investigate the chain structure of ^{13}C labelled copolymer. The torsional angle of the H- ^{13}C - ^{13}C -H part of the anhydride ring was zero degrees, indicating an all *cis* configuration of the H- ^{13}C - ^{13}C -H moiety of the anhydride ring.

Rod-coil block copolymers containing rigid polyampholyte blocks were designed and synthesized by addition-fragmentation chain transfer (RAFT) copolymerization. The rigid polyampholyte blocks were formed by hydrolysis of alternating copolymers and the flexible coil block consists of poly(oligo(ethylene glycol) methacrylate). The rod-coil block copolymers form polyion complex (PIC) aggregates even when the polyampholyte blocks are charge imbalanced. The aggregates did not dissociate upon the addition of high concentrations of NaCl unlike the dissociation of flexible polyampholytes in NaCl solution. These unique solution properties are induced by "like-charge attractions" of the rigid polyampholytic alternating copolymer chains.

An example, of what is birefringent to be a novel class of material, has been prepared which enables the control of the birefringence of a polymer film by controlling the rotation of aromatic groups pendant to the polymer backbone.

A linear rigid bisphenol monomer, 4,4'-dihydroxyterphenyl (DHTP), has been incorporated into poly(aryl ether sulfone)s (PAES) in a study to impart crystallization to these amorphous polymers. Three bisphenols, 4, 4'-isopropylidenediphenol, 4, 4'-(hexafluoroisopropylidene)diphenol and 4,4'-dihydroxybiphenyl have been copolymerized with DHTP and dichlorodiphenylsulfone. Only the segmented polysulfone containing 50% BP and 50% DHTP was semi-crystalline. This PAES had a melting temperature (T_m) 320°C in the first heating cycle of a DSC measurement and the presence of crystallites was confirmed by wide angle X-ray diffraction (WAXS).

Acknowledgements

I would like to take this opportunity to express my gratitude to my research advisor, Dr. S. Richard Turner, for his guidance, inspiration and encouragement throughout the work. I have benefited from his profound knowledge, enormous enthusiasm on science, keen insight in polymer science, tremendous industrial experiences and his great personality. He has provided me many stimulating ideas, careful planning of the research project and endless encouragements. His office door is always open for me to ask for advice and discussion of problems. He is always open-minded and supportive, permits and encourages me to try new things. He spends a lot of off-work time on reading and correcting my manuscripts. It has been really a pleasure to work with him.

I would also like to thank the members of my advisory committee: Dr. Timothy E. Long, Dr. Alan R. Esker, Dr. John G. Dillard and Dr. Richey Davis for their time and guidance through my graduate study at Virginia Tech. Dr. Long treats me as one of his students and provides me the access to his many instruments. Without the tremendous help from him and his group, it would be much more difficult to finish this dissertation. Dr. Esker and Dr. Davis are always willing to discuss the problems with me and provide valuable suggestions. Dr. Dillard corrected my research proposal and taught me how to write a proposal. I also want to thank my former advisor, Dr. William Ducker, who is a great surface chemist and taught me a lot on the colloid and surface science.

This work involved a lot of research cooperation. I thank Professor Michel R. Gagne at University of North Carolina at Chapel Hill for helpful discussion on the ester exchange reaction, Dr. Beth Caba for zeta potential measurements, Dr. Sungsool Wi and

Dr. Chul Kim for the help on solid state NMR measurements, Dr. Herve Marand for the discussions on the polymer crystallization, Professor Steven ZD Cheng and his student Siwei Leng at University of Akron for help on the optical measurements, Dr. Jim Elman at Filmetrics, Inc. for the ellipsometry measurements, and Dr. Sudipto Das for help on DMA and WAXS measurements.

Many thanks go out to all of my colleagues in Dr. Long's group and Dr. Turner's group for their great help on TGA, DSC, SEC and many helpful discussions: Dr. Ann Fornof, Mr. John Layman, Miss Rebecca Huyck, Miss Erika Borgerding, Mr. Tomonori Saito, Miss Gozde Ozturk, Dr. Brian Mather, Miss Emily Anderson, Mrs. Sharlene Williams, Mr. Matthew Cashion, Mr. Andy Duncan, Mr. Matthew Hunley, Dr. Akshay Kokil, Dr. Qin Lin, Dr. Takeo Suga, Dr. William Heath, Dr. Afia Karikari, Mr. Keiichi Osana, Miss Lashonda Cureton, Miss Yi Li, Miss Yanchun Liu, Miss Shauntrece Hardrict and Mr. Bin Zhang. I am especially grateful to Mr. John Layman who taught me how to get persistence length from SEC data and shared his program with me. Mr. Andy Duncan held a lot of interesting discussions with me from science to culture and helped me on the step-growth polymerization and my English. Mr. Matthew Cashion helped me on the free radical polymerization and gave me a lot of help in the lab. Mr. Matthew Hunley helped me on the SEM and electro-spinning. We were the first team in Davidson 113 after it was re-opened as a research lab and I am going to miss the time we spent together.

Special thanks go to Mrs. Mary Jane Smith and Mrs. Tammy Jo Hiner in the office for all of their kind help.

I would also like to acknowledge the financial support of the Department of Chemistry at Virginia Tech and the Donors of the American Chemical Society Petroleum Research Fund.

Finally, I would like to thank my family for their love and great support. My father and mother encouraged me to come to the US for graduate study although they really hoped that their son would stay with them. The unfailing love from my wife Jianying always is my biggest support in the world. My little son Gilbert brings me a lot of joy and he is the strongest driving force for me to work hard.

TABLE OF CONTENTS

List of Schemes -----	x
List of Figures -----	xiii
Lists of Tables -----	xvi
CHAPTER I: Functional Polymers and Their Structure – An Overview	
I.1 Structure of Functional Polymers -----	1
I.2 Positioning the Functional Groups within Functional Polymer – the Obstacles -----	4
I.3 Positioning the Functional Groups within Functional Polymer – the Progress -----	5
I.4 Spatial Arrangement of the Functional Groups within Polymers Synthesized by Alternating Free Radical Polymerization -----	7
CHAPTER II: Polymerization Studies of Substituted Stilbene Monomers	
II.1 Introduction of Highly Functional Polymers and Polymerization of Stilbene -----	13
II.2 Experimental Section -----	15
II.3 Polymerization Studies of Substituted Stilbene with Maleic Anhydride-----	23
II.4 Chain Rigidity of the Substituted Stilbene - Maleic Anhydride or Maleimide Alternating Copolymers-----	26
II.5 Chain Dynamics of the TDAS-MA Alternating Copolymer Probed by ² H-Solid State NMR -----	30
II.6 Attempted Polymerization of Substituted Stilbenes to Make Poly(phenylmethylene) -----	34
II.7 Conclusions -----	36

Chapter III: Chain Configuration of Substituted Stilbene Maleic Anhydride

Alternating Copolymer Probed by Solid State NMR

III.1 Introduction-----	41
III.2 Experimental Section-----	43
III.3 Results and Discussions-----	44
III.4 Conclusions-----	48

Chapter IV: Synthesis and Properties of Rod-coil Block Copolymers Containing Rigid Polyampholyte Blocks Based on N, N, N', N'-tetraalkyl-4, 4'-diaminostilbene and Maleic Anhydride

IV.1 Introduction-----	51
IV.2 Experimental Section-----	52
IV.3 Stimuli Responsive Aggregation of Rod-coil Block Copolymers Containing Rigid Polyampholyte Blocks Based on N, N, N', N'-tetraalkyl-4, 4'-diaminostilbene and Maleic Anhydride-----	57
IV.4 Detailed Discussion of Like Charge Attraction between Rigid Polyampholytes----	63
IV.5 Conclusions-----	67

Chapter V: Rigid Polyelectrolytes Based on Alternating Copolymers from Substituted Stilbene Monomers

V.1 Introduction-----	69
V.2 Experimental Section-----	70
V.3 Results and Discussion-----	78

V.4 Conclusions-----	80
----------------------	----

Chapter VI: Controlling Birefringence of the Polymer Films via Hindered Rotation of the Side Groups of Maleimide - Stilbene Alternating Copolymers

VI.1 Introduction-----	84
VI.2 Experimental Section-----	85
VI.3 Results and Discussions-----	86
VI.4 Conclusions-----	91

Chapter VII: Synthesis and Characterization of Poly(aryl ether sulfone) Copolymers Containing Terphenyl Groups in the Backbone

VII.1 Introduction-----	94
VII.2 Experimental Section-----	95
VII.3 Results and Discussions-----	100
VII.4 Conclusions-----	106

Chapter VIII: Final Conclusions and Future Work

VIII.1 Final Conclusions -----	109
VIII.2 Future Work -----	111

Appendix -----	117
-----------------------	------------

Scheme I.1 Four different levels of structures for functional polymers-----	3
Scheme I.2 The structure comparison between synthetic functional polymer and protein -----	4
Scheme I.3 The “charge transfer complex” (CTC) mechanism and the formation of <i>cis</i> configuration of the succinic anhydride unit-----	8
Scheme II.1 Synthesis of N, N, N', N'-tetraethyl-4, 4'-diaminostilbenes-----	17
Scheme II.2 Synthetic scheme of the di-methylsulfonyl-4,4'-stilbene-----	19
Scheme II.3 Alternating copolymerization of N, N, N', N'-tetraethyl-4, 4'- diaminostilbenes with maleic anhydride-----	23
Scheme II.4 Hydrolysis of N,N-dimethyl-N',N'-dibutyl-4, 4'-diaminostilbene maleic anhydride alternating copolymer in dilute aqueous hydrochloric acid solution-----	28
Scheme II.5 The conversion of stilbene to poly(phenylmethylene)-----	35
Scheme III.1 The synthesis of ¹³ C-labelled TDAS-MA alternating copolymer-----	44
Scheme III.2 Possible chain configuration and spatial arrangement of the functional groups of the TDAS-MA alternating copolymer-----	47
Scheme III.3 Possible chain configuration and spatial arrangement of the functional groups of the hydrolyzed TDAS-MA alternating copolymer-----	47
Scheme IV.1 Synthesis of the rod-coil block copolymers (DHBCs) -----	54
Scheme IV.2 A schematic of the origin of like-charge attraction between rigid polyelectrolyte chains with the presence of divalent counterions -----	64
Scheme IV.3 A schematic of the origin of like-charge attraction between rigid polyampholyte chains-----	65

Scheme IV.4 A schematic of the effects of salt on the PIC aggregates formed by polyelectrolytes with different chain structures-----	66
Scheme V.1 Synthesis of di- <i>t</i> -butyl-trans-4,4'-stilbenedicarboxylate via ester exchange method-----	72
Scheme V.2 Synthesis of dimethylaminopropylmaleimide-----	73
Scheme V.3. Synthesis of rigid polyanion based on alternating copolymerization of DTBSC with maleic anhydride-----	74
Scheme V.4 Synthesis of rigid polycation based on alternating copolymerization of TDAS with DMAPM-----	77
Scheme VI.1 Structures of the maleimide – stilbene alternating copolymers used in this study: <i>N</i> -phenylmaleimide - stilbene copolymer (I); <i>N</i> -(<i>o</i> -tolyl)maleimide – stilbene copolymer (II); <i>N</i> -(<i>o</i> -tolyl)maleimide – stilbene copolymer containing 15% dodecylmaleimide (III)-----	88
Scheme VI.2 Large birefringence originated from the optical anisotropy (a) and ortho-methyl induced orientation of benzene ring (c,d) when polymer chains align parallel to film surface (b)-----	89
Scheme VII.1 The synthesis of 4,4'-dihydroxyterphenyl-----	98
Scheme VII.2 The synthesis of DHTP-BPA random PAES copolymer-----	101
Scheme VII.3 The synthesis of DHTP - BP segmented PAES copolymer-----	102
Scheme VIII.1 A possible strategy to introduce active <i>N</i> -hydroxysuccinimide (NHS) ester groups to the di- <i>t</i> -butyl ester stilbene – maleic anhydride copolymer -----	111
Scheme VIII.2 Possible strategies to introduce acid-labile linkages for the drug delivery -----	112

Scheme VIII.3 Possible strategy to incorporate PEG chains into the polymer-drug conjugates -----	113
Scheme VIII.4 General structures of the copolymers with different amounts of benzene groups-----	116

Figure II.1 Hydrodynamic radius of the N, N-dimethyl-N', N'-dibutyl-4, 4'-
diaminostilbene maleic anhydride alternating copolymer in THF at different temperature
-----27

Figure II.2 Hydrodynamic radius of the neutral and charged forms of the N, N-dimethyl-
N', N'-dibutyl-4, 4'-diaminostilbene maleic anhydride alternating copolymer-----29

Figure II.3 The fitting of $R_g - M_w$ according to ref 29 to obtain persistence length of *N*-
(*o*-tolyl)maleimide – stilbene copolymer backbone-----30

Figure II.4 Solid-state ^2H NMR spectra of unhydrolyzed polymer (A) and hydrolyzed
polymer (B) at 298 K, obtained at a 46.02 MHz resonance frequency with a quadrupole
echo pulse sequence⁸ with proton decoupling. The best fit spectra shown above
experimental spectra based on a rigid-lattice model yields $(e^2qQ/\hbar) = \sim 168$ kHz, a
value for the paraffin hydrocarbons with no motion-----33

Figure II.5 ^2H spectra measured on unhydrolyzed form (A) and on hydrolyzed form (B)
of TDAS-MA copolymer at 25 °C, 120 °C, and 190 °C -----34

Figure II.6 The possible structure of a poly(phenylmethylene) chain -----35

Figure III.1 Pulse sequence for HCCH-2Q-HLF experiment (A), and experimental data
and simulations for the $^{13}\text{C}_2$ -labelled TDAS-MA alternating copolymer (B) and the
hydrolyzed $^{13}\text{C}_2$ -labelled TDAS-MA alternating copolymer (C) samples. A standard
FSLG scaling factor, $k = 0.57$, has been used for our simulations. Simulation results with
torsion angles of 0° and 60° provide best fit to the experimental data of the $^{13}\text{C}_2$ -labelled
TDAS-MA alternating copolymer (B) and the hydrolyzed $^{13}\text{C}_2$ -labelled TDAS-MA
alternating copolymer (C), respectively, as expected-----46

Figure IV.1 IR spectra of the un-hydrolyzed form (a) and hydrolyzed form (b) of OEGMA ₂₆ - <i>b</i> -TDASMA ₃₁ -----	57
Figure IV.2 (a) Structure of the block copolymers. (b) Rod-coil type structure. (c) ζ -potential of the PIC aggregates at different pHs-----	58
Figure IV.3 (a) R_h distributions of PICs formed by OEGMA ₂₆ - <i>b</i> -TDASMA ₃₁ at different pH without the addition of salt; (b) a schematic of pH responsive aggregation of rod-coil block copolymers-----	59
Figure IV.4 (a) Effect of added NaCl on PICs formed by OEGMA ₂₆ - <i>b</i> -TDASMA ₃₁ at pH 7; (b) a schematic of rigid rods packing for various aggregates-----	60
Figure V.1 IR spectra of the di- <i>t</i> -butyl-trans-4,4'-stilbenedicarboxylate maleic anhydride copolymer (a); de-protected form (b); and hydrolyzed form (c)-----	76
Figure V.2 TGA thermogram of the alternating copolymer of di- <i>t</i> -butyl-trans-4,4'-stilbenedicarboxylate with maleic anhydride-----	77
Figure V.3 IR spectrum of the alternating copolymer of N, N, N', N'-tetraethyl-4, 4'-diaminostilbene with dimethylaminopropylmaleimide-----	78
Figure VI.1 Potential energy diagram for internal rotation of benzene ring as a function of torsional angle between the benzene ring and imide ring in <i>N</i> -(<i>o</i> -tolyl)maleimide (a) and <i>N</i> -phenylmaleimide (b)-----	87
Figure VI.2 The refractive indices of films in X,Y and Z directions for <i>N</i> -phenyl maleimide-stilbene copolymer (a) and <i>N</i> -(<i>o</i> -tolyl)maleimide-stilbene copolymer (b)-----	90
Figure VI.3 Effect of film thickness on the birefringent property of the film of <i>N</i> -(<i>o</i> -tolyl)maleimide-stilbene copolymer-----	91

Figure VII.1 Glass transition temperatures of the random BPA-DHTP polysulfone
copolymers containing different amounts of DHTP-----104

Figure VII.2 DSC curves (first and second heating cycles) of the segmented PAES
containing 50% BP and 50% DHTP, obtained at a heating rate of 10 °C/min-----105

Figure VII.3 WAXS pattern of the segmented PAES containing 50% BP and 50% DHTP
-----106

Figure VIII.1 TEM picture of the polymeric aggregates for OEGMA₂₆-*b*-TDASMA₃₁ at
pH 7 with 0.3M NaCl -----114

Table II.1 Solubility of N, N, N', N'-Tetraethyl-4, 4'-diaminostilbene polymers in common solvents-----	24
Table II.2 The compositions of the TDAS-MA copolymer at 60°C with different monomer feeding ratios ($C_{\text{monomer, total}} = 5 \text{ wt\%}$ with 1,2-dichloroethane as the solvent, $C_{\text{initiator}} = 1 \text{ wt\%}$ of monomer)-----	25
Table IV.1 Compositions, molecular weights and molecular-weight distributions of segments and block copolymers-----	55
Table IV.2 Intensity average R_h (Cumulant analysis) of the PIC aggregates formed from the DHBCs under different conditions-----	59
Table V.1 Molecular weights and molecular-weight distributions of polymers I and II -----	79
Table VII.1 Compositions, molecular weights and molecular weight distributions of the random polysulfone copolymers-----	102

Chapter I: Functional Polymers and Their Structure – An Overview

Functional polymers¹ carrying reactive functional groups that can participate in chemical processes have important applications in a great variety of areas such as organic electronics², polymer-drug conjugates^{3,4} and biomaterials.⁵ Synthesis of functional polymers occurs through polymerization of functional monomers or chemical modification of a polymerized substrate. Reactive groups are incorporated into the main chain as pendant groups or as multiple chain ends in dendritic types of molecules. Because of the tolerance of free radical and ring opening metathesis polymerization processes to functional groups,⁷ these two polymerization techniques are the most highly used methods for preparing functional polymers.

The number of functional groups attached and their position within the polymers are two important aspects regarding the specific applications of the functional materials. In the following three sections the spatial arrangement of the functional groups leading to specific structure within the polymers will be addressed. Secondly the free radical alternating copolymerization of 1,2-disubstituted monomers will be discussed with a focus on the structure of the alternating copolymers. Highly functional polymers with a well-defined spatial arrangement of the functional groups can be synthesized via carefully selected 1,2-disubstituted monomers. Variations on this concept form the basis of this dissertation.

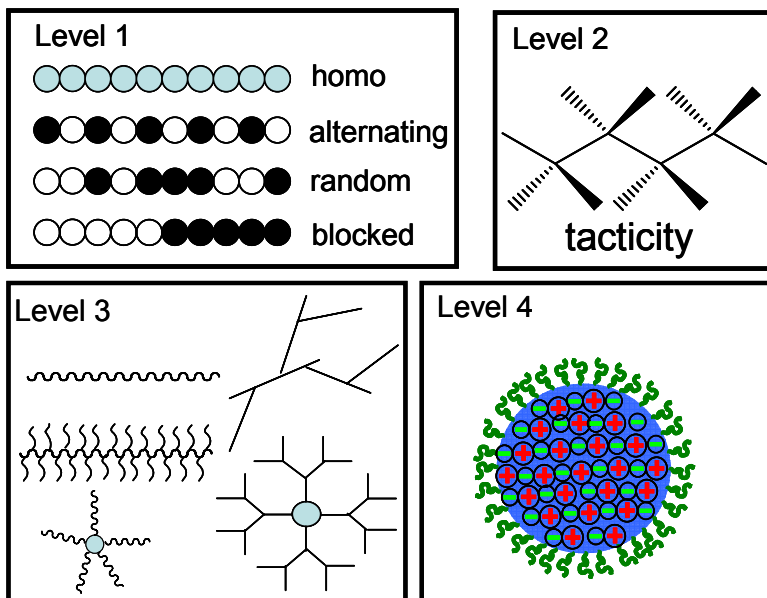
I.1 Structure of Functional Polymers

The actual position of functional groups in a polymer is highly dependent on the 3-D conformation of the polymer chain. For example dendrimers are mono-disperse,

regularly branched polymers with functionality that exponentially expands as the generation number increases.⁸ Many studies have shown that not all of the functional groups are positioned on the surface but many of them are buried inside of the dendrimer “ball”.⁹ Nature provides an excellent example of the spatially positioning of functional groups with proteins whose biological functions are directly determined by four different levels of structures.¹⁰ These macromolecules show the importance of arranging functional groups in defined locations resulting in specific properties for their biological functions. Today more and more functional polymers are needed for enabling materials with specific electronic and biological applications.¹¹ New chemical strategies that can provide precise positioning of functional groups have great potential to lead to novel materials with enhanced application-based performance.

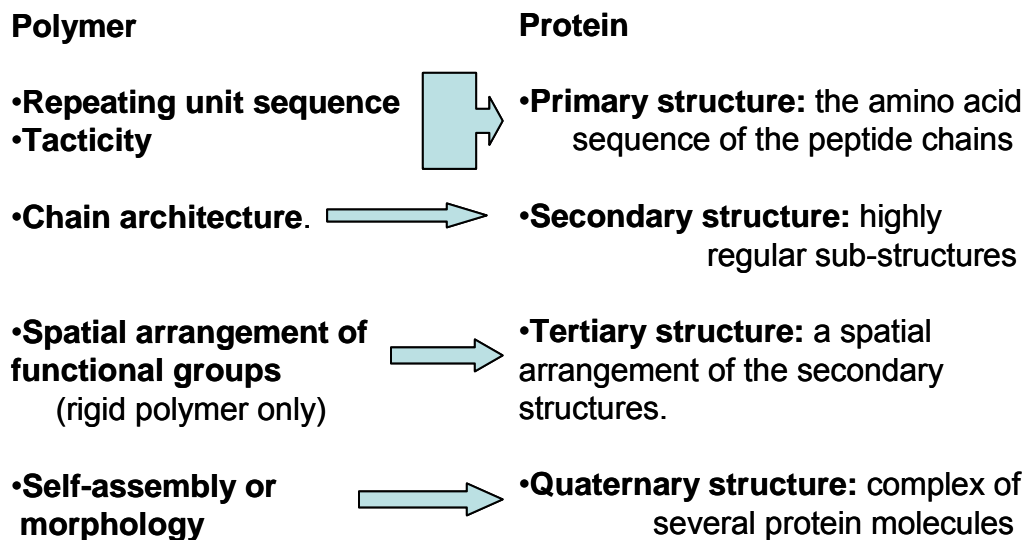
Regarding the spatial arrangement of functional groups, four different structural levels appear based on the dimensional scale (see scheme I.1): 1) the arrangement of the repeat units within a single polymer chain such as homogeneous, random, alternating, blocked or segmented; 2) the relative stereochemistry of adjacent chiral centers within a macromolecule (tacticity); 3) the chain architecture or topology including linear, grafted, star, ladder, branched, hyperbranched, dendritic, crosslinked, etc.; and 4) the packing of polymer chains in various states (morphology and self-assembly). The control of tacticity only has been achieved for some polymer systems via different polymerization techniques and still remains a challenging task.^{13, 14} These four aspects of structure have been extensively explored both in theoretical and experimental studies. To introduce the desired functional groups at pre-defined locations, accurate control is necessary in every facet of the macromolecular structure mentioned above.

Scheme I.1 Four different levels of structures for functional polymers.



Scheme I.2 shows a structural comparison between synthetic polymers and proteins. Tacticity, chemical nature, and arrangement of the synthetic polymer's repeat units correspond to the protein's primary structure (the amino acid sequence of the peptide chains). The chain architecture (i.e. topology) of a synthetic polymer is comparable to a protein's secondary structure. Yet, unlike a protein, a polymer's topology is controlled mainly by the polymerization technique.¹⁵ Only rigid polymers display a well-defined three-dimensional structure similar to a protein. The quaternary structure of proteins is similar to the self-assembly and various states of polymer morphology that stem from tacticity, chemical composition, sequence of repeat units, chain architecture and environmental conditions.

Scheme I.2 The structure comparison between synthetic polymer and protein.



I.2 Positioning the Functional Groups within Functional polymer – Obstacles

Positioning of functional groups is achieved at different scales by varying chain topology, placing functional groups on the main chain, side chain or chain end.¹

However, these structures do not give a well-defined spatial arrangement of the functional groups within the flexible polymer chain. Functional groups also can be positioned in the *meso* scale by polymer self-assembly. For example functional groups can be concentrated within the core or shell of polymeric aggregates.¹⁶ Since these two methods to position functional groups have been extensively explored and are relatively easy to achieve, only the positioning of functional groups within the polymer chain with certain extent of spatial arrangement and obstacles to obtaining this level of control are discussed.

Small organic molecules can be constructed with precise control over the position of functional groups and three-dimensional (stereo-chemical) structure via selective

chemical reactions.¹⁷ A good example is the total synthesis of taxol, a potent anticancer drug with a complex stereo-chemical structure which determines its interactions with cancer tumors.¹⁸ However, synthetic polymer chemists cannot directly employ these selective synthetic organic methods to make polymers with precisely positioned functional groups due to the complex multistage process of polymerization. Tacticity can show a dramatic effect on a polymer's crystallization process as well as mechanical properties.¹⁴ As mentioned before, controlling the configuration of every atom on the backbone of a functional polymer is extremely difficult to achieve.

Due to the segment mobility in flexible synthetic polymers, well-defined spatially arranged functional groups are only observed in the crystalline state or in rigid polymers. In solution or the amorphous state the statistical orientation of the flexible polymer chains "randomizes" the spatial arrangement of the functional groups. Hence a rigid backbone is required to allow positioning of the functional groups within the polymers in a predetermined fashion. Recently, considerable progress in the spatial arrangement of functional groups on rigid polymers has occurred and is summarized in the following section.

I.3 Positioning the Functional Groups within Functional Polymer – Progress

Molecular imprinting is a way to introduce some spatial arrangement of functional groups within cross-linked polymers.^{19, 20} This technique includes the synthesis of cross-linked polymers in the presence of templates which can undergo molecular recognition processes with functional monomers. The templates form a complex with functional monomers. The spatial arrangement of the functional monomers within the

complex is complementary to some structural element of the template. This template-monomer complex is then polymerized and crosslinked to form a rigid, porous polymer matrix. Removal of the template from the rigid porous polymer matrix thus generates an “imprinted surface” decorated with spatially arranged functional groups.

A facially amphiphilic structure commonly found in antimicrobial peptides²¹ was obtained in several rigid synthetic polymers for antimicrobial applications.²²⁻²⁴ DeGrado et al. reported the synthesis of non-toxic membrane-active antimicrobial arylamide oligomers.²² The oligomer chain is rigid due to the amide linkers. Primary amine groups and tert-butyl groups are separately positioned on the two sides of the main chain imparting the facial amphiphilicity. Hydrocarbon-based polymers with similar facially amphiphilic structures, poly(phenylene ethylene)²³ and polynorbornene,²⁴ were also synthesized by Tew et al. via Sonogashira coupling and ring-opening metathesis polymerization. All of these facially amphiphilic functional polymers have rigid backbones and serve as good examples to demonstrate the importance of controlling the spatial arrangement of functional groups within functional polymers.

Moore worked extensively on the synthesis and properties of shape-persistent macrocycles where the functional groups are precisely positioned within the low molecular weight cyclic oligomers via the template method.³¹ Recently a new synthetic route was developed by Tajima to obtain highly regioregular poly[(2-methoxy-5-alkoxy)-1,4 phenylenevinylene]s (PPVs) by the Horner reaction using asymmetrically functionalized monomers.³² In spite of the tremendous progress that has been made to prepare well-defined synthetic polymers via various controlled methods, spatial

arrangement of functional groups in a predetermined manner remains a significant challenge.

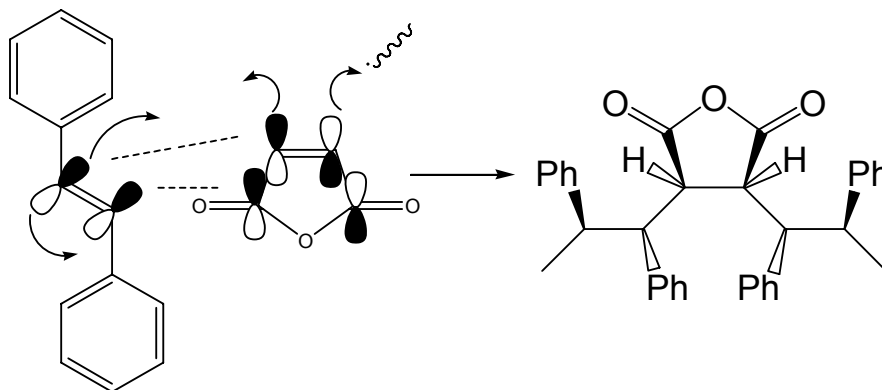
I.4 Spatial Arrangement of the Functional Groups within Polymers Synthesized by Alternating Free Radical Polymerization

Alternating free radical polymerization with 1,2-disubstituted monomers is a convenient and powerful tool to construct highly functional polymeric materials.²⁵ 1,2-Disubstituted monomers have the potential to raise the functionality density along the backbone and thus to increase the functional group concentration as well as impact the chain stiffness. Although 1,2-disubstituted monomers usually are non-homopolymerizable, many of them can be polymerized via so called “alternating free radical polymerization”.²⁵⁻²⁸ Highly functional alternating copolymers can be produced using functional electron-rich (donor) and electron-poor (acceptor) monomer pairs.^{29,30} The type of functional group, molecular weight, polymer architecture, the density of functional groups and stiffness of the polymer chain can be easily controlled. The chemistry of the alternating copolymerization of 1,2-disubstituted monomers will be reviewed in the introduction part of chapter II. The structure of the alternating copolymers is briefly discussed.

To enable the copolymerization of monomers that do not homo-polymerize under free radical conditions at least one electron rich monomer and one electron poor monomer should be involved.²⁸ The driving force for an electron rich radical attacking electron poor double bonds and vice versa is proposed to be the mechanism to overcome the steric/electronic factors that exist as the barriers for the polymerization. An alternative

mechanistic proposal is copolymerization regulated by “donor-acceptor complexes” or “charge transfer complexes”. According to the “charge transfer complex” mechanism significant participation of “charge transfer complexes” in the polymerization would induce the succinic anhydride units to mainly adopt the *cis* configuration for the stilbene maleic anhydride alternating copolymer (Scheme I.3).³³ Many research efforts have been dedicated to investigate the *cis/trans* configurations of the polymer chain to elucidate the mechanism of the alternating polymerization.

Scheme I.3 The “charge transfer complex” (CTC) mechanism and the formation of the *cis* configuration of the succinic anhydride unit.



Solution NMR has been employed to investigate the chain configuration of many alternating copolymers since *cis* and *trans* configurations should display different ¹H and ¹³C NMR signals. Olson and Butler employed ¹³C NMR spectroscopy to investigate the stereochemistry of the *N*-phenyl maleimide/2-chloroethyl vinyl ether alternating copolymers to elucidate the mechanism of the alternating free radical polymerization.³⁴⁻³⁷ After comparing the ¹³C NMR spectra of the polymers with the corresponding model compounds they concluded that the succinimide units mainly adopt the *cis* configuration

indicating the significant participation of a donor-acceptor “charge transfer complex” in the alternating copolymerization. However, ^{15}N NMR spectroscopy of alkene/N-methyl maleimide copolymers and ^{13}C NMR spectroscopy of alkene/maleic anhydride copolymers showed mostly *trans* enchainment of the maleimide units.³⁸⁻⁴⁰

At least one of the monomers used in each of the above mentioned studies is homopolymerizable which may contribute to the controversial conclusions from the different systems. If both monomers are nonhomopolymerizable such as *trans*-stilbene and maleic anhydride, the “charge transfer complexes” may be more significantly involved in the alternating copolymerization process and induce the succinic anhydride units to mainly adopt the *cis* configuration. Because of strong steric hindrance, the two bulky substituted phenyl groups of the stilbene should primarily adopt the *trans* configuration. If this is the case such systems can be utilized to make highly functional polymers with spatially positioned functional groups. Moreover, since the synthetic routes of substituted stilbenes and maleimide with various functional groups have been well developed this strategy will be a powerful tool to easily enchain and position different functional groups onto the desired polymers.

This study presents an effort to synthesize and characterize highly functional polymers with spatially arranged functional groups based on the alternating copolymerization of substituted stilbenes and maleic anhydride or substituted maleimide. Chapter II describes the synthesis and characterization of highly functional polymers from substituted stilbenes with maleic anhydride. Chapter III presents the solid state NMR studies of the chain structure for the substituted stilbenes - maleic anhydride alternating copolymer. The functional groups of the polymer are spatially arranged along

the polymer backbone. Chapter IV focuses on the synthesis and properties of rod-coil block copolymers containing rigid polyampholyte blocks based on N, N, N', N'-tetraalkyl-4, 4'-diaminostilbene and maleic anhydride. Chapter V describes the synthesis of polyelectrolytes based on substituted stilbenes with maleic anhydride or dimethylaminopropylmaleimide. Chapter VI shows how the spatial arrangement of the functional groups can be utilized to tune the optical properties of the polymer film. Chapter VII describes the synthesis and characterization of semi-crystalline poly(aryl ether sulfone)s containing terphenyl groups in the backbone.

References

- (1) Fréchet, J.M.J. *Science*, **1994**, *263*, 1710-1715.
- (2) Fréchet, J.M.J. *Prog. Polym. Sci.*, **2005**, *30*, 844–857.
- (3) Khandare, J.; Minko, T. *Prog. Polym. Sci.*, **2006**, *31*, 359–397.
- (4) Duncan, R. *Nature Reviews*, **2003**, *2*, 347-360.
- (5) Mammen, M.; Choi, S.K.; Whitesides G.M. *Angew. Chem. Int. Ed.* **1998**, *37*, 2754-2794.
- (6) Braun, D.; Hu, F.C. *Prog. Polym. Sci.*, **2006**, *31*, 239–276.
- (7) Allen, M.J.; Raines, R.T.; Kiessling, L.L. *J. Am. Chem. Soc.* **2006**, *128*, 6534-6535.
- (8) Fréchet, J.M.J. *J. of Polym. Sci.: A Polym. Chem.*, **2004**, *41*, 3713–3725.
- (9) Boris, D.; Rubinstein, M. *Macromolecules*, **1996**, *29*, 7251-7260.
- (10) Banaszak, L.J. *Foundations of Structural Biology*. Academic Press, **2000**.
- (11) Langer, R.; Tirrell, D.A. *Nature*, **2004**, *428*, 487-492.
- (12) Hawker, C.J.; Wooley, K.L. *Science*, **2005**, *309*, 1200-1205.

- (13) Rosa, C.D.; Auriemma, F. *Prog. Polym. Sci.*, **1988**, *13*, 189–276.
- (14) Hatada, K.; Kitayama, T.; Ute, K. *Prog. Polym. Sci.*, **2006**, *31*, 145–237.
- (15) Odian, G. *Principle of Polymerization*, 4th edition. John Wiley & Sons, Inc.: Hoboken, New Jersey, **2004**.
- (16) Haag, R. *Angew. Chem. Int. Ed.* **2004**, *43*, 278-282.
- (17) Corey, E. J.; Cheng, X-M. *The Logic of Chemical Synthesis*. John Wiley & Sons, Inc.: Hoboken, New Jersey, **1995**.
- (18) Nicolaou, K.C.; Yang, Z.; Liu, J. J.; Ueno, H.; Nantermet, P. G.; Guy, R. K.; Claiborne, C. F.; Renaud, J.; Couladouros, E. A.; Paulvannan, K.; Sorensen, E. J. *Nature* **1994**, *367*, 630 – 634.
- (19) Sellergren, B. *Angew. Chem. Int. Ed.* **2000**, *39*, 1031-1037.
- (20) Whitcombe, M.J.; Vulfson, E.N. *Adv. Mater.* **2001**, *13*, 467-478.
- (21) Zasloff, M. *Nature*, **2002**, *415*, 389-395.
- (22) Liu, D.H.; Choi, S.W.; Chen, B.; Doerksen, R.J.; Clements, D.J.; Winkler, J.D.; Klein, M.L.; DeGrado, W.F. *Angew. Chem. Int. Ed.* **2004**, *43*, 1158-1162.
- (23) Arnt, L.; Nusslein, K.; Tew, G.N. *J. of Polym. Sci.: A Polym. Chem.*, **2004**, *42*, 3860–3864.
- (24) Ilker, M.F.; Nusslein, K.; Tew, G.N.; Coughlin, E.B. *J. Am. Chem. Soc.* **2004**, *126*, 15870-15875.
- (25) Zhang, X.; Li, Z.C.; Li, K.B.; Lin, S.; Du, F.S.; Li, F.M. *Prog. Polym. Sci.*, **2006**, *31*, 893–948.
- (26) Hall, H.K.; Padias, A.B. *J. of Polym. Sci.: A Polym. Chem.*, **2004**, *42*, 2845–2858.
- (27) Hall, H.K.; Padias, A.B. *J. of Polym. Sci.: A Polym. Chem.*, **2001**, *39*, 2069–2077.

- (28) Rzaev, Z.M.O. *Prog. Polym. Sci.*, **2000**, *25*, 163–217.
- (29) Mao, M.; Turner, S.R. *Polymer* **2006**, *47*, 8101-8105.
- (30) Mao, M.; Turner, S.R. *J. Am. Chem. Soc.* **2007**, *129*, 3832-3833.
- (31) Zhang, W.; Moore, J.S. *Angew. Chem. Int. Ed.* **2006**, *45*, 4416-4439.
- (32) Suzuki, Y.; Hashimoto, K.; Tajima, K. *Macromolecules*, **2007**, *46*, ASAP.
- (33) Mulliken, R.S.; Person, W.B. “Molecular Complex: A Lecture and Reprint Volume”; Wiley-Interscience: New York, **1969**.
- (34) Olson, K.G.; Butler, G.B. *Macromolecules*, **1983**, *16*, 707-710.
- (35) Butler, G.B.; Olson, K.G.; Tu, C.L. *Macromolecules*, **1984**, *17*, 1884-1887.
- (36) Olson, K.G.; Butler, G.B. *Macromolecules*, **1984**, *17*, 2480-2486.
- (37) Olson, K.G.; Butler, G.B. *Macromolecules*, **1984**, *17*, 2487-2501.
- (38) Komber, H.; Jakisch, L.; Zschoche, S.; Mobus, H.; Ratzsch, M.; Scheller, D.
Makromol. Chem., Rapid Commun. **1991**, *12*, 547-552.
- (39) Ratzsch, M.; Zschoche, S.; Steinert, V.; Schlothauer, K. *Makromol. Chem.*, **1986**,
187, 1669-1679.
- (40) Komber, H. *Makromol. Chem. Phys.* **1995**, *196*, 669-678.

Chapter II: Polymerization Studies of Substituted Stilbene Monomers

“Reprinted from Polymer, Vol 47, Min Mao, S Richard Turner, Synthesis and Characterization of Highly Functionalized Polymers Based on N, N, N', N'-Tetraalkyl-4, 4'-diaminostilbene and Maleic Anhydride, Pages 8101-8105, Copyright (2006), with permission from Elsevier.”

II.1 Introduction of Highly Functional Polymers and Polymerization of Stilbene

Synthetic macromolecules containing functional groups pendant to the polymer backbone enable an expanding number of important applications including drug delivery¹, waste water purification², stabilization of micro and nano particles³, surface modification for improved adhesion⁴, etc. Because of the tolerance of free radical polymerization processes to functional groups, free radical polymerization is the most highly used process for preparing functional polymers. In addition to the type of functional group, molecular weight control, and polymer architecture, the density of functional groups and stiffness of the polymer chain can be an important parameter for imparting specific properties. 1,2-Disubstituted monomers have the potential to raise the functionality density along the backbone and thus to increase the functional group concentration as well as impact the chain stiffness.

Although 1,2-disubstituted monomers can be problematic in polymerizations there are several examples of very interesting polymers that are prepared from 1,2-disubstituted monomers. One important family of 1,2-substituted polymer backbone polymers is based on fumarate esters. Fumarate esters are readily polymerizable to poly(substituted methylenes) and these polymers and polymerizations have been the subject of several studies^{5,6}. Cyclic 1,2-monomers, in particular N-substituted maleimides, have been studied as monomers for homopolymerizations via free radical and anionic processes⁷⁻¹⁰. The resulting homopolymers have stiff chains predominately

formed by *trans* addition of the double bonds of the maleimides and consequently these polymers have very high glass transition temperatures.

The incorporation of N-substituted maleimides in free radically prepared copolymers has been an extensively studied area.¹¹⁻¹⁶ Because of the strong electronegativity of the maleimide double bond, maleimide copolymers have a strong propensity to be alternating.¹² The ease of preparing N-functionalized maleimides has resulted in the preparation of various functionalized alternating copolymers where the fundamental physical properties have been studied. The fundamental studies with these polymers have subsequently led to the design and synthesis of specific structures and functionality for candidates in a large variety of potential applications¹¹⁻¹⁶. The combination of high levels of functionality that can be readily and precisely modified and the stiffness of the chain imparted by 1,2-disubstituted monomers continues to be an area of high scientific output as well as offering the possibility of obtaining novel polymers with a wide range of potential useful properties as specific structure property relationships are understood.

trans-Stilbene or 1,2-diphenylethylene is another 1,2-disubstituted monomer that can be readily functionalized and that can be anticipated to have a significant impact on chain dimensions due to an expected predominant *trans* enchainment mode of the monomer and steric repulsion of the pendant aromatic substituents along the chain. Unlike the fumarates and N-substituted maleimides, stilbene and its derivatives are electron rich or donor 1,2-monomers. Stilbene forms alternating copolymers with maleic anhydride and this system has been studied as a classical donor/acceptor comonomer system¹⁷⁻²¹. Maleimide, N-ethylmaleimide, and N-phenylmaleimide form alternating

copolymers with stilbene²². As an example of a functionalized maleimide stilbene copolymer poly(N-(p-acetoxyphenylmaleimide)-alt-stilbene) was readily prepared and readily deprotected to the phenolic copolymer. This copolymer showed miscibility with novolac resins and was developed as a T_g enhancer for positive photoresists²³⁻²⁵.

Other than thermal studies and previous work on blends for photoresists,²³ to the best of our knowledge no work on preparing functional stilbene alternating copolymers and characterizing the properties of these novel structures has been reported. These novel rigid alternating copolymers contain groups that can be converted to ionic groups to promote water solubility. Therefore N, N, N', N'-tetraalkyl-4, 4'-diaminostilbenes (TDAS) based on the well developed synthetic routes of substituted stilbenes²⁶ are prepared and their copolymerization with maleic anhydride is studied. Such copolymers can be the basis of novel rigid polyelectrolytes and strictly alternating polyampholytes which potentially will possess unique solution and other physical characteristics. At the end of this chapter, the attempted polymerization of substituted stilbenes to make polybenzyl also will be discussed.

II.2 Experimental Section

General considerations. All reagents were purchased from Aldrich and were used as received. Maleic anhydride-d₂ (98 atom % D) was purchased from Aldrich and used as received. ¹H NMR spectra were determined at 25°C in CDCl₃ at 400 MHz with a Varian Unity spectrometer. IR spectra were recorded with a MIDAC M2004 FT-IR spectrophotometer in the reflection mode. Melting points of monomers were measured on

BUCHI Melting Point B-540 instrument. The elemental analysis was done by Atlantic Microlab, Inc. (Norcross, Georgia).

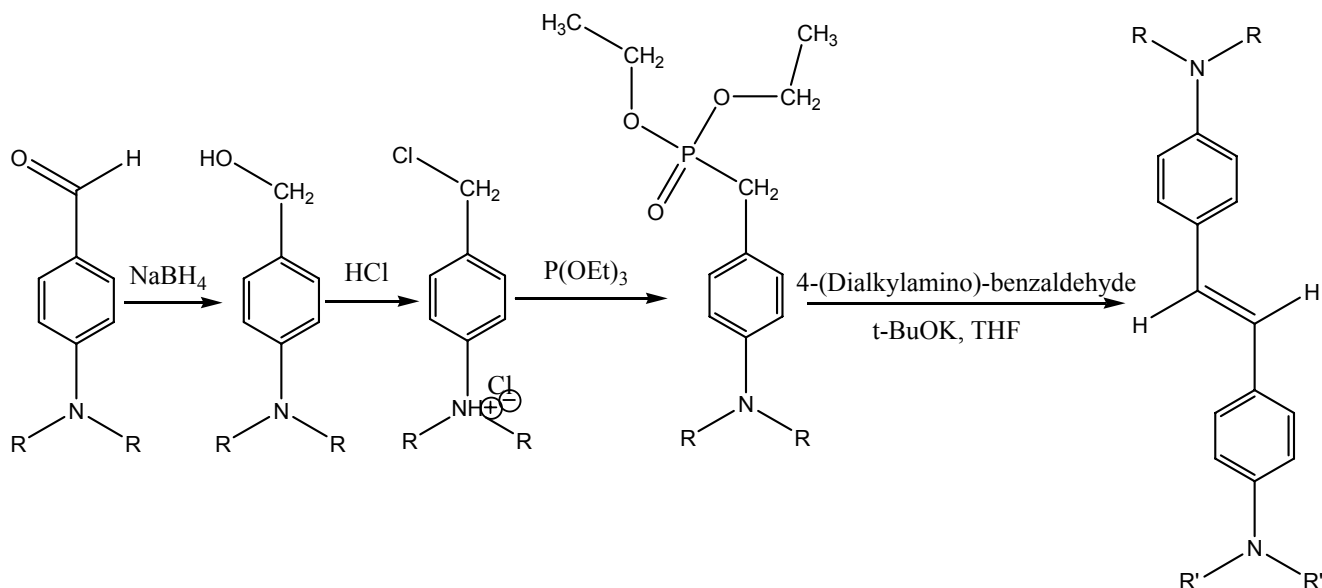
Thermogravimetric analysis (TGA) was conducted under nitrogen, from 25 to 600 °C at a heating rate of 10 °C using a TA Instrument TGA 295. Glass transition temperatures were determined using a Perkin-Elmer Pyris 1 DSC at a heating rate of 20°C/min under nitrogen. Molecular weights of synthesized polymers were determined using size exclusion chromatography (SEC) using a Waters 717 Autosampler equipped with three in-line PLgel 5 mm Mixed-C columns, Waters 410 RI detector, Viscotek 270 dual detector, and in-line Wyatt Technology miniDAWN multiple angle laser light scattering (MALLS) detector. The dn/dc values were determined on-line using the calibration constant for the RI detector and the mass of the polymer sample. SEC measurements were performed at 40 °C in tetrahydrofuran at a flow rate of 1.0 mL/min. For all samples, it was assumed that 100% of the polymer eluted from the column during the measurement.

Dynamic light scattering measurements were performed using a Malvern CGS-3 light scattering instrument with a He-Ne laser ($\lambda= 632.8$ nm) as the incident source. The sample chamber was thermostated and could be controlled to within 0.1 °C. The intensity-intensity time correlation functions were analyzed by means of the CONTIN method.

Synthesis of N, N, N', N'-tetraalkyl-4, 4'-diaminostilbenes (TDAS). Horner-Emmons condensation of an aldehyde with a phosphonate is employed to synthesize these TDASs ²⁷ (Scheme II.1). 4-N,N-dibutylaminobenzyl phosphonate and 4-N,N-

diethylaminobenzyl phosphonate were prepared following a previously published procedure²⁸.

Scheme II.1 Synthesis of N, N, N', N'-tetraethyl-4, 4'-diaminostilbenes.



TDAS-I: R=methyl, R'=butyl

TDAS-II: R=methyl, R'=ethyl

TDAS-III: R, R' = ethyl

A typical procedure to prepare N, N-dimethyl-N', N'-dibutyl-4, 4'-diaminostilbene (TDAS-I) is as follows: to a solution of 4-N,N-dibutylaminobenzyl phosphonate (2.61gram, 7.35mmol) and 4-N,N-dimethylaminobenzaldehyde (1.10gram, 7.35mmol) in dry THF (15ml) cooled in a ice-water bath was added KO^tBu (1.0M in THF, 12ml) slowly over 10 minutes. The solution was stirred at room temperature for 3 hours. After that, the reaction was poured into 100ml water. The product precipitated out from the solution and was collected by filtration. The crude product was purified by recrystallization from methanol. Yield: 70%. ¹H NMR (CDCl₃, 400MHz) δ ppm: 7.32

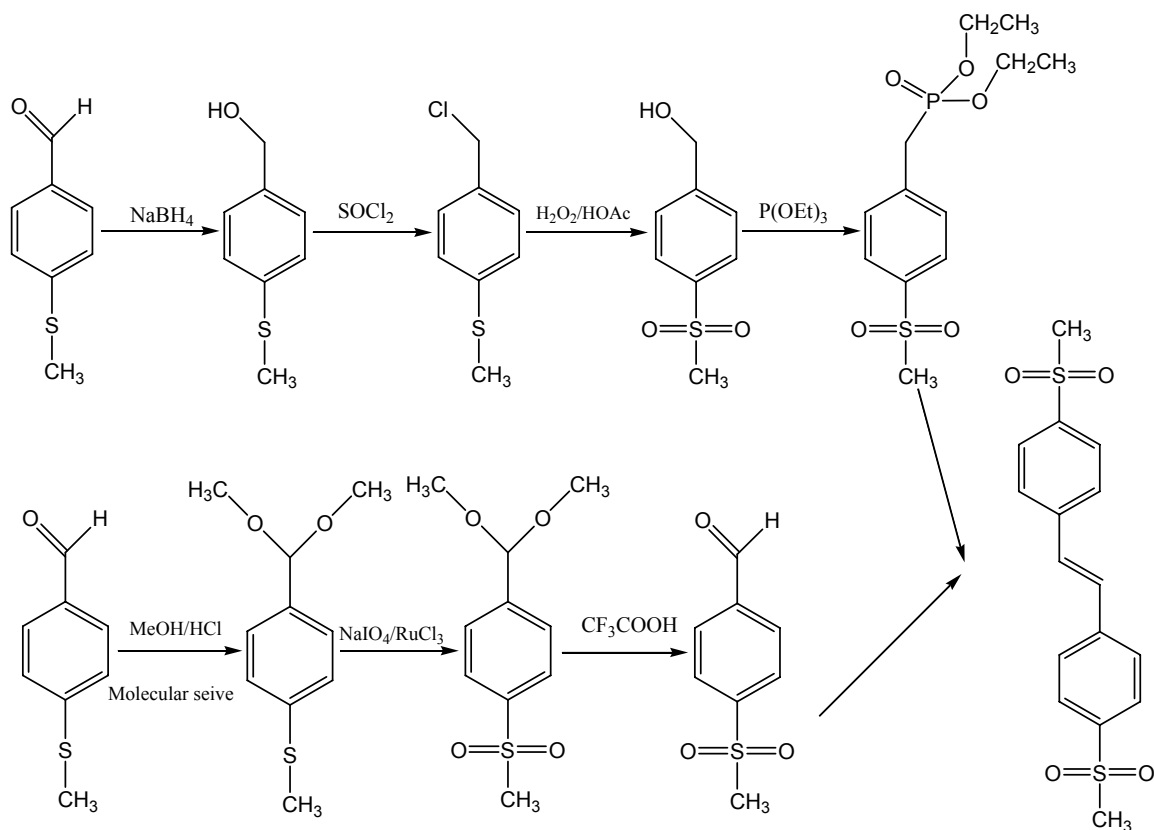
(m, 4H, Ar-H), 6.82 (s, 2H, vinyl), 6.70 (m, 4H, Ar-H), 3.25 (m, 4H, NCH₂), 2.95 (s, 6H, NCH₃), 1.60 (m, 4H, CH₂), 1.40-1.30 (m, 4H, CH₂), 0.95 (t, 6H, CH₃). ¹³C NMR (CDCl₃, 400MHz) δ ppm: 149.3, 147.2, 127.1, 126.8, 125.4, 124.9, 123.9, 112.7, 111.7, 50.8, 40.6, 29.4, 20.3, 14.0. Elemental Analysis: Calculated C, 82.23; H, 9.78; N, 7.99. Found: C, 82.12; H, 9.90; N, 7.91. Mp: 87.1-87.4°C.

N, N-dimethyl-N', N'-diethyl-4, 4'-diaminostilbene (TDAS-II) was synthesized via the condensation of 4-N,N-diethylaminobenzyl phosphonate with N,N-dimethylaminobenzaldehyde. The crude product was purified by recrystallization from acetone. Yield: 75%. ¹H NMR (CDCl₃, 400MHz) δ ppm: 7.34 (m, 4H, Ar-H), 6.82 (s, 2H, vinyl), 6.65 (m, 4H, Ar-H), 3.32 (q, 4H, NCH₂), 2.92 (s, 6H, NCH₃), 1.12 (t, 6H, CH₃). ¹³C NMR (CDCl₃, 400MHz) δ ppm: 149.5, 146.7, 127.2, 127.0, 126.9, 125.7, 124.9, 124.1, 112.7, 111.9, 44.4, 40.6, 12.7. Elemental Analysis: Calculated C, 81.59; H, 8.90; N, 9.51. Found: C, 81.52; H, 9.14; N, 9.48. Mp: 155.4-155.8°C.

N, N, N', N'-tetraethyl-4, 4'-diaminostilbene (TDAS-III) was synthesized via the condensation of 4-N,N-diethylaminobenzyl phosphonate with N,N-diethylaminobenzaldehyde. The crude product was purified by recrystallization from acetone. Yield: 68%. ¹H NMR (CDCl₃, 400MHz) δ ppm: 7.30 (m, 4H, Ar-H), 6.80 (s, 2H, vinyl), 6.62 (m, 4H, Ar-H), 3.32 (q, 4H, NCH₂), 1.12 (t, 6H, CH₃). ¹³C NMR (CDCl₃, 400MHz) δ ppm: 146.7, 127.1, 125.8, 124.2, 111.9, 44.4, 12.6. Elemental Analysis: Calculated: C, 81.94; H, 9.38; N, 8.69. Found: C, 81.94; H, 9.38; N, 8.53. Mp: 136.3-136.9°C.

Synthesis of di-methylsulfonyl-4,4'-stilbene. Similar to N, N, N', N'-tetraalkyl-4, 4'-diaminostilbenes, Horner-Emmons condensation of an aldehyde with a phosphonate is employed to synthesize di-methylsulfonyl-4,4'-stilbene.²⁷ The following is the synthetic scheme. The 4-(Methylmercapto)benzylaldehyde has to be protected before the oxidation step. The details for each step are described below:

Scheme II.2 Synthetic scheme of the di-methylsulfonyl-4,4'-stilbene.



4-(Methylmercapto)benzyl Chloride. In a 250mL, three-necked, round-bottomed flask equipped with a dropping funnel and a reflux condenser was charged with 100 mL of toluene and 10 g (64.9 mmol) of 4-(methylmercapto)benzyl alcohol. Thionyl chloride (8 mL) was added dropwise with stirring. When the addition of the thionyl chloride was completed, the reaction mixture was heated to 80 °C and stirred for 2h. The

mixture was then cooled to room temperature. Toluene and excess thionyl chloride were evaporated under reduced pressure and yielded NMR pure compound. ^1H NMR (CDCl_3 , 400MHz) δ ppm: 7.28 (m, 4H, Ar-H), 4.57 (s, 2H, Ar- CH_2), 2.50 (s, 3H, SCH_3).

Diethyl 4-(Methylmercapto)benzyl phosphonate. In a 100 mL flask was charged with triethyl phosphite (16 ml) and 11.16 g of 4-(methylmercapto)benzyl chloride. The reaction was refluxed for 4 hours. Excess triethyl phosphite was removed under reduced pressure. The product was used without further purification for the next step of reaction. ^1H NMR (CDCl_3 , 400MHz) δ ppm: 7.20 (m, 4H, Ar-H), 4.00 (m, 4H, P(=O)OCH_2), 3.10 (d, Ar- CH_2), 2.45 (s, 3H, SCH_3), 1.22 (t, 6H, CH_3).

Diethyl 4-(Methylsulfonyl)benzyl phosphonate. In a 100 ml flask charged with 50 mL of glacial acetic acid, 20 ml of H_2O_2 (30% in water) was added 20 grams of diethyl (methylmercapto)benzyl phosphonate. The reaction mixture was refluxed at 100°C for 8 hours. The water and acetic acid were evaporated under reduced pressure, and the residue was a very viscous liquid which solidified on standing. ^1H NMR (CDCl_3 , 400MHz) δ ppm: 7.82 (d, 2H, Ar-H), 7.44 (d 2H, Ar-H), 4.00 (m, 4H, P(=O)OCH_2), 3.20 (d, Ar- CH_2), 3.00 (s, 3H, SCH_3), 1.22 (t, 6H, CH_3).

1-(Dimethoxymethyl)-4-(methylthio)-benzene. A mixture of [4-(methylthio)phenyl]oxo-methyl (1 gram, 6.58 mmol), 20 ml methanol and 0.5 ml of 37% HCl was refluxed for 3 hrs over 4A molecular sieves. The mixture was filtered over Celite and evaporated to give acetal as a colorless oil. ^1H NMR (CDCl_3 , 400MHz) δ ppm: 7.38 (d, 2H, Ar-H), 7.22 (d, 2H, Ar-H), 5.38 (s, 1H, OCHO), 3.30 (s, 6H, OCH_3), 2.50 (s, 3H, SCH_3).

1-(Dimethoxymethyl)-4-(Methylsulfonyl)-benzene. To a 100 ml flask with a magnetic stirrer were sequentially added 1-(dimethoxymethyl)-4-(methylthio)-benzene (1.23 gram, 6.21 mmol), carbon tetrachloride (10m), acetonitrile (10 ml), water (20 ml) and sodium periodate (3,986 gram, 18.64 mmol). To this suspension was added ruthenium trichloride hydrate (2mg, 0.05 mol%). The resulting mixture was stirred at room temperature. A white precipitate was formed during the reaction. After 45 minutes, water and ether were added to the reaction. After separation, the ether layer was washed with saturated sodium bicarbonate and sodium chloride solutions and dried over magnesium sulfate. After the removal of solvent the product was isolated in 2.0 gram (90%) yield as a NMR-pure compound.

4-(Methylsulfonyl)-benzaldehyde. The acetal was hydrolyzed by stirring in a mixture of chloroform and 50% aqueous trifluoroacetic acid (2:1) at 0°C for 90 minutes. After that, aqueous sodium carbonate solution was added to neutralize the acid. The mixture was extracted three times with ethyl ether and after the combined organic layer was washed with brine and dried over magnesium sulfate. After the removal of solvent the product was isolated in 8.0 gram (97%) yield as a NMR-pure compound. The product was used directly for the next step of the synthesis. ¹H NMR (CDCl₃, 400MHz) δ ppm: 10.18 (s, 1H, CHO), 8.10 (m, 4H, Ar-H), 3.10 (s, 3H, SO₂CH₃).

Di-methylsulfonyl-4,4'-stilbene. To a solution of diethyl 4-(methylmercapto)benzyl phosphonate (7.35mmol) and 4-(methylsulfonyl)-benzaldehyde (7.35mmol) in dry THF (15ml) cooled in a ice-water bath was added KO^tBu (1.0M in THF, 12ml) slowly over 10 minutes. The solution was stirred at room temperature for 3 hours. After that, the reaction was poured into 100ml water. The product precipitated out

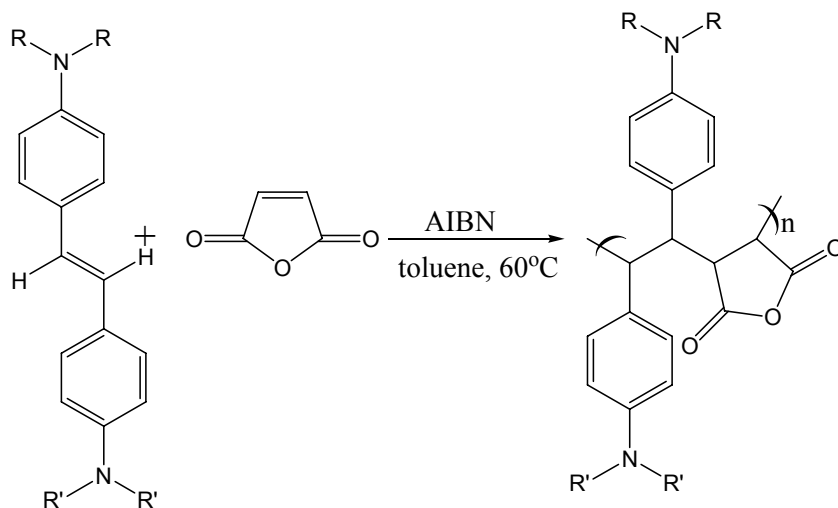
from the solution and was collected by filtration. Yield: 99% as a white solid. $^1\text{H NMR}$ (CDCl_3 , 400MHz) δ ppm: 7.90 (m, 8H, Ar-H), 7.58 (s, 2H, vinyl), 3.22 (s, 3H, SO_2CH_3).

N, N, N-trimethylammonium bromide-N', N'-diethylamino-4, 4'-stilbene.

This asymmetrical stilbene was synthesized by reacting N, N-dimethyl-N', N'-dibutyl-4, 4'-diaminostilbene with 1 eq CH_3I in THF. The final product precipitated out as a pure compound. Only the dimethylamino group reacted with CH_3I due to the steric hindrance. $^1\text{H NMR}$ (CDCl_3 , 400MHz) δ ppm: 7.40 (m, 8H, Ar-H), 6.64 (s, 2H, vinyl), 4.00 (s, 9H, NCH_3), 3.40 (q, 4H, NCH_2), 1.20 (t, 6H, CH_3).

Polymerization. The TADS, maleic anhydride, and toluene were added together with an initiator [2,2'-azobisisobutyronitrile (AIBN)] in a 50-mL, septum sealed glass bottle equipped with a magnetic stirrer. The polymerization solution turned dark red immediately upon mixing the two monomers. All of the copolymerizations contained an equal molar ratio of TDAS and maleic anhydride. The initiator concentration varied from 0.1 wt% to 1 wt%. The mixture was degassed by purging with argon for 20 min and polymerized at 60 °C for 24 hours (Scheme II.3). The copolymers were then isolated by precipitation into hexane. The collected crude products were re-dissolved in chloroform and precipitated in hexane. The cycle was repeated for three times to remove the unreacted monomers. The copolymer formed by TDAS-II and maleic anhydride is insoluble in any organic solvent and was freed from monomers by repeated rinsing with chloroform. All polymers were dried in the vacuum oven at 60°C overnight before characterization. Two peaks associated with the anhydride groups of the copolymers (1841 cm^{-1} and 1772 cm^{-1}) were clearly observed in the IR spectrum, and the peak from the free carboxylic acid groups was absent.

Scheme II.3 Alternating copolymerization of N, N, N', N'-tetraethyl-4, 4'-diaminostilbenes with maleic anhydride.



III.3 Polymerization Studies of Substituted Stilbene with Maleic Anhydride

Free radical alternating copolymerization of electron rich and electron poor monomers is a well-documented polymerization process for enabling the copolymerization of monomers that do not homopolymerize under free radical conditions.³¹ The stilbene maleic anhydride comonomer pair and the vinyl ether maleic anhydride comonomer pair are classical examples of this phenomenon since neither stilbene, vinyl ethers, nor maleic anhydride is homopolymerize in a radical process, yet the alternating copolymerization of these comonomer pairs readily yields as a high molecular weight copolymer²⁹⁻³¹.

Since amino groups are very strong electron-donating groups, TDASs readily copolymerize with maleic anhydride to yield soluble high molecular weight alternating copolymers with almost 100% conversion. After TDASs were mixed with maleic anhydride, the solutions turned dark red immediately, which may be due to the formation

of donor-acceptor complexes. The color of the solutions disappeared after about two hours. This polymerization process is not spontaneous. Without the addition of initiator, the color did not fade and on precipitation no polymer was isolated. Unlike the stilbene maleic anhydride copolymer, these copolymers are soluble in organic solvents. The solubility and molecular weight data are shown in Table II.1.

Table II.1 Solubility of N, N, N', N'-tetraethyl-4, 4'-diaminostilbene polymers in common solvents.

Polymer	water	methanol	THF	chloroform	toluene	hexane
R=methyl, R'=ethyl	-	-	-	-+	-	-
R, R' = ethyl	-	-	-+	+	-+	-
R=methyl, R'=butyl	-	-	+**	+	+	-

* - insoluble, -+ slightly soluble, + soluble; ** MALLS-SEC: $\bar{M}_n = 94600$ g/mole;

$$\bar{M}_w = 164600 \text{ g/mole}; \bar{M}_w / \bar{M}_n = 1.74$$

As shown in Table II.1, the solubility characteristics of these polymers in organic solvents are dependent on the length of the N-alkyl substituents. Long alkyl chains on the amino groups, acting as the solvating segments, significantly increase the solubility of these polymers in organic solvents. Water solubility of these copolymers is pH dependent. They are very soluble in dilute aqueous hydrochloric acid solution. After the pH of the solution is increased to 4.9, the polymers will precipitate. Further raising the

pH to 12 yields a slightly turbid solution. The low solubility of these polymers in basic aqueous solution can be attributed to the hydrophobic amine-substituted phenyl groups.

The effect of the comonomer feed ratio on the composition of the TDAS-MA copolymer was also investigated. The comonomer feed ratio of TDAS to MA was varied from 7:3 to 1:9. The homo-polymerization of TDAS or maleic anhydride was not observed. The compositions of the polymers are almost identical, indicating, as expected, the strictly alternating structure of the TDAS-MA copolymer (Table II.2).

Table II.2 The compositions of the TDAS-MA copolymer at 60°C with different monomer feeding ratios ($C_{\text{monomer, total}} = 5 \text{ wt\%}$ with 1,2-dichloroethane as the solvent, $C_{\text{initiator}} = 1 \text{ wt\%}$ of monomer).

monomer feeding ratio, TDAS:MA	composition from elemental analysis		
	C	H	N
1:0	no polymer recovered		
7:3	74.03%	7.67%	6.76%
1:1	74.05%	7.66%	6.55%
3:7	73.44%	7.58%	6.63%
1:9	no polymer recovered		
0:1	no polymer recovered		
theoretical 1:1	74.26%	7.67%	6.66%

II.4 Chain Rigidity of the Substituted Stilbene - Maleic Anhydride or Maleimide Alternating Copolymers

The polymers are thermally stable up to 300 °C (measured by TGA). Similar to polyfumarates,⁵ there is no observed glass transition for these polymers up to 280°C, which indicates very stiff polymer backbones. Moreover, in the 400 MHz ¹H NMR spectrum of the TDAS-I maleic anhydride alternating copolymer, the aromatic hydrogen atoms show very broad peaks, and the peaks of the hydrogen atoms on the polymer backbone are almost invisible. A similar phenomenon is also observed for the TDAS-III maleic anhydride alternating copolymer. Such greatly broadened peaks are consistent with severely restricted rotation of the polymer backbones.

The backbone rigidity of these TDAS maleic anhydride copolymers is further corroborated by the dynamic light scattering measurements. The hydrodynamic radius (R_h) of the TDAS-I maleic anhydride alternating copolymer chains in THF was monitored as a function of temperature (Figure II.1). At the temperature range from 10°C to 40°C, the copolymer has almost the same R_h , around 10nm. If the polymer chains adopt a coil conformation in solution, their size will vary with the change of temperature, unless THF is an extremely good solvent for this alternating copolymer so the polymer chains are already highly extended at the low temperature.

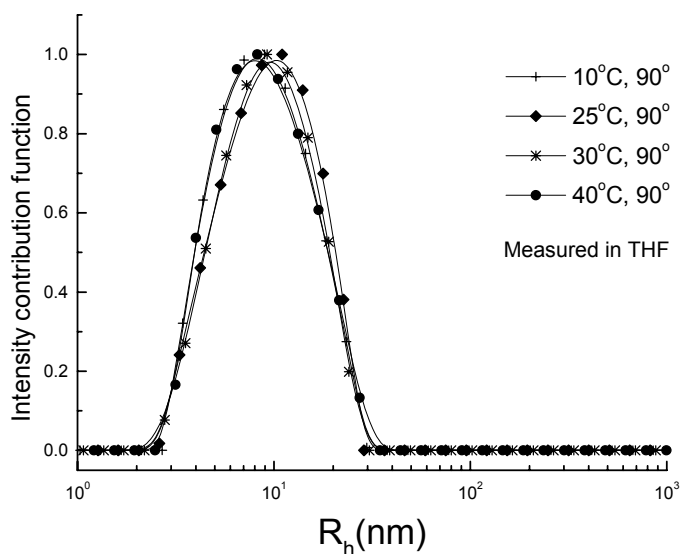
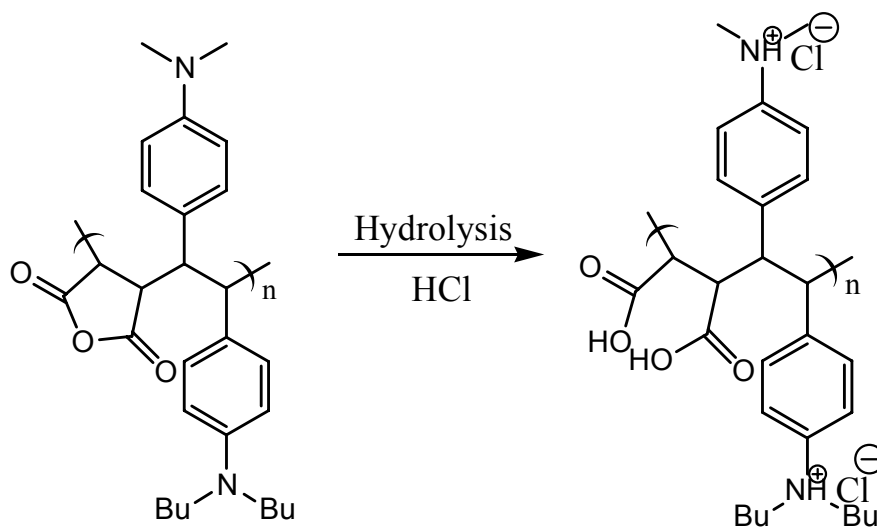


Figure II.1 Hydrodynamic radius of the N, N-dimethyl-N', N'-dibutyl-4, 4'-diaminostilbene maleic anhydride alternating copolymer in THF at different temperature.

Due to the polyelectrolyte effect the charges on the polymer chains will expand the backbones from the electrostatic repulsion between the charged groups. As stated before, these TDAS maleic anhydride copolymers are soluble in dilute aqueous hydrochloric acid and turn into cationic polyelectrolytes. If the chains of these alternating copolymers in neutral form are coils, the introduced charges on the polymer chains would stretch the coils into rods. The TDAS-I maleic anhydride alternating copolymer was dissolved in 0.01M hydrochloric acid aqueous solution, subsequently it was hydrolyzed and highly charged (Scheme II.4). The hydrolyzed and positively charged polymer was isolated by precipitation into THF and dried in a vacuum oven at 70 °C overnight. Besides the disappearance of the peaks from the anhydride group (1841 cm^{-1} and 1772 cm^{-1}), a strong absorption peak associated with the free carboxylic acid (1721 cm^{-1}) was

observed in the IR spectrum, indicating complete hydrolysis of the anhydride group. The hydrodynamic radius of the neutral form copolymer (dissolved in chloroform) was identical to the R_h of the hydrolyzed, highly charged form of the polymers dissolved in acidic water (Figure 2), suggesting that the neutral initial chain is rigid. Due to the hydrophobic butyl chains on the amino groups, the copolymer in dilute aqueous hydrochloric acid solution is a partially hydrophobic polyelectrolyte which forms large aggregates. The nature of such aggregates has not been studied.

Scheme II.4 Hydrolysis of N,N-dimethyl-N',N'-dibutyl-4,4'-diaminostilbene maleic anhydride alternating copolymer in dilute aqueous hydrochloric acid solution.



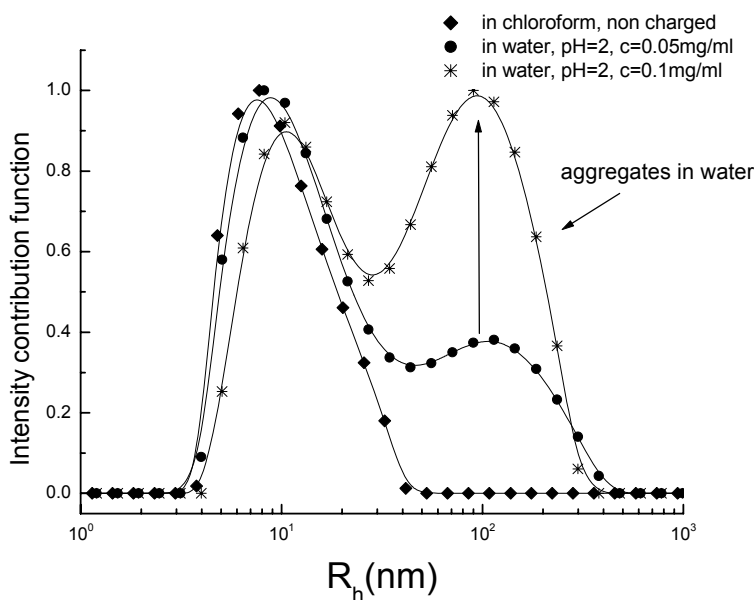


Figure II.2 Hydrodynamic radius of the neutral and charged forms of the N, N-dimethyl-N', N'-dibutyl-4, 4'-diaminostilbene maleic anhydride alternating copolymer.

Persistence length is introduced by Kratky and Porod as a direct measure of the intrinsic chain stiffness for a linear polymer chain.³⁸ Recently Mourey proposed a method to obtain the persistence length of the polymer by fitting the molecular weight versus radius of gyration (R_g) data obtained from MALLS-SEC measurement with a semi-flexible chain model.³⁹ For *N*-(*o*-tolyl)maleimide – stilbene copolymer (see chapter VI for the synthetic details) the persistence length of the polymer backbone is around 10 nm fitted from the molecular weight versus radius of gyration (R_g) data obtained from MALLS-SEC measurement with a semi-flexible chain model (Figure II.3):

$$R_g^2 = \frac{l_p M}{3M_L} - l_p^2 + \frac{2l_p M_L}{M} - \frac{2l_p^4 M_L^2}{M^2} \left(1 - e^{-\frac{M}{l_p M_L}}\right)$$

where l_p is the persistence length and M_l is the molar mass per unit contour length. Such a persistence length is comparable to that of rigid rod poly(p-phenylene) (around 13 nm).⁴⁰

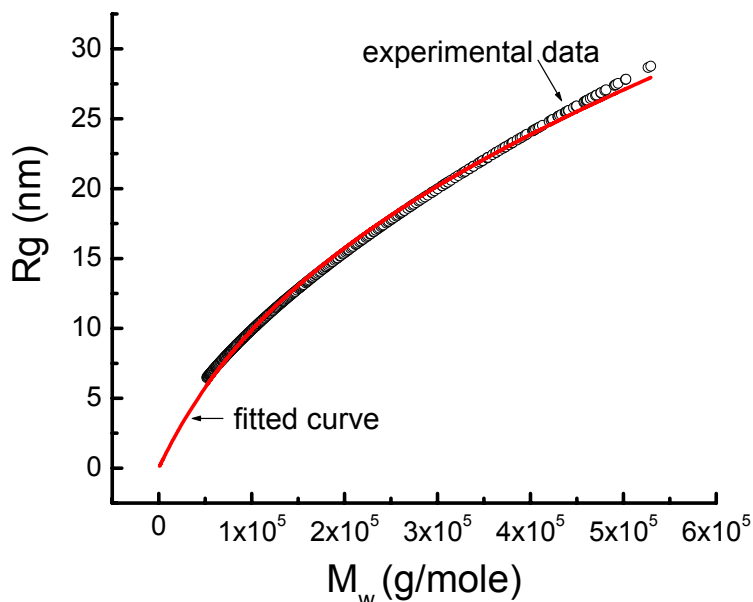


Figure II.3 The fitting of $R_g - M_w$ according to ref 29 to obtain persistence length of *N*-(*o*-tolyl)maleimide – stilbene copolymer backbone.

II.5 Chain Dynamics of the TDAS-MA Alternating Copolymer Probed by ²H-Solid State NMR

Other strong piece of evidence for the rigid backbone of the substituted stilbene – maleic anhydride alternating copolymer comes from the solid state ²H NMR. The deuterium nucleus has a spin of 1, resulting in three energy levels in a magnetic field and a non-zero quadrupole moment.³³ Deuterium NMR spectroscopy in the solid state offers some distinct advantages for the study of molecular motion in solid polymers since deuterium NMR quadrupolar powder pattern (lineshape), the well-known Pake spectrum,

is sensitive to motions that have correlation times of ca. 10^{-4} - 10^{-7} s.³⁴ The splitting between the two peaks in the powder pattern, given by the following equation, corresponds to nuclear sites oriented at $\theta = 90^\circ$ with respect to the magnetic field.

$$\Delta\nu = \frac{3}{4} \chi (3 \cos^2 \theta - 1 - \eta \sin^2 \theta \cos^2 \Phi)$$

where χ is the quadrupolar coupling constant defined as e^2qQ/\hbar (where e is the elementary charge, Q is the quadrupole moment of the nucleus, q is the electric field gradient and \hbar is Planck's constant), θ and Φ are polar angles specifying the orientation of the magnetic field with the principal axis system of the electric field gradient tensor, η is the asymmetry parameter.³⁵ η is zero for the case of axial symmetry such as the aliphatic C-D bond. In the absence of motion, the deuterium lineshape is a result only of the angle the C-D bond forms with respect to the magnetic field and the two allowed transition. A rigid-lattice model yields the quadrupolar coupling constant (e^2qQ/\hbar) = \sim 168 kHz for the paraffin hydrocarbons.³⁶ Molecular motion which changes the C-D bond orientation is accounted for by the use of averaged terms for χ and η . Motion introduces a significant and predictable change in the width and shape of the deuterium NMR spectrum.³⁷

Based on the magnitude of deuterium quadrupolar coupling constant, e^2qQ/\hbar , in the solid state, ^2H NMR spectroscopy has been used to characterize the motional mobility of N, N, N', N'-tetraethyl-4, 4'-diaminostilbene (TDAS) and maleic anhydride (MA) alternating copolymer synthesized in the previous section. Solid-state ^2H NMR spectra were obtained on a Bruker Avance II spectrometer with a quadrupole echo pulse sequence by using a static ^1H -X double resonance probe tuned at 301 MHz and at 46.02

MHz for ^1H and ^2H channels, respectively. Typically, the delay between pulses was 30 ~ 40 μs , and the dwell time was 2 μs . The maximum allowed pulse power of the probe at the ^2H frequency provided a 90° degree pulse length 4.5 μs . 20 – 30 mg of sample required 2048 scans with a recycle time of 3s. 400 Hz Lorentzian line broadening was applied to the ^2H NMR spectra of the compounds.

The ^2H NMR spectrum of both unhydrolyzed (Fig.II.4A) and hydrolyzed forms (Fig.II.4B) of the deuterated N, N, N', N'-tetraethyl-4, 4'-diaminostilbene (TDAS) and maleic anhydride (MA) alternating copolymer are shown in Fig.II.5, together with a rigid-lattice simulation of the line shape. The simulation yields the quadrupole coupling constants, $(e^2qQ/\hbar) = \sim 168$ kHz, for both polymers, indicating that the polymer backbone skeleton of both types of polymers are rigid.⁷ For the hydrolyzed polymer, there are many charged quaternary ammonium groups and hydrogen bonding formation carboxylate acid groups. The strong inter-chain interactions will block all of the possible motions of the polymer backbone.

A closer look at the spectra (Fig. II4A), however, indicates that the magnitude of the coupling constant of the unhydrolyzed form is somewhat smaller than that of the hydrolyzed form. To elucidate the possible motion of the unhydrolyzed polymer backbone, the deuterium NMR spectra of both polymers were measured at various temperatures. However, within the temperature range from 25°C to 190°C, the splitting between the two peaks in the powder pattern remained the same (Fig.II.5). As mentioned before, the molecular motion leads to an averaging of the quadrupolar interactions, resulting in decreased line widths. In the region of the fast exchange, $\tau < 10^{-8}$ s, line width and lineshape of the spectrum depend on the type of the molecular motion. Increasing

velocity of the motions does not result in an additional decrease of the line width. Molecular motions with correlation time $\tau > 10^{-4}$ s are slow with respect to the time resolution of the ^2H NMR and can be observed by a change of the resonance line. In the intermediate range $10^{-4} > \tau > 10^{-8}$ s the averaging is not complete and the line width depends on the type of the molecular motion as well as on the rate and shows the temperature dependence. So the slightly smaller line width of the unhydrolyzed polymer may reflect a rapid, small-amplitude motion of the anhydride plane.

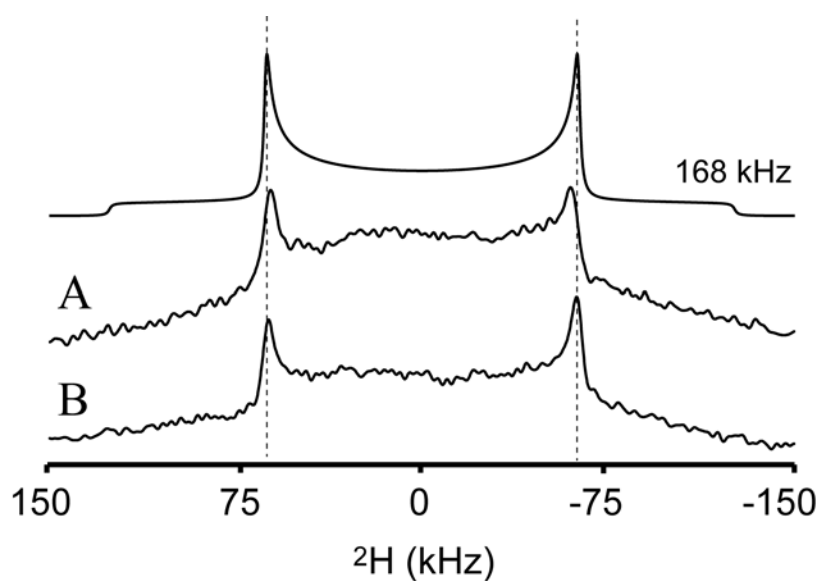


Figure II.4 Solid-state ^2H NMR spectra of unhydrolyzed polymer (A) and hydrolyzed polymer (B) at 298 K, obtained at a 46.02 MHz resonance frequency with a quadrupole echo pulse sequence⁸ with proton decoupling. The best fit spectra shown above experimental spectra based on a rigid-lattice model yields $(e^2qQ/\hbar) = \sim 168$ kHz, a value for the paraffin hydrocarbons with no motion.

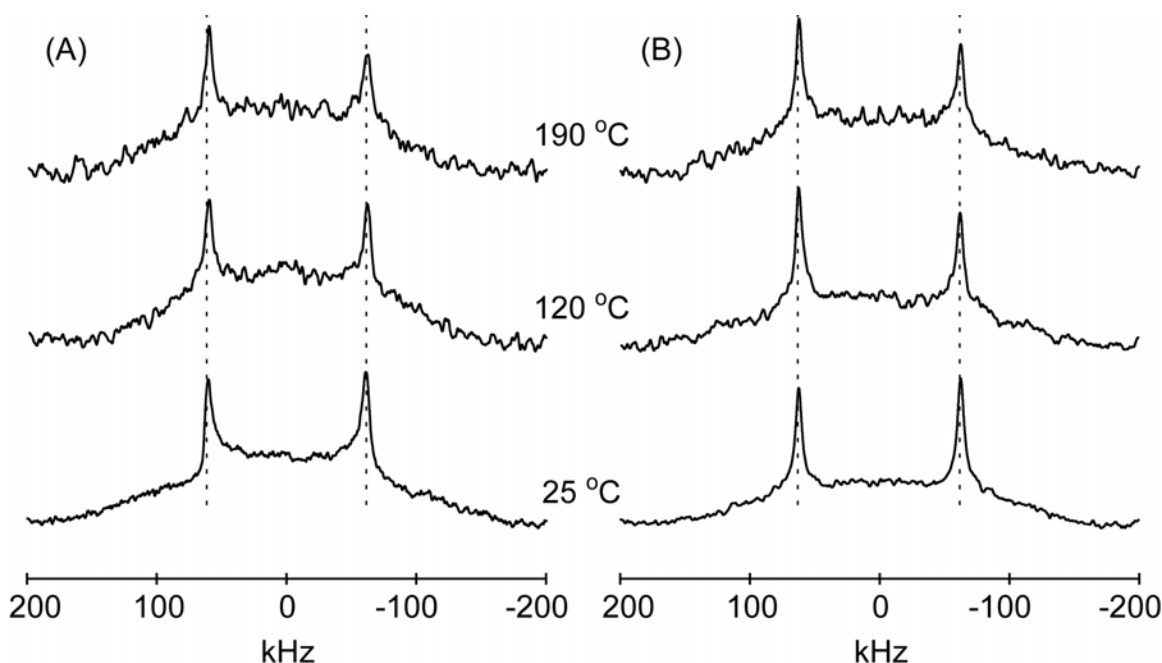


Figure II.5 ^2H spectra measured on unhydrolyzed form (A) and on hydrolyzed form (B) of TDAS-MA copolymer at 25 °C, 120 °C, and 190 °C.

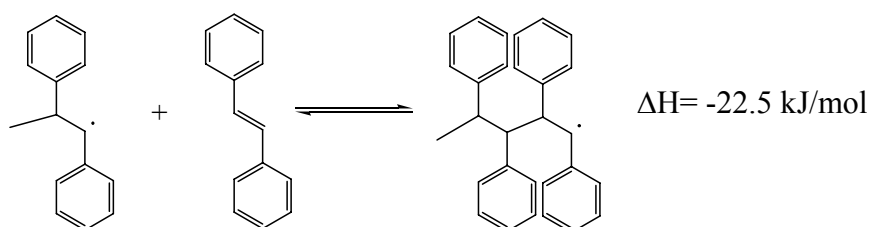
II.6 Attempted Polymerization of Substituted Stilbenes to Synthesize Poly(phenylmethylene)

Free radical alternating copolymerization of electron rich and electron poor monomers is a well-documented polymerization process for enabling the copolymerization of monomers that do not homopolymerize under free radical conditions. The driving force of electron rich radical attacking electron poor double bonds and vice versa is proposed to be the strong driving force to overcome the steric/electronic factors that are the barriers for the polymerization (an alternative mechanistic proposal is copolymerization regulated by donor-acceptor complexes).^{30,31}

The reasons for the failure of stilbene to homopolymerize have not been elucidated. It has been shown that, in the presence of methacrylate or styrene, stilbene

and some of the halogenated derivatives of stilbene react with benzoyl peroxide as an anitiator and then add to methyl methacrylate or styrene to form chains with terminal stilbene units.³² However stilbene propagation itself was not observed. From quantum calculations with Gaussian98, we modeled the conversion of stilbene to poly(phenylmethylene) chain and found that the heat of this reaction is calculated to be -22.5 kJ/mol (scheme II.5).

Scheme II.5 The conversion of stilbene to poly(phenylmethylene).



A poly(phenylmethylene) chain could possess interesting and unusual rod-like properties due to the steric interactions of the pendant phenyl groups on each carbon atom. Molecular models indicate that the phenyl groups most likely would align perpendicular to the chain as shown in Figure II.6.

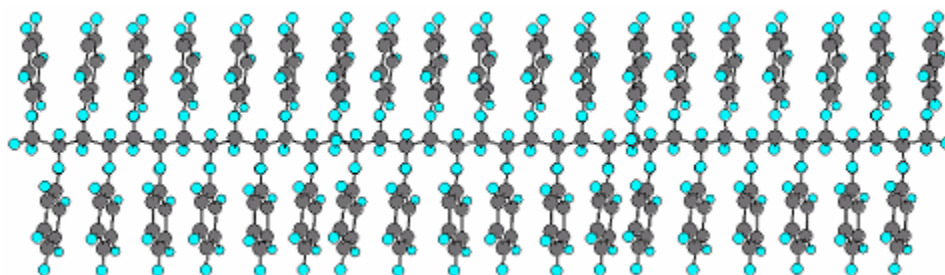


Figure II.6 The possible structure of a poly(phenylmethylene) chain.

One possible strategy to prepare the unknown poly(phenylmethylene)s is based on the alternating copolymerization of electron donor and electron acceptor substituted

stilbenes. The driving force of alternating copolymerization of these donor and acceptor monomers may provide the energetics to overcome the transition state problems and permit the formation of high molecular weight poly(phenylmethylene)s. The first system investigated is N, N-dimethyl-N', N'-dibutyl-4, 4'-diaminostilbene as the donor and di-*t*-butyl-*trans*-4,4'-stilbenedicarboxylate (the synthesis of this monomer is described in chapter V) as the acceptor. However the free radical polymerization using benzoyl peroxide and AIBN in toluene failed to produce polymer in this system. There was no color change when donor-acceptor monomers were mixed together.

Three new stilbene monomers were prepared to explore the homopolymerization of stilbenes further (see the experimental section of this chapter for the details of the synthesis). Sulfone groups are relatively strong electron withdrawing functionalities. However the free radical polymerization using benzoyl peroxide and AIBN in DMF failed to produce polymer with N, N-dimethyl-N', N'-dibutyl-4, 4'-diaminostilbene as the donor and di-methylsulfonyl-4,4'-stilbene as the acceptor. Asymmetrical stilbenes, N, N, N-trimethylammonium bromide-N', N'-diethylamino-4, 4'-stilbene, with the electron-donating groups (amino group) on one end and the electron-withdrawing groups (quaternary ammonium) on the other end were also synthesized. However this unsymmetrical stilbene also failed to homopolymerize to produce polymer.

II.7 Conclusions

In summary a series of novel, highly functional rod-like copolymers by the alternating copolymerization of TDAS with maleic anhydride has been synthesized and some of their properties have been characterized. These alternating copolymers possess

some unusual and fundamentally interesting solution properties. Increasing the length of alkyl chains on the amino group significantly enhances the solubility of these alternating copolymers in organic solvents. Depending on solution pH, the alternating copolymers can be converted into strictly alternating polyampholytes, cationic or anionic polyelectrolytes with different solubility in aqueous solution. The hydrodynamic radius (R_h) of these alternating copolymers does not change upon increasing temperature or introducing charges to the amino groups, indicating the presence of very rigid polymer backbones. There is no observed glass transition below 280°C which corroborates the chain rigidity. The persistence length of the alternating copolymers is around 10 nm. ^2H solid state NMR is also employed to study the chain dynamics of the alternating copolymers and reveals the high rigidity of the polymer backbone. These results indicate that a wide variety of responsive rod-like copolymers are readily accessible using substituted stilbene monomers.

The polymerization of stilbene monomers with electron-donating and electron-withdrawing groups to synthesize poly(phenylmethylene)s was also investigated. To date the homopolymerization of substituted stilbenes has not been successful.

References

- (1) Giles, E. R.; Frechet, J.M. J. *Drug Discovery Today* **2005**, *10*, 35.
- (2) Bolto, B.A. *Prog. Polym. Sci.* **1995**, *20*, 987.
- (3) Foerster, S.; Abetz, V.; Muller, A. H. E. *Advances in Polym. Sci.* **2004**, *166*, 173.
- (4) Pasquier, N.; Keul, H.; Moeller, M. *Designed Monomers and Polymers* **2005**, *8*, 679.

- (5) Otsu, T., Yasuhara, T., Matsumoto, A. *J. Macromol. Sci. Chem.* **1988**, A25, 537.
- (6) Murata, Y.; Koinuma, Y.; Amaya, N.; Otsu, T.; Nisimura, M. *Eur. Pat. Appl.* 233299 AL (1987) to Nippon Oils & Fats Co.
- (7) Otsu, T., Matsumoto, A., Kubota, T., Mori, S. *Polymer Bulletin* **1990**, 23, 43 and Matsumoto, A., Kubota, T., Otsu, T. *Macromolecules* **1990**, 23, 4508.
- (8) Nakayama, Y.; Smets, G. *J. Polym. Sci. Part A-1*, **1967**, 5, 1619.
- (9) Cubbon, R.C. P. *Polymer* **1965**, 6, 419.
- (10) Balta-Calleja, F.J.; Ramos, J. G.; Barrales-Rienda, J.M. *Kolloid-Z.u.Z Polymere* **1972**, 250, 474.
- (11) Kim, S-T., Kim, J-B., Chung, C-M., Ahn, K-D. *J. Appl. Polym. Sci.* **1997**, 66, 2507.
- (12) Turner, S. R.; Anderson, C.C.; Kolterman, K.M.; Seligson, D. *ACS Symposium Series* **1989**, 381, 172.
- (13) Gangadhara, P.; Noel, C.; Reyx, D.; Kajzar, F. *J. Polym. Sci. Part A*, **1999**, 37, 513.
- (14) Appelhans, D.; Zhong-Gang, W.; Zschoche, S.; Zhuang, R-C.; Haussler, L.; Friedel, P.; Simon, F.; Jehnichen, D.; Grundke, K.; Eichhorn, K-J.; Komber, H.; Voit, B. *Macromolecules* **2005**, 38, 1655.
- (15) Lange, R.F.; Meijer, E. W. *Macromolecules* **1995**, 28, 782.
- (16) Perez-Camacho, O.; Sepulveda-Guzman, S.; Perez-Alvarex, M.; Garcia-Zamora, M.; Cadenas-Pliego, G. *Polymer Int.* **2005**, 54, 1626.
- (17) Hallensleben, M. *European Polymer Journal* **1973**, 9, 227.
- (18) Tanaka, T.; Vogl, O. *Polymer Journal* **1974**, 6, 522.

- (19) Kellou, M.; Jenner, G. *European Polymer Journal* **1977**, *13*, 9.
- (20) Ebdon, J. R.; Hunt, B. J.; Hussein, S. *British Polymer Journal* **1987**, *19*, 333.
- (21) McNeill, I. C.; Polishchuk, A.Y.; Azikov, G. E. *Polymer Degradation and Stability* **1995**, *47*, 319.
- (22) Rzaev, Z. M. O.; Milli, H.; Akovali, G. *Polymer International* **1996**, *41*, 259.
- (23) Turner, S. R.; Arcus, R. A.; Houle, C. G.; Schleigh, W. R. *Polymer Engineering and Science* **1986**, *26*, 1096.
- (24) Turner, S. R.; Houle, C. G. U. S. Patent 4,663,268 (1987) to Eastman Kodak Company.
- (25) Turner, S. R. unpublished results.
- (26) Becker, K. B. *Synthesis*, **1983**, 341.
- (27) Wadsworth, W.S.; Emmons, W.D. *J. Amer. Chem. Soc.* **1961**, *83*, 1733.
- (28) Marder, S.R.; Perry, J.; Zhou, W.; Kuebler, S.M.; Cammack, J.K. WO 2002079691.
- (29) Odian, G., "Principles of Polymerization," Fourth Edition, Wiley Interscience, 498.
- (30) Hall, H. K.; Padias, A. B., *Acc. Chem. Res.* **1997**, *30*, 322 (discusses mechanisms of copolymerization).
- (31) Rzaev, Z. M. O., *Prog. Polym. Sci.* **2000**, *25*, 163.
- (32) Bevington, J.C.; Breuer, S.W.; Huckerby, T.N. *Angew. Makromol. Chem.* **1988**, *9*, 791.
- (33) Duer, M.J. "Solid-State NMR Spectroscopy: Principles and Applications"; Blackwell Science Ltd.: Oxford, **2004**.
- (34) Spiess, H.W. *Colloid & Polymer Science*, **1983**, *261*, 193-209.
- (35) Matsunami, S.; Kakuchi, T.; Ishii, F.; *Macromolecules*, **1997**, *30*, 1074-1078.

- (36) Burnett, L. J.; Muller, B. H. *J. Chem. Phys.* **1971**, *55*, 5829-5831.
- (37) Jelinski, L.W.; Dumais, J.J.; Engel, A.K. *Macromolecules*, **1983**, *16*, 492-496.
- (38) Yamazaki, S.; Muroga, Y.; Noda, I. *Langmuir*, **1999**, *15*, 4147-4149.
- (39) Mourey, T.; Le, K.; Bryan, T.; Zheng, S.Y.; Bennett G. *Polymer* **2005**, *46*, 9033-9042.
- (40) Vanhee, S.; Rulkens, R.; Lehmann, U.; Rosenauer, C.; Schulze, M.; Kohler, W.; Wegner, G. *Macromolecules* **1996**, *29*, 5136-5142

Chapter III: Chain Configuration of Substituted Stilbene Maleic Anhydride Alternating Copolymer Probed by Solid State NMR

III.1 Introduction

Functional polymers¹ carrying reactive functional groups that can participate in chemical processes have tremendous applications in a great variety of areas such as organic electronics², polymer-drug conjugates^{3,4} and biomaterials.⁵ The reactive groups can be incorporated along the main chain as pendant groups or as multiple chain ends in star or dendritic molecules. Because of the tolerance of free radical polymerization processes to functional groups, free radical polymerization is one of the most highly used methods for preparing functional polymers.

Alternating free radical polymerization with multi-substituted monomers is a convenient and powerful tool to construct highly functional polymeric materials.⁶ Multi-substituted monomers have the potential to raise the functionality density along the backbone and thus to increase the functional group concentration. Although multi-substituted monomers usually are nonhomopolymerizable, many of them can be polymerized via so called “alternating free radical polymerization”.⁶⁻¹⁰ Highly functional alternating copolymers can be produced by using functional electron-rich (donor) and electron-poor (acceptor) monomer pairs.^{11,12,31} The type of functional group, molecular weight, polymer architecture, the density of functional groups and stiffness of the polymer chain can be controlled using this strategy. Because of the alternating nature of the alternating free radical polymerization, regular placement of functional groups along the backbone, important for certain applications,¹³ is possible.

Solution NMR has been employed to investigate the chain configuration of many alternating copolymers since *cis* and *trans* configurations should have different ^1H and ^{13}C NMR signals. Olson and Butler used ^{13}C NMR spectroscopy to investigate the stereochemistry of the *N*-phenyl maleimide/2-chloroethyl vinyl ether alternating copolymers to elucidate the mechanism of the alternating free radical polymerization.¹⁴⁻¹⁷ After comparing the ^{13}C NMR spectra of the polymers with the corresponding model compounds, they concluded that the succinimide units mainly adopt the *cis* configuration indicating the significant participation of a donor-acceptor complex or “charge transfer complex” in the alternating copolymerization. However ^{15}N NMR spectroscopy of alkene/*N*-methyl maleimide copolymers and ^{13}C NMR spectroscopy of alkene/maleic anhydride copolymers showed mostly *trans* enchainment of the maleimide units.¹⁸⁻²⁰ All of the above studies relied on the comparison between the NMR spectra of model compounds and the polymers, where it is inherently difficult to assign the NMR signals correctly due to the broad signal, signal overlap, and small chemical shift differences.

During the last decade tremendous progress in the solid state NMR technique has made this technique valuable for the study of polymer structure.²¹⁻²³ Double quantum solid state NMR has been successfully used to determine the *cis/trans* chain configurations of various polymers.^{24,25} The torsional angle of isotopic labelled peptide segments also can be measured by solid state NMR.^{26,27} Among numerous solid state NMR methods, double quantum heteronuclear local field solid state NMR spectroscopy (2Q-HLF Solid State NMR) developed by Levitt ten years ago, is able to measure the torsional angle of a $^{13}\text{C}_2$ -labelled H-C-C-H moiety with a resolution of $\approx \pm 20^\circ$ in the neighborhood of the *cis* configuration and $\approx \pm 10^\circ$ in the neighborhood of the *trans*

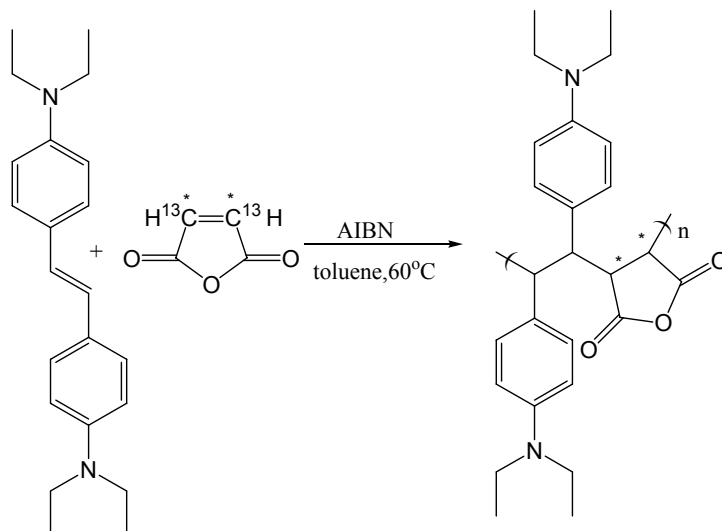
configuration.^{27,28} This technique is well suited for the study of the chain configuration in alternating copolymers avoiding the difficulties of solution NMR studies to determine the backbone stereochemistry. For this study, the N, N, N', N'-tetraethyl-4, 4'-diaminostilbene (TDAS) and maleic anhydride (MA) alternating copolymer was synthesized using ¹³C-labelled maleic anhydride and characterized following the procedure described elsewhere (scheme III.1).¹¹

III.2 Experimental Section

HCCH-2Q-HLF Solid State NMR exploits the evolution of the excited double-quantum coherence between the neighboring ¹³C spins in the presence of local heteronuclear ¹H-¹³C dipolar fields from the directly bonded ¹H spins.²⁷ The pulse sequence for the HCCH-2Q-HLF experiment is shown in Figure III.1A. After the cross-polarization pulse and a 90° pulse, the homonuclear recoupling sequence $R26_4^{11}$ creates double-quantum coherences which evolve under ¹H-¹³C dipolar couplings while suppressing ¹H-¹H dipolar couplings (FSLG) for a fraction of a rotation period (t_f). Then double-quantum coherences are reconverted to observable ¹³C magnetization by a second $R26_4^{11}$ block, with a standard double-quantum filtering phase cycle, followed by a 90° pulse. The experiments were performed at a magnetic field of 7.1 T and under magic-angle-spinning with a spinning frequency of $\nu_r = 3673$ Hz. The amplitude and duration of double-quantum excitation block $R26_4^{11}$ is 23.87 kHz (= 6.5 ν_r) and 1.09 ms (= 4 τ_r) respectively. The maximum Frequency-Switched Lee-Goldburg (FSLG) off-resonance (¹H offset frequency = ± 63.64 kHz; rf -pulse power $\nu_{rf} = 90$ kHz) spin-locking period to suppress ¹H-¹H homonuclear dipolar interaction during the double-quantum evolution

period is one τ_r , which is 15 times a t_l increment that corresponds to a basic FSLG unit, $(9.07 \mu\text{s})_0(9.07 \mu\text{s})_{180}$, where 0 and 180 designate rf -pulse phase of FSLG spin-locking pulse irradiation. The proton decoupling powers during $R26_4^{11}$ block and two-pulse phase modulated (TPPM) decoupling scheme²⁹ for signal acquisition are 80 kHz and 66 kHz, respectively. Total 2048 transient signals were accumulated for each t_l slice with acquisition delay for 2s on 30 mg of ^{13}C -labeled samples.

Scheme III.1 The synthesis of ^{13}C -labelled TDAS-MA alternating copolymer.



III.3 Results and Discussions

The torsional angle of the $\text{H}-^{13}\text{C}-^{13}\text{C}-\text{H}$ part of the anhydride ring is zero degrees (Figure III.1B), indicating the predominately *cis* configuration of the $\text{H}-^{13}\text{C}-^{13}\text{C}-\text{H}$ linkage of the anhydride ring. Considering the $\pm 20^\circ$ resolution of the torsional angle measurement of the 2Q-HLF Solid State NMR method, at least 80% of the $\text{H}-^{13}\text{C}-^{13}\text{C}-\text{H}$ part of the anhydride ring adopts the *cis* configuration. Olson and Butler have claimed

that the *cis* configuration results from the direct copolymerization of a charge transfer complex of the donor and acceptor comonomers.^{14-17, 30} Because of strong steric hindrance, the two bulky substituted phenyl groups of the stilbene should mainly adopt the *trans* configuration. Based on this assumption, a possible picture of the chain configuration of the TDAS-MA alternating copolymer is shown in Scheme III.2: the polymer backbone is highly kinked due to the predominately *cis* configuration of the **H-¹³C-¹³C-H** part of the anhydride ring. With such a structure, the functional groups are arranged in a regular way i.e. the diethylamino phenyl groups are on the two sides of the backbone plane and the anhydride groups are within the backbone plane. This spatial arrangement of functional groups along the backbone may open up opportunities for modification reactions that can lead to unique polymers with potentially useful properties. Currently we are actively pursuing targets derived from these structures.

When the amino groups are protonated and charged, they will experience strong electrostatic repulsion. If the above picture of the chain configuration of the TDAS-MA copolymer is correct, the electrostatic repulsion between the charged amino groups will rotate the polymer backbone to minimize the unfavorable repulsion, since they are concentrated on the both sides on the polymer backbone plane (Scheme III.3). When the anhydride ring is opened, such rotation of the polymer backbone will be possible and the torsional angle of the **H-¹³C-¹³C-H** moiety of the hydrolyzed anhydride will be changed. Dihedral angle measurement of the hydrolyzed TDAS-MA copolymer is consistent with this hypothesis. The ¹³C-labelled TDAS-MA copolymer was hydrolyzed in dilute HCl solution. The hydrolysis of the anhydride ring was confirmed by the disappearance of the peaks from the anhydride groups (1841 cm⁻¹ and 1772 cm⁻¹) and appearance of a strong

absorption peak associated with the free carboxylic acid (1721cm^{-1}) in the IR spectrum. The HCCH-2Q-HLF Solid State NMR spectrum of the dried hydrolyzed ^{13}C -labelled TDAS-MA copolymer is shown in Figure III.1C. The torsional angle of the $\text{H}-^{13}\text{C}-^{13}\text{C}-\text{H}$ moiety of the hydrolyzed anhydride groups appears to be 60° , indicating the significant rotation of the polymer backbone.

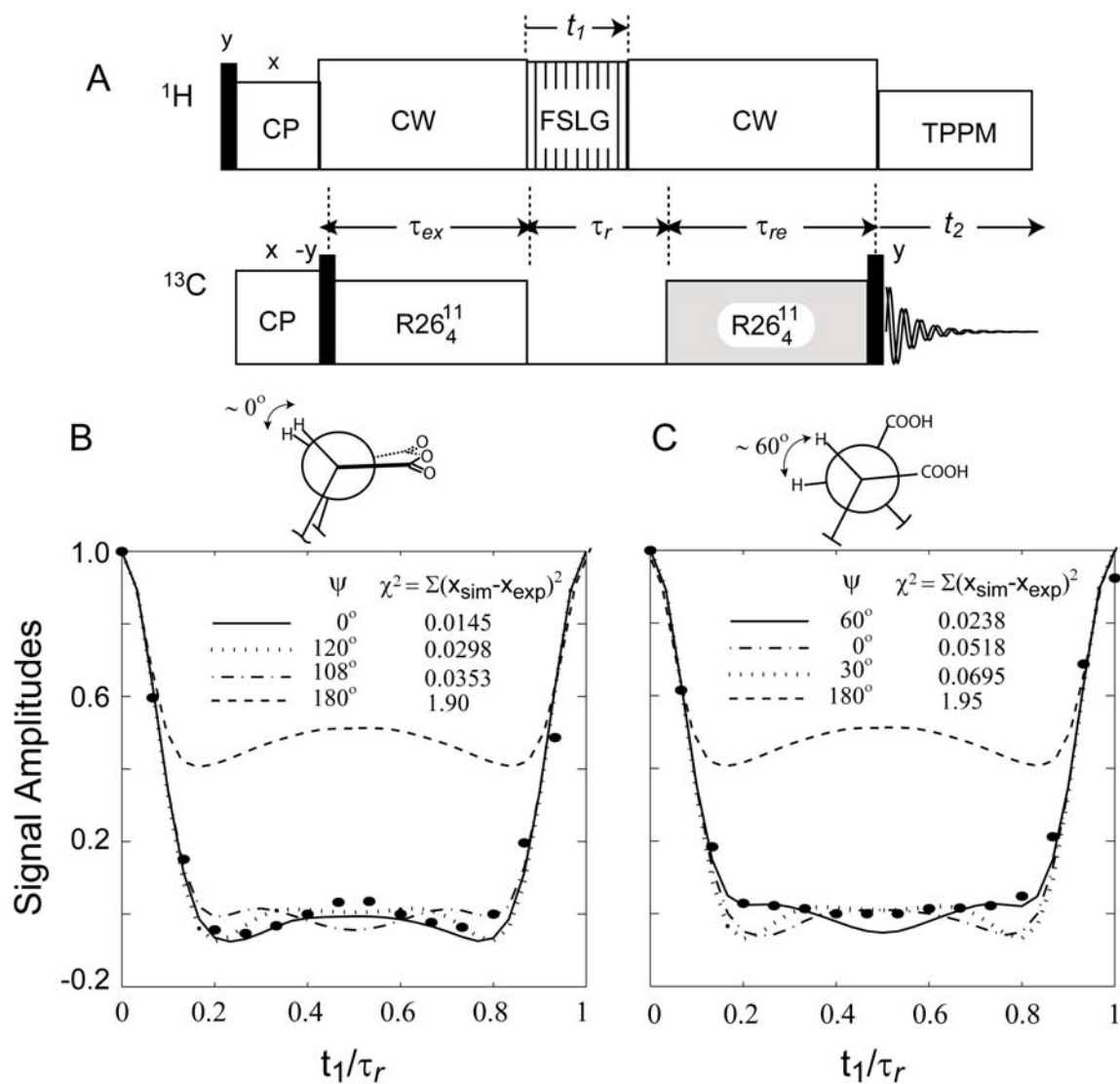
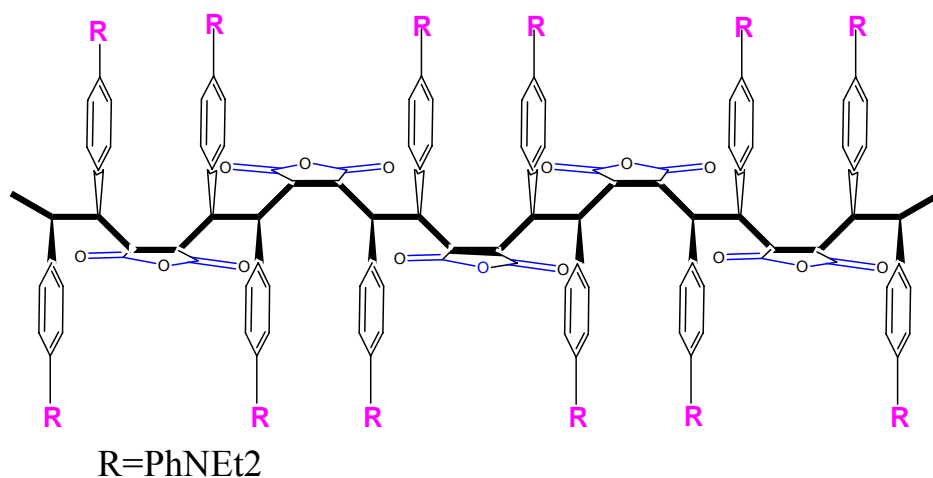


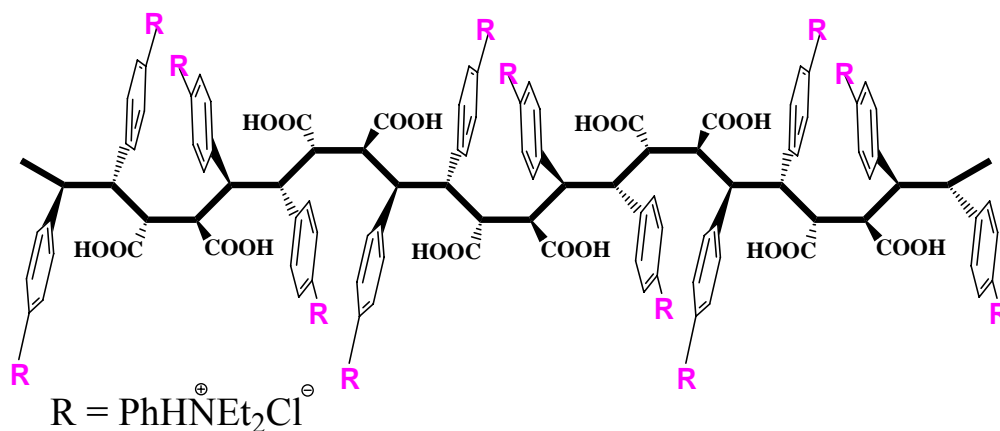
Figure III.1 Pulse sequence for HCCH-2Q-HLF experiment (A), and experimental data and simulations for the $^{13}\text{C}_2$ -labelled TDAS-MA alternating copolymer (B) and the

hydrolyzed $^{13}\text{C}_2$ -labelled TDAS-MA alternating copolymer (C) samples. A standard FSLG scaling factor, $k = 0.57$, has been used for our simulations. Simulation results with torsion angles of 0° and 60° provide best fit to the experimental data of the $^{13}\text{C}_2$ -labelled TDAS-MA alternating copolymer (B) and the hydrolyzed $^{13}\text{C}_2$ -labelled TDAS-MA alternating copolymer (C), respectively, as expected.

Scheme III.2 Possible chain configuration and spatial arrangement of the functional groups of the TDAS-MA alternating copolymer.



Scheme III.3 Possible chain configuration and spatial arrangement of the functional groups of the hydrolyzed TDAS-MA alternating copolymer.



III.4 Conclusions

In a conclusion, the result of the solid state NMR torsional angle measurement of the TDAS-MA copolymer has shown that the H-¹³C-¹³C-H linkages in the maleic anhydride units are enchainned in a predominately *cis* configuration. This could result in a chain structure that positions the diethylamino phenyl groups in an alternating arrangement on both sides of the plane of the backbone with the anhydride groups within the backbone plane. When the anhydride groups are hydrolyzed, there is a 60° rotation of the H-¹³C-¹³C-H linkage in the maleic anhydride units. Continuing studies include reacting the anhydride groups to precisely place various functional groups along the backbone and structure analysis of other examples of these stilbene copolymers.

References

- (1) Fréchet, J.M.J. *Science*, **1994**, *263*, 1710-1715.
- (2) Fréchet, J.M.J. *Prog. Polym. Sci.*, **2005**, *30*, 844–857.
- (3) Khandare, J.; Minko, T. *Prog. Polym. Sci.*, **2006**, *31*, 359–397.
- (4) Duncan, R. *Nature Reviews*, **2003**, *2*, 347-360.
- (5) Mammen, M.; Choi, S.K.; Whitesides G.M. *Angew. Chem. Int. Ed.* **1998**, *37*, 2754-2794.
- (6) Braun, D.; Hu, F.C. *Prog. Polym. Sci.*, **2006**, *31*, 239–276.
- (7) Zhang, X.; Li, Z.C.; Li, K.B.; Lin, S.; Du, F.S.; Li, F.M. *Prog. Polym. Sci.*, **2006**, *31*, 893–948.
- (8) Hall, H.K.; Padias, A.B. *J. of Polym. Sci.: A Polym. Chem.*, **2004**, *42*, 2845–2858.
- (9) Hall, H.K.; Padias, A.B. *J. of Polym. Sci.: A Polym. Chem.*, **2001**, *39*, 2069–2077.

- (10) Rzaev, Z.M.O. *Prog. Polym. Sci.*, **2000**, *25*, 163–217.
- (11) Mao, M.; Turner, S.R. *Polymer* **2006**, *47*, 8101-8105.
- (12) Mao, M.; Turner, S.R. *J. Am. Chem. Soc.* **2007**, *129*, 3832-3833.
- (13) Wulff, G.; Schauhoff, S. *J. Org. Chem.* **1991**, *56*, 395-400.
- (14) Olson, K.G.; Butler, G.B. *Macromolecules*, **1983**, *16*, 707-710.
- (15) Butler, G.B.; Olson, K.G.; Tu, C.L. *Macromolecules*, **1984**, *17*, 1884-1887.
- (16) Olson, K.G.; Butler, G.B. *Macromolecules*, **1984**, *17*, 2480-2486.
- (17) Olson, K.G.; Butler, G.B. *Macromolecules*, **1984**, *17*, 2487-2501.
- (18) Komber, H.; Jakisch, L.; Zschoche, S.; Mobus, H.; Ratzsch, M.; Scheller, D.
Makromol. Chem., Rapid Commun. **1991**, *12*, 547-552.
- (19) Ratzsch, M.; Zschoche, S.; Steinert, V.; Schlothauer, K. *Makromol. Chem.*, **1986**,
187, 1669-1679.
- (20) Komber, H. *Makromol. Chem. Phys.* **1995**, *196*, 669-678.
- (21) Duer, M.J. Ed. *Solid-state NMR spectroscopy Principles and Applications*,
Blackwell Science Ltd: Oxford, **2002**.
- (22) Schmidt-Rohr, K.; Spiess, H.W. Eds. *Multidimensional solid-state NMR and
Polymers*, Academic Press: London, **1994**.
- (23) Spiess, H.W. *J. of Polym. Sci.: A Polym. Chem.*, **2004**, *42*, 5031–5044.
- (24) Harris, D.J.; Bonagamba, T.J.; Hong, M.; Schmidt-Rohr, K. *Polymer* **2005**, *46*,
11737–11743.
- (25) Schmidt-Rohr, K.; Hu, W.; Zumbulyadis, N. *Science*, **1998**, *280*, 714-717.
- (26) Wi, S.; Sun, H.; Oldfield, E.; Hong, M. *J. Am. Chem. Soc.*, **2005**, *127*, 6451-6458.
- (27) Feng, X.; Eden, M.; Brinkmann, A.; Luthman, H.; Eriksson, L.; Graslund, A.;

- Antzutkin, O. N.; Levitt, M. H. *J. Am. Chem. Soc.*, **1997**, *119*, 12006-12007.
- (28) Feng, X.; Lee, Y.K.; Sandstrom, D.; Eden, M.; Maisel, H.; Sebald, A.; Levitt, M.H. *Chem. Phys. Lett.*, **1996**, *257*, 314-320.
- (29) Benett, A. E.; Rienstra, C. M.; Auger, M.; Lakshmi, K. V.; Griffin, R. G. *J. Chem. Phys.* **1995**, *103*, 6951-6958.
- (30) Mulliken, R.S.; Person, W.B. "Molecular Complex: A Lecture and Reprint Volume"; Wiley-Interscience: New York, **1969**.
- (31) Turner, S.R.; Anderson, C.C.; Kolterman, K.M. *J. of Polym. Sci.: C Polym. Lett.*, **1989**, *27*, 253-258.

Chapter IV: Synthesis and Properties of Rod-coil Block Copolymers

Containing Rigid Polyampholyte Blocks Based on N, N, N', N'-

Tetraalkyl-4, 4'-diaminostilbene and Maleic Anhydride

(Published as: Mao, M.; Turner, S. R. *J. Am. Chem. Soc.* **2007**, *129*, 3832-3833.)

IV.1 Introduction

The electrostatic interaction (neutralization) between a pair of oppositely charged blocks can act as the driving force for the formation of polyion complex (PIC) micelles and vesicles which combine properties of polyelectrolytes and block copolymer aggregates.¹⁻⁵ It has been suggested that these PIC aggregates could be used as controlled drug delivery systems and carriers of DNA for gene therapy.⁶ PICs are also employed to enhance the stability of polymeric aggregates.^{7,8} Since the driving force of the PIC formation is electrostatic attraction, the reported PIC aggregates are salt-sensitive and they fall apart as the salt concentration reaches a critical value.^{2,3} Chemical cross-linking can be employed to stabilize PIC aggregates.^{3,9} Another possible way to enhance the stability is to increase the rigidity of the polyelectrolyte backbones since attractive interactions are possible between stiff polyelectrolytes.¹⁰⁻¹²

Recently, the synthesis of rigid pH responsive polyampholytes via alternating copolymerization of *N,N,N',N'*-tetraalkyl-4,4'-diaminostilbenes (TDAS) with maleic anhydride and the subsequent hydrolysis of the anhydride groups was reported.¹³ In this contribution, the synthesis of novel rod-coil block copolymers containing the polyampholyte based on *N,N,N',N'*-tetraethyl-4,4'-diaminostilbene and a poly(methoxy-capped oligo- (ethylene glycol)methacrylate) (OEGMA) block for the investigation of the

aggregation process driven by electrostatic interactions between the rigid polyampholyte blocks is given. To the best of our knowledge, this is the first study of the solution properties of rigid polyampholyte based rod-coil block copolymers. Rigid polyampholytes exhibit intriguing differences from flexible ones.¹⁴

IV.2 Experimental Section

General considerations. All reagents were purchased from Aldrich and were used as received. HPLC grade water was used for the preparation of aqueous solutions in this study. ¹H NMR spectra were determined at 25°C in CDCl₃ at 400 MHz with a Varian Unity spectrometer. IR spectra were recorded with a MIDAC M2004 FT-IR spectrophotometer in the reflection mode. pH measurements were performed using an Oakton pH1100 pH meter.

Zeta potential measurements were performed using a MALVERN Zetasizer (Nano ZS, ZEN3600) with a He-Ne laser ($\lambda = 632.8$ nm) and a folded capillary cell (DTS1060). pH of the solutions (polymer concentration is around 10 mg/mL with 1-3 mmol/L NaCl) was checked before the zeta potential measurements.

Synthesis of double hydrophilic block copolymers. The synthesis of N, N, N', N'-tetraethyl-4, 4'-diaminostilbene was described elsewhere.¹³ Poly(ethylene glycol) methyl ether methacrylate (methoxy-capped oligo(ethylene glycol) methacrylate (OEGMA), average Mn ~ 300) was purified by filtration through neutral alumina to remove inhibitors. The chain transfer agent cumyl dithiobenzoate (CDB) was synthesized following a published procedure.²¹

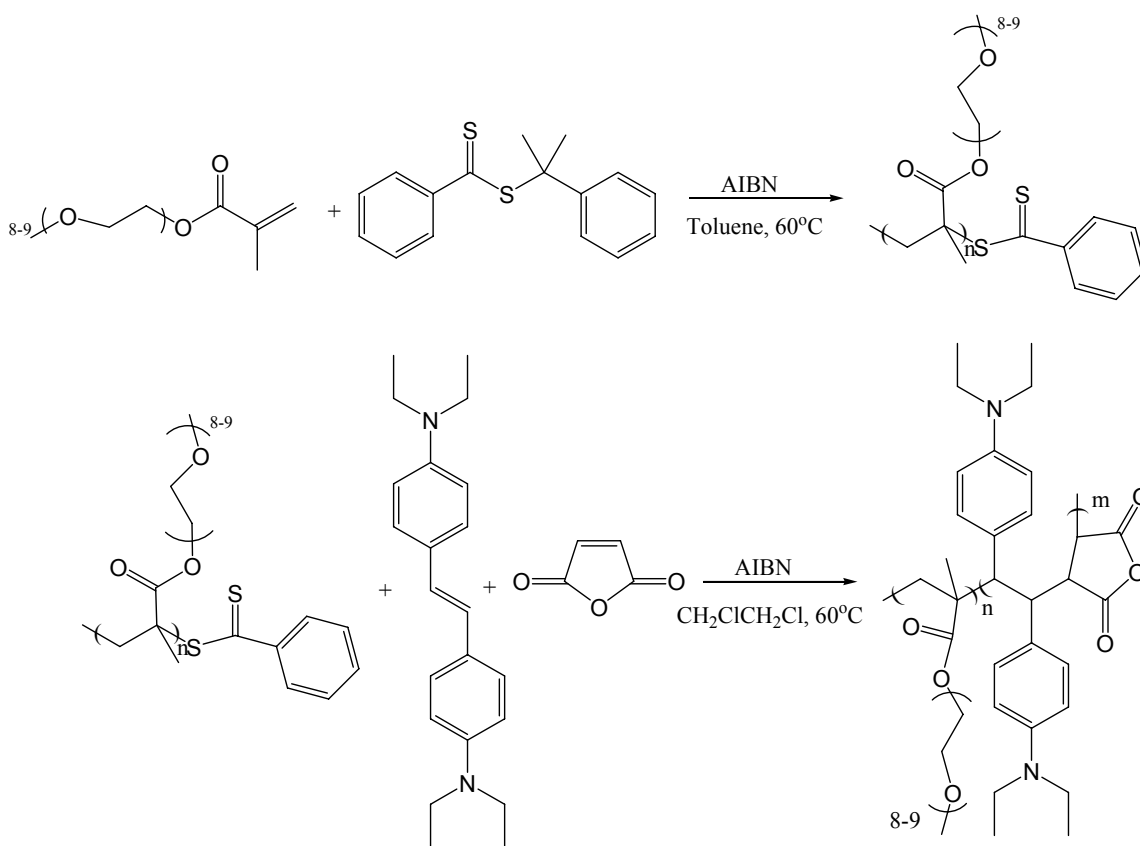
The rod-coil block copolymers were synthesized by reversible addition-fragmentation chain transfer (RAFT) polymerization using cumyl dithiobenzoate as the chain transfer reagent (Scheme IV.1).

The polyOEGMA blocks were synthesized first and used as the macro RAFT agents for the polymerization of the second polyampholyte block. Toluene was used as solvent for the RAFT polymerization of the polyOEGMA block. 2, 2'-azobisisobutyronitrile (AIBN) was used as initiator and its concentration was kept to half of the chain transfer agent. The OEGMA (~20 wt%), AIBN, cumyl dithiobenzoate and toluene was mixed together in a 50-mL, septum sealed glass bottle equipped with a magnetic stirrer. The mixture was degassed by purging with argon for 20 min and polymerized at 60 °C for 16 hours. The polymers were then isolated by precipitation into hexane. The collected crude products were re-dissolved into chloroform and precipitated in hexane. The cycle was repeated three times to remove the unreacted monomers. All polymers were dried in the vacuum oven at 60°C overnight before characterization.

The block copolymerizations were performed using polyOEGMA as a macromolecular chain transfer agent. The polyOEGMA, N, N, N', N'-tetraethyl-4, 4'-diaminostilbene, maleic anhydride, AIBN and 1, 2-dichloroethane were mixed together in a 50-mL, septum sealed glass bottle equipped with a magnetic stirrer. All of the polymerizations contained an equal molar ratio of N, N, N', N'-tetraethyl-4, 4'-diaminostilbene and maleic anhydride. The mixture were degassed by purging with argon for 20 min and polymerized at 60 °C for 18 hours. The copolymers were then isolated by precipitation in hexane. The collected crude products were re-dissolved into chloroform and precipitated in a hexane/chloroform (3:1) mixture. The cycle was repeated three

times to remove the unreacted monomers. All polymers were dried in a vacuum oven at 60°C overnight before characterization. Two peaks associated with the anhydride groups of the copolymers (1841 cm^{-1} and 1772 cm^{-1}) were clearly observed in the IR spectrum, and the peak from the free carboxylic acid groups was absent. The IR spectra of the unhydrolyzed and hydrolyzed double hydrophilic block copolymer (OBGMA₂₆-*b*-TDASMA₃₁) are shown in Figure IV.1.

Scheme IV.1 Synthesis of the rod-coil block copolymers (DHBCs).



Molecular weight determination. Molecular weights of synthesized polymers were determined using size exclusion chromatography (SEC) using a Waters 717 Autosampler equipped with three in-line PLgel 5 mm Mixed-C columns, a Waters 410 RI detector, a Viscotek 270 dual detector, and an in-line Wyatt Technology miniDAWN

multiple angle laser light scattering (MALLS) detector. The dn/dc values were determined on-line using the calibration constant for the RI detector and the mass of the polymer sample. SEC measurements were performed at 40 °C in tetrahydrofuran at a flow rate of 1.0 mL/min. For all samples, it was assumed that 100% of the polymer eluted from the column during the measurement.

Table IV.1 Compositions, molecular weights and molecular-weight distributions of segments and block copolymers.

entry	structure	M_n	M_w/M_n
1	OEGMA ₂₆	7860	1.09
2	OEGMA ₁₀₅	31600	1.15
3	OEGMA ₂₆ - <i>b</i> -TDASMA ₃₁	20800	1.23
4	OEGMA ₁₀₅ - <i>b</i> -TDASMA ₃₈	47600	1.14

Dynamic light scattering experiments. Dynamic light scattering measurements were performed using a Malvern CGS-3 light scattering instrument equipped with a He-Ne linear polarized laser ($\lambda= 632.8$ nm) and an ALV-5000/EPP Multiple Tau Digital Correlator. The samples were kept at constant temperature (25.0 °C) during all the experiments. The concentration of the polymer for all samples was kept constant at 1 mg/mL. Quartz cells with 10 mm diameter were used for the measurements. The cells were cleaned in a 3:1 (v/v) mixture of concentrated H₂SO₄ and 30% H₂O₂ at ~ 80 °C for 1 h. *Caution: this mixture reacts violently with organic materials and must be handled with great care.* The cells were further freed from dust via the acetone vapor rinse method. The minimum sample volume required for the experiment was 1 mL. The data

acquisition was done with the ALV-Correlator Control Software, and the counting time was set to 300 s. The intensity-intensity time correlation functions were analyzed by means of CONTIN method to obtain distributions of hydrodynamic radii of the PIC aggregates. The Cumulant method was employed to determine the average R_h of the PIC aggregates.

Hydrolysis of rod-coil block copolymers. The rod-coil block copolymers were dissolved in dilute HCl solution (pH 3) and aged for two hours for the complete hydrolysis of the anhydride groups. The hydrolysis of OEGMA was checked with ^1H and ^{13}C NMR. In order to avoid the effect of H_2O on the NMR experiments, we prepared 0.001M H_2SO_4 in D_2O and monitored the ^1H and ^{13}C NMR of the OEGMA block under the same conditions used for the preparation of the rod-coil block copolymer samples. We did not observe any change on the ^1H and ^{13}C NMR of the OEGMA block, indicating that hydrolysis of the methacrylate groups in the polyOEGMA block is insignificant during the hydrolysis of the anhydride groups.

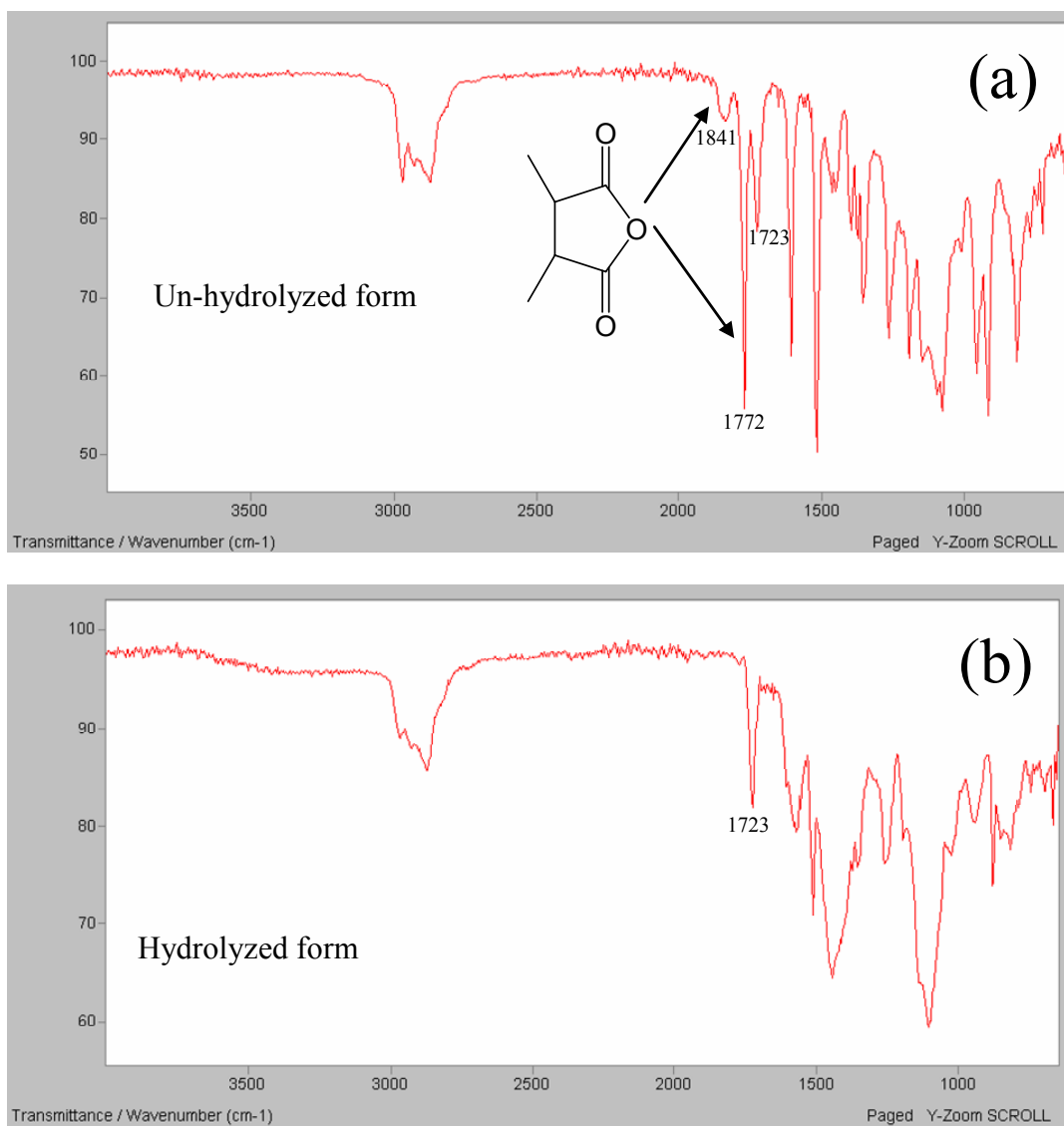


Figure IV.1 IR spectra of the un-hydrolyzed form (a) and hydrolyzed form (b) of OBGMA₂₆-*b*-TDASMA₃₁.

IV.3 Stimuli Responsive Aggregation of Rod-coil Block Copolymers Containing Rigid Polyampholyte Blocks Based on N, N, N', N'-Tetraalkyl-4, 4'-diaminostilbene and Maleic Anhydride

The rod-coil block copolymers were dissolved in dilute HCl solution (pH 3) and aged for 2 h for the complete hydrolysis of the anhydride groups. To locate the isoelectric

point (IEP), the ζ -potential of the polymeric aggregates was monitored as a function of pH (Figure IV.2). A simple acid-base equilibrium calculation¹⁵ shows that theoretical IEP is 5.9 at which point 80% of the amine and carboxylate acid groups are charged, (pKas 4.16 and 5.61 for succinic acid and 6.61 for *N,N*-diethylaniline). The experimental IEP of the polyampholyte was found to be around 5.7, very close to the theoretical value.

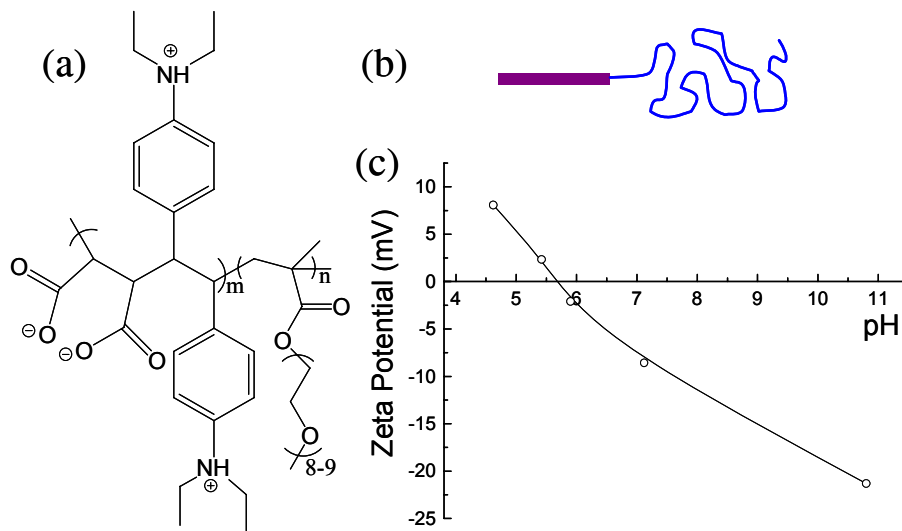


Figure IV.2 (a) Structure of the block copolymers. (b) Rod-coil type structure. (c) ζ -potential of the PIC aggregates at different pH .

For PIC aggregates from oppositely charged PEG-poly(amino acid) block copolymers, the charged segments must have matched chain lengths to diminish the electrostatic repulsion from excess charges.⁴ For block copolymers, the PIC aggregates can still exist when pH deviates from the IEP by about 1 unit ($5 < \text{pH} < 7$), where the rigid polyampholyte segments are net positively or negatively charged. The hydrodynamic radii (R_h) of the polymeric aggregates formed from OEGMA₂₆-*b*-TDASMA₃₁ as a function of pH were monitored by dynamic light scattering (DLS) (Figure IV.3a). The R_h of the aggregates was pH dependent and reached a maximum

around the IEP. At low (pH 3) and high pH (pH 10.8) conditions, the polymer was highly positively or negatively charged and no aggregates were observed. As the pH approached the IEP, the rod-coil block copolymers started to form polymeric aggregates where the polyampholyte blocks form the core surrounded by a polyOEGMA corona (Figure IV.3b). At pH 5.5, close to the IEP, a bimodal distribution of the PIC aggregates was observed, indicating the incomplete transition of the PIC aggregates which was also observed in other polymer systems.¹⁶ The pH responsive aggregation was also observed for OEGMA₁₀₅-*b*-TDASMA₃₈ with a longer OEGMA block (Table IV.2). The effect of pH change is much weaker when the OEGMA block is larger.

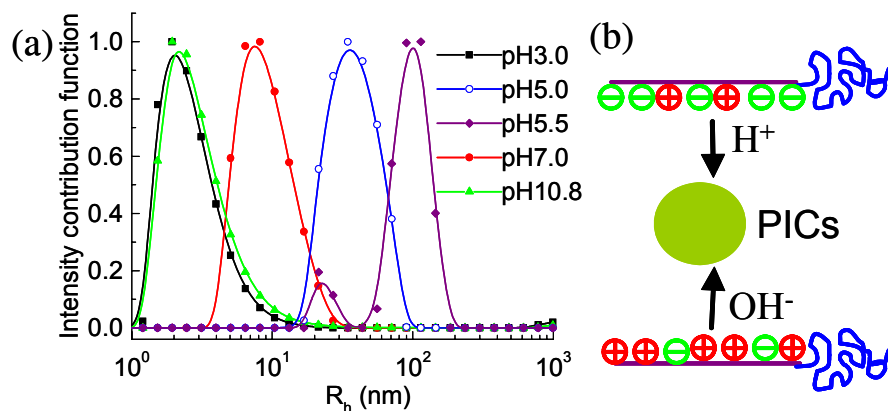


Figure IV.3 (a) R_h distributions of PICs formed by OEGMA₂₆-*b*-TDASMA₃₁ at different pH without the addition of salt; (b) a schematic of pH responsive aggregation of rod-coil block copolymers.

Table IV.2 Intensity average R_h (Cumulant analysis) of the PIC aggregates formed from the DHBCs under different conditions.

pH	pH = 3	pH = 10.8	pH = 7		pH = 5.5	
Concentration of NaCl	0.1M	0.1M	0.01M	0.5M	0.01M	1.0M
OEGMA ₁₀₅ - <i>b</i> -TDASMA ₃₈ R_h (nm)	6±1	6±1	12±1	17±1	15±1	21±1
OEGMA ₂₆ - <i>b</i> -TDASMA ₃₁ R_h (nm)	4±1	5±1	9±1	430±10	80±5	turbid

The aggregation process was also affected by the addition of NaCl. PIC aggregates did not dissociate upon the addition of salt but grew with increasing salt concentration. For OEGMA₂₆-*b*-TDASMA₃₁ at pH 7, 25 °C, and 0.3 M NaCl, larger aggregates with R_h around 150 nm were observed in addition to the smaller aggregates (Figure IV.4a). After increasing the salt concentration to 0.5 M, the smaller aggregates were undetectable and the larger aggregates grew to an average R_h around 500 nm. When the salt concentration was increased to 1.0 M, the solution became turbid. For OEGMA₁₀₅-*b*-TDASMA₃₈, the effect of added salt is much weaker (Table IV.2).

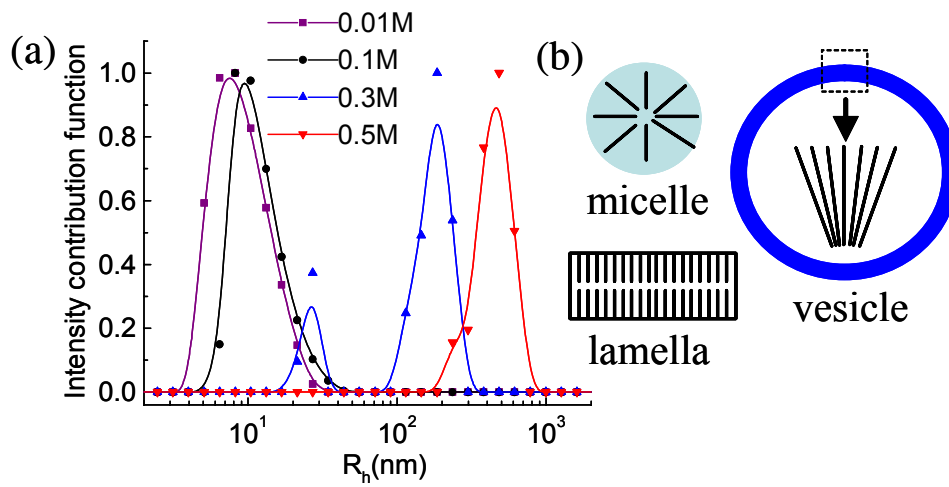


Figure IV.4 (a) Effect of added NaCl on PICs formed by OEGMA₂₆-*b*-TDASMA₃₁ at pH 7; (b) a schematic of rigid rods packing for various aggregates.

The aggregation of the rigid charge-imbalanced polyampholyte segments indicates the existence of attractive interchain interactions, significantly different from flexible polyampholytes. For example, charge-imbalanced flexible polyampholytes are soluble through electrostatic repulsions.¹⁵ Like-charge attractions between rod-like polyelectrolytes are relevant to a wide range of colloidal and biomedical processes and

have been observed in various systems, such as DNA forming bundles in the presence of divalent counterions.¹⁷ The attractive interactions are suggested to originate from positional counterion correlations, similar to van der Waals interactions: a rigid polyelectrolyte chain with condensed divalent counterions can be treated as a charged rigid polyampholyte (Figure 1 in ref 11), and strong dipole-dipole attractions can overcome repulsions from the net charges on the rods.^{10,11} Added univalent salt reduces the effective charge on the rods, while the binding of multivalent ions is unchanged, giving rise to the increase in the net effective attraction.¹⁸ A detailed discussion of like-charge attraction is given in the next section.

The same picture is also applicable for the rigid polyampholytes. Negative and positive charges attached to the rigid polyampholyte backbones will impart large dipoles, thereby inducing strong attractions between them.¹⁹ Since the acid-base equilibrium is mainly dependent on the solution pH, the addition of NaCl will not change the surface charge on the polyampholyte blocks but the effective charge will be reduced. As stated above, added NaCl will increase the net effective attraction and therefore promote the aggregation of the rigid polyampholyte blocks.

The effect of NaCl on the water solubility of the TDASMA alternating copolymer was also studied. The TDASMA alternating copolymer is soluble in water when the pH is lower than 4.9. At pH 4.8 the polymer solution remained clear. However with the addition of **ONLY** 0.03M NaCl at this pH, the clear solution turned turbid. Further increasing the salt concentration to 1.0M did not lead to resolubilizing the polymer to a clear solution. When the pH of the solution was adjusted to 2.0 or 12.5, the turbid solution with 0.03M NaCl became clear. Hydrophobic polyelectrolytes can become

insoluble in water with the addition of salt. This is often termed as “salting out”, due to the increased polarity of the aqueous solution. These observations indicate that this is not the case for the TDASMA homopolymer. At pH 12.5 all of the dialkyl amino groups of the stilbene derived units are deprotonated and noncharged. This should be the most hydrophobic state of this alternating copolymer. However the TDASMA alternating copolymer is insoluble at pH 4.8 with the addition of 0.03M NaCl but soluble at pH 12.5 with the same amount of NaCl. This indicates that at pH 4.8 TDASMA became insoluble in water with the addition of 0.03M NaCl due to reduced electrostatic repulsions instead of the increased polarity of the aqueous solution. This observation suggests that the effect of the salt on the rod-coil blocks in this manuscript is NOT a result of “salting out” the TDASMA blocks.

Since a “salting out” phenomenon was observed for PEG²², the salt responsive behavior of the polyOEGMA segment was studied. For this purpose, the R_h of a polyOEGMA homo-polymer with $M_w = 60000$ g/mole was monitored as a function of salt concentration. The solution stayed clear with the addition of 1M NaCl and the R_h of the polymer chain did not change, excluding the possibility of salting out triggering the salt responsive aggregation of these copolymers.

Figure IV.4b shows different ways that rods can pack in aggregates. Denser packing will favor the formation of larger aggregates.¹⁹ For example, vesicles instead of micelles become the predominant aggregates for block copolymers with a rigid block.²⁰ Adding salt or adjusting pH close to the IEP will diminish the electrostatic repulsions to allow the polyampholyte segments to pack more densely, thereby increasing the size of the PIC aggregates. Interplay between electrostatic interactions and block length can

affect the aggregation process. Longer polyOEGMA blocks will occupy more volume and interfere with the packing of polyampholyte blocks. Consequently, OEGMA₁₀₅-*b*-TDASMA₃₈ will form smaller aggregates, and the effects of pH and added salt are much weaker compared to OEGMA₂₆-*b*-TDASMA₃₁.

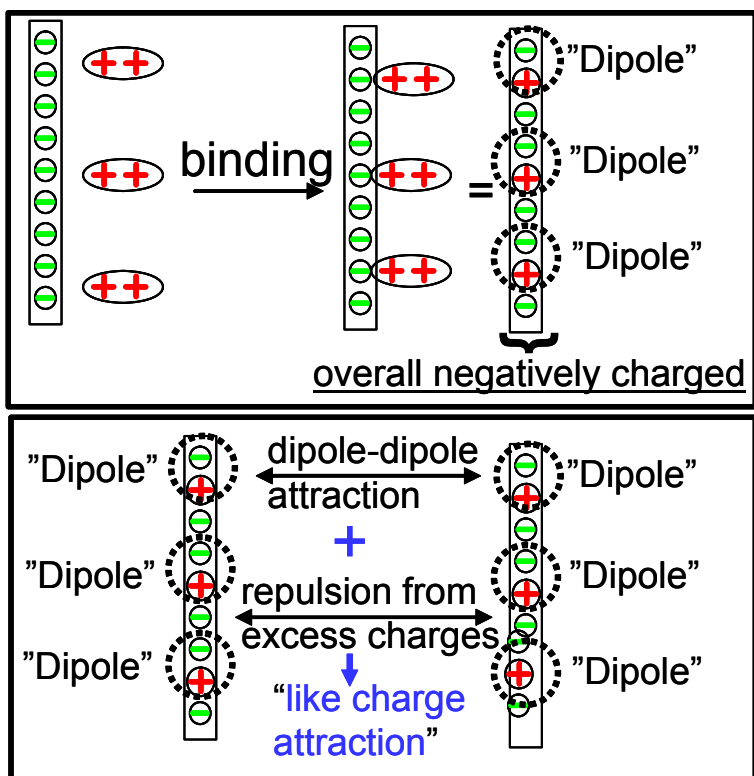
IV4. Detailed Discussion of Like Charge Attraction Between Rigid Polyampholytes

It is generally true that like-charges repel and the unlike ones attract each other. But it is found that under certain conditions like-charged colloids can attract one another, which is counter intuitive. Like-charge attractions between rod-like polyelectrolytes are relevant to a wide range of colloidal and biomedical processes and have been observed in various systems. It is also very important in biological systems and one particular example is the DNA condensation. In aqueous solution DNA is highly negatively charged, one negative charge every 1.7Å°. Some viruses use multivalent cations to pack over a meter of highly charged DNA into a nucleus of few micrometers. The multivalent counterions must induce attraction between the highly negatively charged DNA chains. This effect is termed as “like-charge attraction” and is still not fully understood and an active debate is ongoing about the precise mechanism that induces such attractions.

The widely used mean-field theory of electrostatic interactions between macroions, the Poisson-Boltzmann (PB) theory, predicts that two parallel cylinders with the same charge always repel each other. Various theories have been developed to account for the like-charge attraction.^{10-12, 17,18} It is generally accepted that the like-charge attraction is due to some form of positional counter-ion correlations.¹⁷ A “dipole” model has been used to illustrate the electrostatic origin of the like-charge attraction.¹¹ The

attractive interactions are suggested to originate from positional counterion correlations, similar to “van der Waals” interactions: a rigid polyelectrolyte chain with condensed divalent counterions can be treated as a charged rigid polyampholyte, and strong dipole-dipole attractions can overcome repulsions from the net charges on the rods. Scheme IV.2 is used to illustrate the origin of like charge attraction between rigid polyelectrolyte chains. Scheme IV.2 is based on figure 1 in Reference 11:

Scheme IV.2 A schematic of the origin of like-charge attraction between rigid polyelectrolyte chains with the presence of divalent counterions.

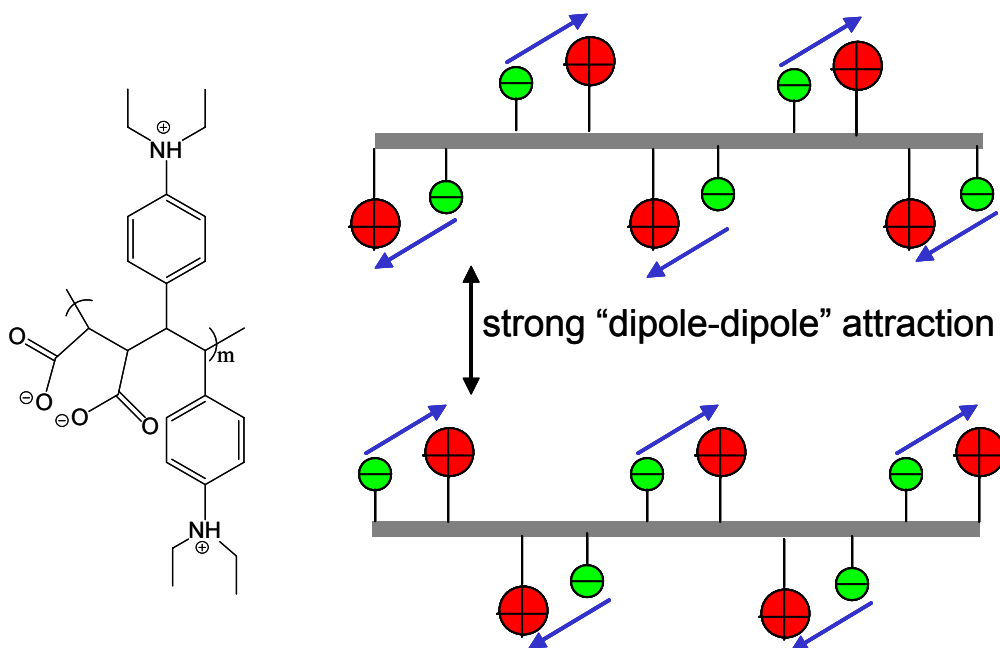


Recently Gelbert et al. theoretically addressed the effect of 1:1 salts on like-charge attractions.¹⁸ The addition of 1:1 salts would reduce the effective charge on the rods and thus screen the repulsion from the excess charges. The binding of the multivalent counterions onto the rods remains unaffected. So overall, the attractive

interaction between charged rods would be enhanced by the addition of 1:1 salts. There is no experimental evidence published that confirms this theoretical prediction.

The negatively charged rods with divalent counterions illustrated in Scheme IV.2 are treated as rigid “polyampholytes” for the theoretical calculations. The aggregation of the rigid charge-imbalanced polyampholyte segments in our study indicates the existence of attractive inter-chain interactions, significantly different from flexible polyampholytes.¹⁶ For example, charge-imbalanced flexible polyampholytes are soluble through electrostatic repulsions.¹⁶

Scheme IV.3 A schematic of the origin of like-charge attraction between rigid polyampholyte chains.

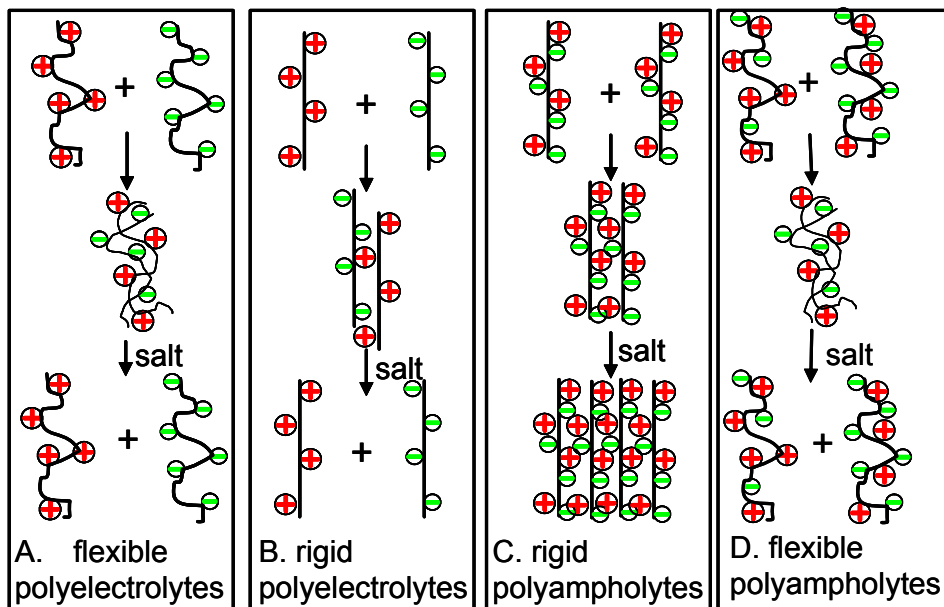


The attractive inter-chain interaction originates from the like-charge attraction.

Scheme IV.3 shows the structure of the rigid polyampholyte. Negative and positive

charges attached to the rigid polyampholyte backbones will impart large dipoles thereby inducing strong attractions between them. Since the acid-base equilibrium is mainly dependent on the solution pH, the surface charge of the polyampholyte blocks will not be changed but the effective charge will be reduced by the addition of NaCl. As stated above, added NaCl will increase the net effective attraction and therefore promote the aggregation of the rigid polyampholyte blocks. This salt effect is totally different from that on flexible charged polymers. For example flexible polyampholytes become soluble at IEP upon the addition of certain amount of salt.¹⁶ In Scheme IV.4 the effects of salt on the PIC aggregates formed by polyelectrolytes with different chain structures are compared. The rigid polyampholyte has a unique response to added salt.

Scheme IV.4 A schematic of the effects of salt on the PIC aggregates formed by polyelectrolytes with different chain structures.



IV5. Conclusions

In summary, novel rod-coil block copolymers containing rigid polyampholyte segments were synthesized and investigated. The chain rigidity has a dramatic effect on the electrostatic interactions between polyelectrolytes. The PIC aggregates formed from these rod-coil block copolymers were found to be responsive to pH changes and added salt. The unique solution properties of the rigid polyampholytes are induced by the like-charge attractions imparted by the rigid chains.

References

- (1) Lutz, J.F. *Polymer International* **2006**, *55*, 979-993, and references therein.
- (2) Kabanov, A.V.; Bronich, T.K.; Kabanov, V.A.; Yu, K.; Eisenberg, A. *Macromolecules* **1996**, *29*, 6797-6802.
- (3) Kakizawa, Y.; Harada, A.; Kataoka, K. *J. Am. Chem. Soc.* **1999**, *121*, 11247-11248.
- (4) Harada, A.; Kataoka, K. *Science* **1999**, *283*, 65-67.
- (5) Koide, A.; Kishimura, A.; Osada, K.; Jang, W.D.; Yamasaki, Y.; Kataoka, K. *J. Am. Chem. Soc.* **2006**, *128*, 5988-5989.
- (6) Nishiyama, N.; Kataoka, K. *Adv. Polym. Sci.* **2006**, *193*, 67-101.
- (7) Li Y.T.; Lokitz B.S.; McCormick, C.L. *Angew. Chem. Int. Ed.* **2006**, *45*, 5792-5795.
- (8) Weaver, J.V.M.; Tang, Y.Q.; Liu, S.Y.; Iddon, P.D.; Grigg, R.; Billingham, N.C.; Armes, S.P.; Hunter, R.; Rannard, S.P. *Angew. Chem. Int. Ed.* **2004**, *43*, 1389-1392.
- (9) Bronich, T. K.; Keifer, P. A.; Shlyakhtenko, L. S.; Kabanov, A. V. *J. Am. Chem. Soc.* **2005**, *127*, 8236-8237.

- (10) Jensen, N.G.; Mashl, R.J.; Bruinsma, R.F.; Gelbart, W.M. *Phys. Rev. Lett.* **1997**, *78*, 2477-2480.
- (11) Ha, B.Y.; Liu, A.J. *Phys. Rev. Lett.* **1997**, *79*, 1289-1292.
- (12) Ray, J.; Manning, G.S. *Langmuir*, **1994**, *10*, 2450-2461.
- (13) Mao, M.; Turner, S.R. *Polymer* **2006**, *47*, 8101-8105.
- (14) Tsitsilianis, C.; Gotzamanis, G. *Macromol. Rapid Commun.* **2006**, *27*, 1757-1763.
- (15) Bhargava, P.; Tu Y. F.; Zheng, J.X.; Xiong, H.M.; Quirk, R.P.; Cheng, S.Z.D. *J. Am. Chem. Soc.* **2007**, *129*, 1113-1121.
- (16) Lowe, A.B.; McCormick, C.L. *Chem. Rev.* **2002**, *102*, 4177-4189.
- (17) Angelin, T.E.; Liang, H.J.; Wriggers, W.; Wong, G.C. *Proc. Natl. Acad. Sci. USA* **2003**, *100*, 8634-8637, and references therein.
- (18) Lee, K.C.; Borukhov, I.; Gelbart, W.M.; Liu, A.J.; Stevens, M.J. *Phys. Rev. Lett.* **2004**, *93*, 128101.
- (19) Israelachvili, J. *Intermolecular and Surface Forces*, Academic Press, London, 1992.
- (20) Antonietti, M.; Forster, S. *Adv. Mater.* **2003**, *15*, 1323-1333.
- (21) Moad, G.; Chiefari, J.; Krstina, J.; Postma, A.; Mayadunne, R. T. A.; Rizzardo, E.; Thang, S. H. *Polym. Int.* **2000**, *49*, 993-1001.
- (22) Hey, M.J.; Jackson, D.P.; Yan, H. *Polymer* **2005**, *46*, 2567-2572.

Chapter V: Rigid Charged Polyelectrolytes Based on Alternating

Copolymers from Substituted Stilbene Monomers

V.1 Introduction

Polyelectrolytes combine properties of polymer and electrolytes, play very important roles in nature, and have broad applications in various industrial processes. Many experimental¹ and theoretical² studies of the solution and bulk state properties of polyelectrolytes have been reported. The complexity of the properties of polyelectrolytes originates from a combination of many variables such as chemical structure of the polymer backbone, molecular weight, chain architecture, the type, concentration and distribution of the ionic groups and different solution conditions in which these polymers are studied. Usually these parameters are interrelated with each other and make the task of understanding the effect of each individual parameter formidable. Recently polyelectrolytes with well-defined structures have been synthesized to simplify the situation and assist in the understanding of structure-property relationship.³

Electrostatic interactions determine the properties of polyelectrolytes both in solution and in bulk.² Chain conformations of flexible polyelectrolytes are dominated by long range Coulombic forces between charged species which are also strongly affected by the conformational change of the polymer backbones.² Rigid polyelectrolytes maintain the same chain conformation regardless of the variation of electrostatic interactions, allowing the investigation only of the effects of Coulombic interactions on the solution properties of polyelectrolytes.⁴⁻⁸ The study of rigid polyelectrolytes can help develop a better understanding of the fundamental properties of these highly charged macromolecules.

Biological rigid polyelectrolytes such as DNA are found in nature.⁹ The most reported synthetic rigid polyelectrolytes are based on poly(p-phenylene) synthesized by Pd-catalyzed aryl-aryl coupling reactions.^{4,7,10,11,12} Solubilizing side chains usually are required to enhance the solubility of the poly(p-phenylene) precursors in organic solvents. Usually the long alkyl solubilizing side chains induce additional hydrophobic interactions between the polyelectrolyte chains when the rigid polyelectrolytes are dissolved in water.^{6,8,13}

Since free radical polymerization is tolerant to many kinds of functional groups,¹⁴ it is possible to synthesize rigid polyelectrolytes via free radical polymerization. For example rigid dendronized polymers^{15,16} have been synthesized by free radical polymerization and can be converted into rigid polyelectrolytes.^{17,18,19} Recently the synthesis of rigid polyampholytes based on N, N, N', N'-tetraalkyl-4, 4'-diaminostilbenes (TDAS) and maleic anhydride (MA) via free radical polymerization was reported.²⁰ Based on this strategy the synthesis and properties of rod-coil block copolymers containing rigid polyampholyte segments using RAFT controlled free radical polymerization was also reported.²¹ Here the facile synthesis of rigid anionic and cationic polyelectrolytes based on the alternating copolymers of substituted stilbenes is presented. The synthetic schemes of the rigid polyelectrolytes are shown below.

V.2 Experimental Section

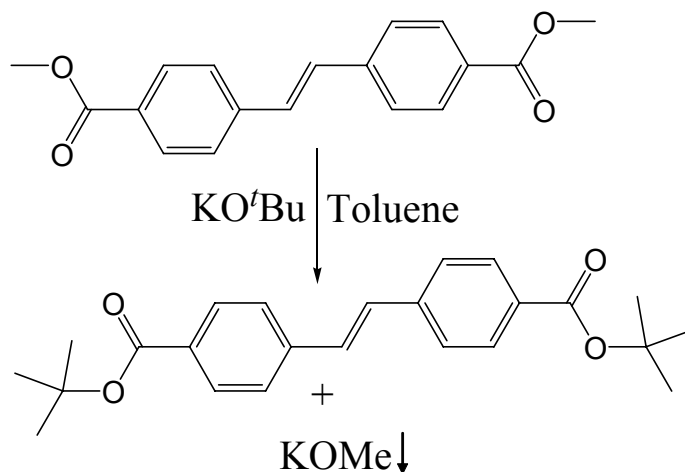
Reagents and analyses. All reagents were purchased from Aldrich and were used as received. The synthesis of N, N, N', N'-tetraethyl-4, 4'-diaminostilbene was described in Chapter II. ¹H and ¹³C NMR spectra were determined at 25°C in CDCl₃ at 400 MHz

with a Varian Unity spectrometer. IR spectra were recorded with a MIDAC M2004 FT-IR spectrophotometer in the reflection mode. The elemental analysis was done by Atlantic Microlab, Inc. (Norcross, Georgia). Thermogravimetric analysis (TGA) was conducted under nitrogen, from 25 to 600 °C at a heating rate of 10 °C using a TA Instrument TGA 295. Molecular weights of synthesized polymers were determined using size exclusion chromatography (SEC) using a Waters 717 Autosampler equipped with three in-line PLgel 5 mm Mixed-C columns, Waters 410 RI detector, Viscotek 270 dual detector, and in-line Wyatt Technology miniDAWN multiple angle laser light scattering (MALLS) detector. The dn/dc values were determined on-line using the calibration constant for the RI detector and the mass of the polymer sample. SEC measurements were performed at 40 °C in tetrahydrofuran at a flow rate of 1.0 mL/min.

Synthesis of di-*t*-butyl-trans-4,4'-stilbenedicarboxylate (DTBES). Dimethyl-trans-4,4'-stilbenedicarboxylate (DMES) was received as a gift from Eastman Chemical Company and is highly insoluble in most organic solvents. The ester exchange method was used to convert the methyl ester into the more soluble *t*-butyl ester derivative.²² The ester exchange reaction was driven by the precipitation of potassium methoxide (KOMe) (Scheme V.1). A typical procedure to prepare di-*t*-butyl-trans-4,4'-stilbenedicarboxylate is as follows: to a suspension of dimethyl-trans-4,4'-stilbenedicarboxylate (0.77g, 2.6mmol) in toluene (15ml) heated in a oil bath at 110°C was added KOtBu (1.0M in THF, 10ml) slowly over 10 minutes. After refluxing for 30 minutes, the reaction mixture was cooled down to room temperature and stirred overnight. During the reaction dimethyl-trans-4,4'-stilbenedicarboxylate was gradually dissolved and the potassium methoxide precipitated out to drive the reaction to completion. After that, the reaction

was poured into 100 ml concentrated NH_4Cl aqueous solution. The organic layer was collected and dried with MgSO_4 . Evaporation of the solvent gave crude product 0.7 g (70%). The crude product was purified by column chromatography (hexane/ethyl acetate) yielding a white solid. ^1H NMR (CDCl_3 , 400MHz) δ ppm: 7.99 (d, 4H, Ar-H), 7.56 (d, 4H, Ar-H), 7.21 (s, 2H, vinyl), 1.61 (s, 18H, CH_3). ^{13}C NMR (CDCl_3 , 400MHz) δ ppm: 165.6, 140.9, 131.4, 130.0, 129.9, 126.5, 81.2, 28.3. This compound is thermally unstable (decomposition of *t*-Bu ester group) above 190°C .

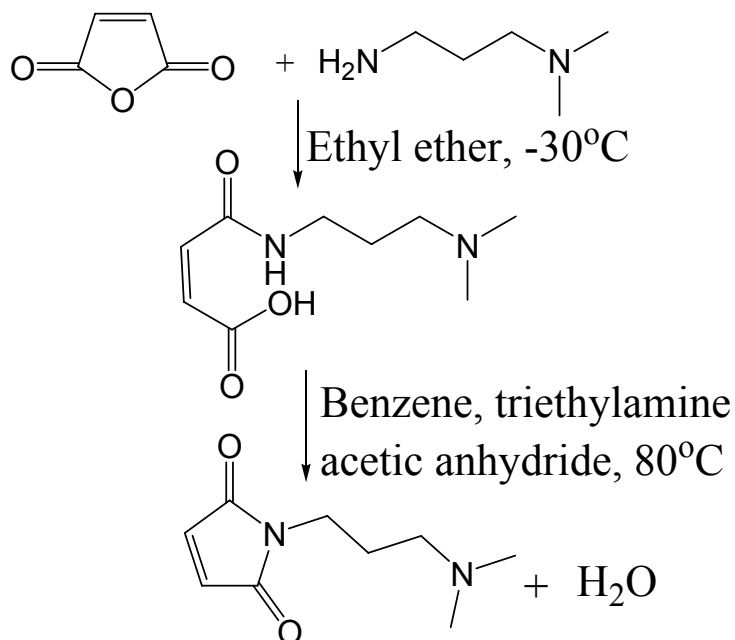
Scheme V.1 Synthesis of di-*t*-butyl-*trans*-4,4'-stilbenedicarboxylate via ester exchange method.



Synthesis of dimethylaminopropylmaleimide (DMAPM). The DMAPM was synthesized as shown in Scheme V.2.²³ A typical procedure to prepare DMAPM is as follows: to a solution of maleic anhydride (7.82 g, 80mmol) in ethyl ether (100ml) cooled in acetone-dry ice bath was added dimethylaminopropylamine (8.14 g, 80mmol) slowly over 30 minutes. The reaction mixture was cooled and stirred for four hours. During the reaction the maleic acid precipitated as a white solid. After the reaction the ethyl ether

was decanted. The white solid was mixed with triethyl amine (19.7 g), acetic anhydride (9.4g) and benzene (90ml) and the reaction mixture was heated at 80°C overnight. Afterwards, the reaction was washed three times with 100ml water. The organic layer was collected and dried with MgSO₄. Evaporation of the solvent gave crude product 1.45 g (10%). The crude product was purified by column chromatography (hexane/ethyl acetate) resulted as yellow liquid. ¹H NMR (CDCl₃, 400MHz) δ ppm: 6.69 (s, 2H, vinyl), 3.58 (t, 2H, NCH₂), 2.27 (t, 2H, NCH₂), 2.19 (s, 6H, NCH₃), 1.74 (m, 2H, CH₂). ¹³C NMR (CDCl₃, 400MHz) δ ppm: 170.9, 134.2, 57.0, 45.5, 36.3, 26.7.

Scheme V.2 Synthesis of dimethylaminopropylmaleimide.

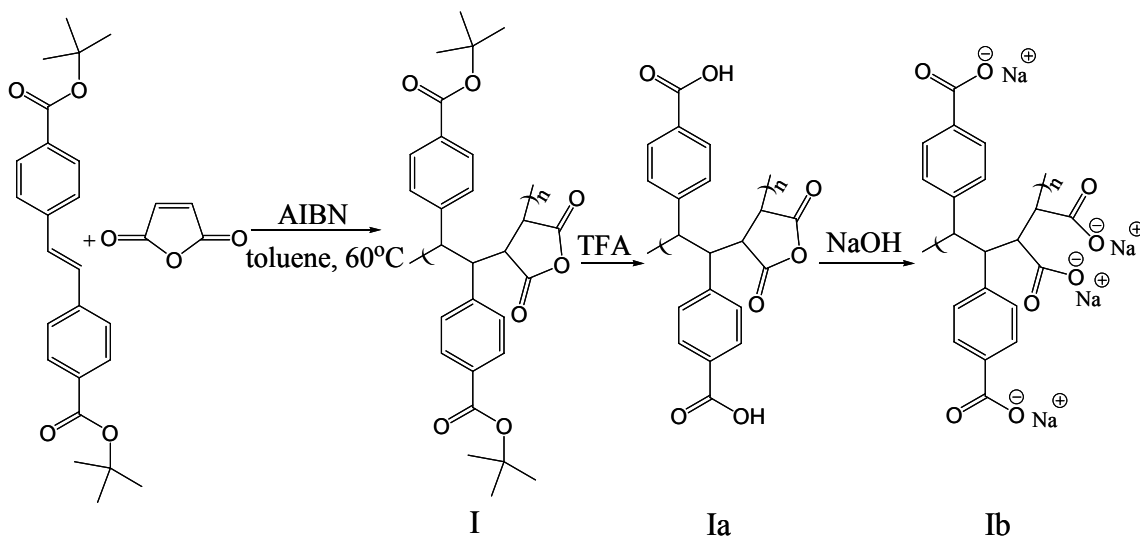


Polymerization. The monomers (DTBSC with maleic anhydride, TDAS with DMAPM, 1:1 mixing ratio, ~10 wt%) and THF were added together with an initiator [2,2'-azobisisobutyronitrile (AIBN)] in a 50-mL, septum sealed glass bottle equipped with a magnetic stirrer. The initiator concentration was 1 wt%. The mixtures were

degassed by purging with argon for 20 min and polymerized at 60 °C for 24 hours. The copolymers were then isolated by precipitation into hexane. The collected crude products were re-dissolved into chloroform and precipitated in hexane. The cycle was repeated for three times to remove unreacted monomers. All polymers were dried under vacuum at 60°C overnight before characterization.

The alternating copolymer of di-*t*-butyl-*trans*-4,4'-stilbenedicarboxylate with maleic anhydride (Scheme V.3). The 1:1 structure of the copolymer was confirmed by elemental analysis. Elemental Analysis: Calculated C, 70.28; H, 6.32; Found: C, 69.84; H, 6.39.

Scheme V.3 Synthesis of rigid polyanion based on alternating copolymerization of DTBSC with maleic anhydride.



The presence of anhydride groups after the polymerization was confirmed by IR spectroscopy. Two peaks associated with the anhydride groups of the copolymers (1841 cm⁻¹ and 1777 cm⁻¹) were clearly observed in the IR spectrum, and the peak from free

carboxylic acid groups was absent (Figure V.1a). The *t*-butyl ester groups were easily cleaved by trifluoroacetic acid (TFA) (200 mg of the polymer stirring with 4 ml CH₂Cl₂/TFA (50/50) mixture for 30 min at room temperature). After the cleavage of the *t*-butyl ester groups, the anhydride groups remained intact (Figure V.1b). The adsorption peaks from the anhydride groups disappeared with the subsequent hydrolysis in the 0.01M NaOH solution for 30 minutes (Figure V.1c). The hydrolyzed form of the di-*t*-butyl-trans-4,4'-stilbenedicarboxylate maleic anhydride copolymer was very soluble in water.

The *t*-butyl ester groups are thermally unstable and can be cleaved by heating to 200 °C (see Figure V.2).

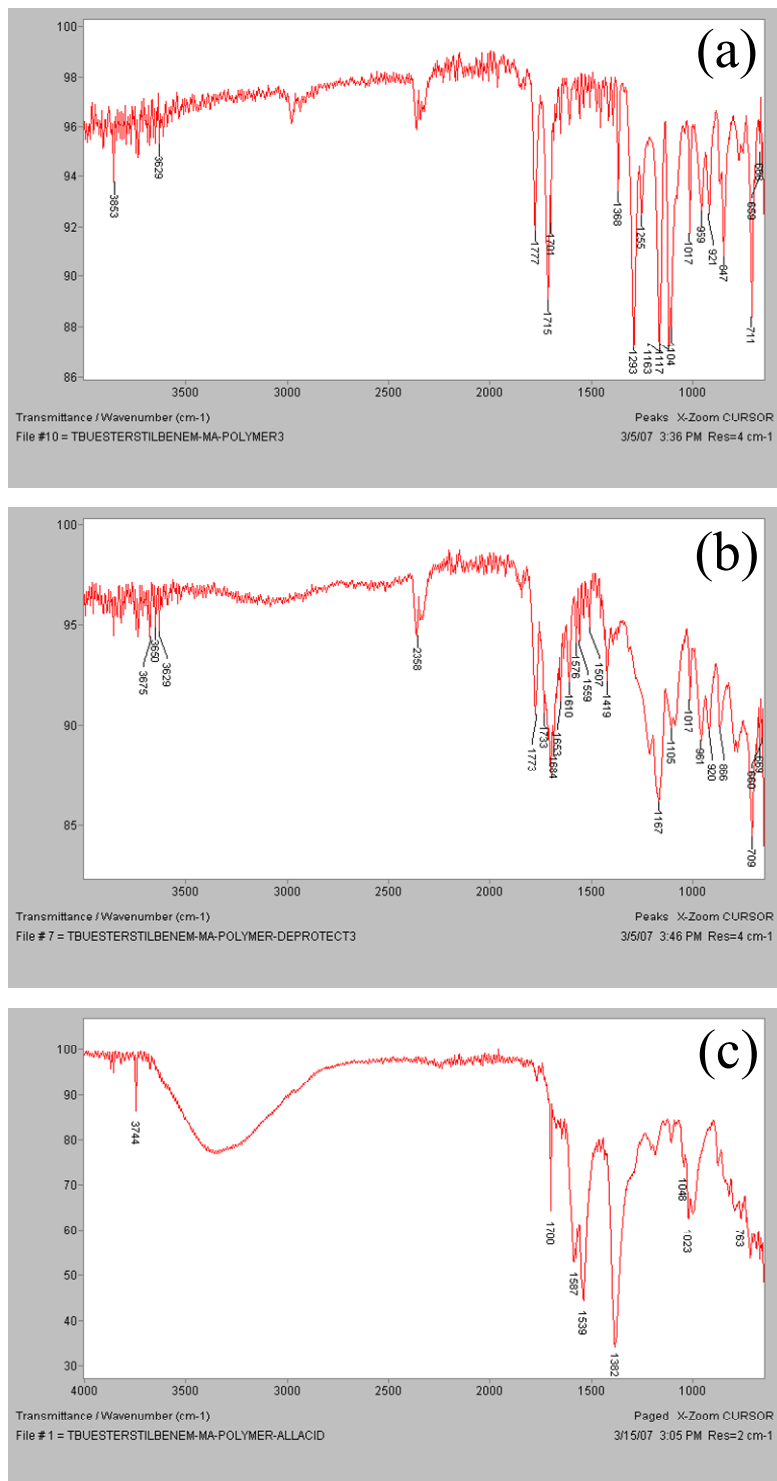


Figure V.1 IR spectra of the di-*t*-butyl-*trans*-4,4'-stilbenedicarboxylate maleic anhydride copolymer (a); de-protected form (b); and hydrolyzed form (c).

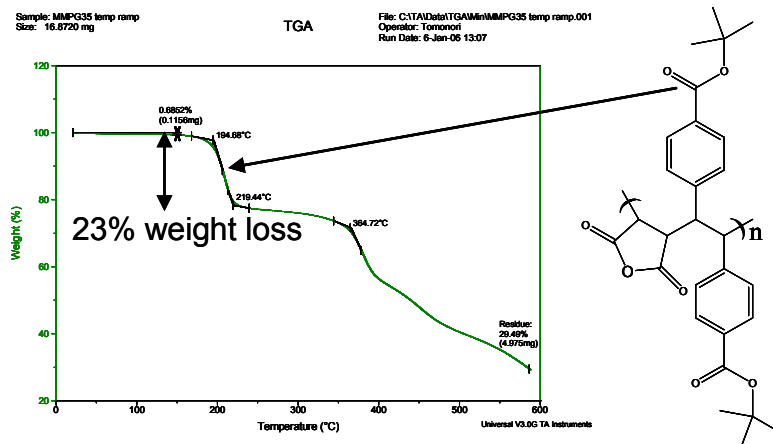
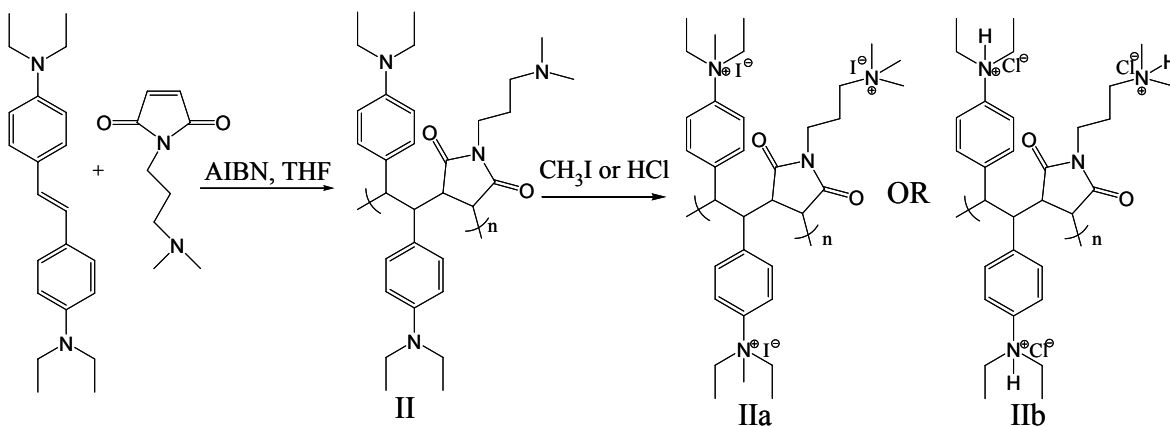


Figure V.2 TGA thermogram of the alternating copolymer of di-*t*-butyl-*trans*-4,4'-stilbenedicarboxylate with maleic anhydride.

The alternating copolymer of N, N, N', N'-tetraethyl-4, 4'-diaminostilbene with dimethylaminopropylmaleimide (Scheme V.4). The IB spectrum shown in Figure V.3 indicates the presence of imide rings. The 1:1 structure of the copolymer was confirmed by elemental analysis. Elemental Analysis: Calculated C, 73.77; H, 8.79; N, 11.10; Found: C, 71.38; H, 8.61; N, 11.23.

Scheme V.4 Synthesis of rigid polycation based on alternating copolymerization of TDAS with DMAPM.



elemental analysis. For I the 1:1 structure can be further corroborated by the mass loss (23%) at 200 °C due to the cleavage of thermally unstable *t*-butyl ester groups, which is exactly equal to the theoretical mass loss assuming the strictly alternating structure. Since the substituted stilbenes and maleic anhydride do not homo-polymerize and the maleimide homo-polymerizes very slowly, the 1:1 copolymers are alternating. The details of the structural characterization of these two copolymers are described in the experimental section.

Table V.1 Molecular weights and molecular-weight distributions of polymers I and II.

Polymer	M_n (g/mole)	M_w/M_n
I, the precursor for the polyanion	18100	1.18
II, the precursor for the polycation	10900	1.20

To convert I into a polyanion, the *t*-butyl ester groups were cleaved by trifluoroacetic acid (TFA) in dichloromethane. After that the de-protected polymer Ia was dissolved in dilute NaOH (0.001M) solution and converted into a rigid polyanion (scheme V.3). II can be easily dissolved in dilute aqueous hydrochloric acid and converted into a rigid polycation. The amine groups attached to the backbone of II also can be converted into quaternary ammonium groups by reacting with CH₃I (scheme V.4). Since amine and carboxylate groups are pH responsive, the charge density of these two rigid polyelectrolytes can be regulated by varying the solution pH to tune the electrostatic interactions between polymer chains.

Dynamic light scattering studies have shown that the TDAS/maleic anhydride alternating copolymers have a rigid backbone.²⁰ No glass transition temperatures were observed even up to the decomposition temperatures of these copolymers. Preliminary ²H solid state NMR studies on N, N, N', N'-tetraethyl-4, 4'-diaminostilbene maleic anhydride alternating copolymer confirm the chain rigidity of the polymer backbone.²⁶

The positively and negatively charged polyelectrolytes (Ib and IIa) are synthesized from easily accessible comonomers. These comonomers readily undergo alternating copolymerization which can be controlled by living free radical polymerization.²¹ The alternating copolymers have functional groups regularly positioned from each carbon atom of the polymer backbone. These functional groups are easily converted to charged groups which yield rigid polyelectrolytes with a variety of structures.

When mixed in the aqueous solution, the polyanion and polycation formed a polyion complex (PIC) and the solution turned turbid, similar to flexible polyelectrolytes or polyampholytes.^{27,28} With addition of 0.4M NaCl, the turbid solution became clear indicating the break-up of the polyion complex. The effect of salt on the PIC formed by rigid polyelectrolytes is similar to that on the PIC formed by flexible polyelectrolytes or polyampholytes but very different from that on the PIC formed by rigid polyampholytes based on the substituted stilbenes maleic anhydride backbones.²¹

V.4 Conclusions

Free radical alternating copolymerization was used to prepare rigid anionic and cationic polyelectrolytes. The polyanion was obtained from the di-t-butyl-trans-4,4'-

stilbenedicarboxylate maleic anhydride copolymer by hydrolysis of the t-butyl group and the polycation was prepared from the copolymer of N,N-dimethylaminopropyl maleimide with N, N, N', N'-tetraethyl-4, 4'-diaminostilbene by treating with hydrochloric acid or methyl iodide. The oppositely charged rigid polyelectrolytes formed a polyion complex (PIC) when mixed in aqueous solution. The PIC aggregates dissociated upon the addition of sodium chloride.

References

- (1) Radeva T., *Physical chemistry of polyelectrolytes*, Marcel Dekker: New York, **2001**.
- (2) Dobrynin, A.V.; Rubinstein, M. *Prog. Polym. Sci.* **2005**, *30*, 1049–1118.
- (3) Bohrisch, J.; Eisenbach, C.D.; Jaeger, W.; Mori, H.; Muller, A.H.E.; Rehahn, M.; Schaller, C.; Traser, S.; Wittmeyer, P. *Adv. Polym. Sci.* **2004**, *165*, 1-41.
- (4) Brodowski, G.; Horvath, A.; Ballauff, M.; Rehahn, M. *Macromolecules*, **1996**, *29*, 6962-6965.
- (5) Liu, T.; Rulkens, R.; Wegner, G.; Chu, B. *Macromolecules*, **1998**, *31*, 6119-6128.
- (6) Holm, C.; Rehahn, M.; Oppermann, W.; Ballauff, M. *Adv. Polym. Sci.* **2004**, *166*, 1-27.
- (7) Balanda, P.B.; Ramey, M.B.; Reynolds, J.R. *Macromolecules*, **1999**, *32*, 3970-3978.
- (8) Kroeger, A.; Deimede, V.; Belack, J.; Lieberwirth, I.; Fytas, G.; Wegner, G. *Macromolecules*, **2007**, *40*, 105-115.
- (9) Nicolai, T.; Mandel, M. *Macromolecules*, **1989**, *22*, 438-444.
- (10) Child, A.D.; Reynolds, J.R. *Macromolecules*, **1994**, *27*, 1975-1977.

- (11) Rulkens, R.; Schulze, M.; Wegner, G. *Macromol. Chem., Rapid Commun.* **1994**, *15*, 669-676.
- (12) Rulkens, R.; Wegner, G.; Enkelmann, V.; Schulze, M. *Ber. Bunsen-Ges. Phys. Chem.* **1996**, *100*, 707-714.
- (13) Bockstaller, M.; Kohler, W.; Wegner, G.; Vlassopoulos, D.; Fytas, G.; *Macromolecules*, **2000**, *33*, 3951-3953.
- (14) Braunecker, W.A.; Matyjaszewski, K. *Prog. Polym. Sci.* **2007**, *32*, 93-146.
- (15) Yoshida, M.; Fresco, Z.M.; Ohnishi, S.; Frechet, J.M. *Macromolecules*, **2005**, *38*, 334-344.
- (16) Schluter, A.D.; Rabe, J.P. *Angew. Chem. Int. Ed.* **2000**, *39*, 864 – 883.
- (17) Lubbert, A.; Nguyen, T.Q.; Sun, F.; Sheiko, S.S.; Klok, H.A. *Macromolecules*, **2005**, *38*, 2064-2071.
- (18) Gossel, I.; Shu, L.J.; Schluter, A.D.; Rabe, J.P. *J. Am. Chem. Soc.* **2002**, *124*, 6860-6865.
- (19) Al-Hellani, R.; Schluter, A.D. *Macromolecules* **2006**, *39*, 8943-8951.
- (20) Mao, M.; Turner, S.R. *Polymer* **2006**, *47*, 8101-8105.
- (21) Mao, M.; Turner, S.R. *J. Am. Chem. Soc.* **2007**, *129*, 3832-3833.
- (22) Kissling, R.M.; Gagne, M.R. *Org. Lett.* **2000**, *2*, 4209-4212.
- (23) Joyce, K.C. Ph.D. Dissertation, University of Florida, **1966**.
- (24) Kellou, M.; Jenner, G. *European Polymer Journal* **1977**, *13*, 9-14.
- (25) Ebdon, J. R.; Hunt, B. J.; Hussein, S. *British Polymer Journal* **1987**, *19*, 333-337.
- (26) Duer, M.J. In *Solid-State NMR spectroscopy: Principles and Applications*; Duer, M.J., Ed; Blackwell Sciences Ltd: London, **2002**.

- (27) Lowe, A.B.; McCormick, C.L. *Chem. Rev.*, **2002**, *102*, 4177-4189.
- (28) Mertoglu, M.; Gamier, S.; Laschewsky, A.; Skrabania, K.; Storsberg, J. *Polymer*, **2005**, *46*, 7726-7740.
- (29) Mourey, T.; Le, K.; Bryan, T.; Zheng, S.Y.; Bennett G. *Polymer* **2005**, *46*, 9033-9042.
- (30) Vanhee, S.; Rulkens, R.; Lehmann, U.; Rosenauer, C.; Schulze, M.; Kohler, W.; Wegner, G. *Macromolecules* **1996**, *29*, 5136-5142.
- (31) Yamazaki, S.; Muroga, Y.; Noda, I. *Langmuir*, **1999**, *15*, 4147-4149.

Chapter VI: Controlling Birefringence of the Polymer Films via Hindered Rotation of the Side Groups of Maleimide - Stilbene Alternating Copolymers

VI.1 Introduction

Birefringence ($n_{TE}-n_{TM}$) (TE = transverse electric; TM = transverse magnetic) indicates the optical anisotropy of a material and is closely related to the performance of optical polymers which are widely used such as lenses and optical waveguides.¹⁻⁴ Though optical polymers usually are amorphous isotropic materials and birefringence is undesired,^{5,6} there is great interest in anisotropic optical polymers with well-defined birefringent properties.⁷ For example, specially functionalized polyimide films are finding commercial application as compensators for normally white twisted nematic liquid crystal display (LCD).^{8,9} The birefringence of polymeric materials due to the orientation of polymer chains induced by crystallization or mechanical deformation such as injection, extrusion and drawing has been extensively explored.^{10,11} For instance, a biaxially orientated poly(methyl methacrylate) (PMMA) film shows a negative birefringence on the order of 0.0001.⁶ Since many functional groups attached to polymers are asymmetrical in polarizability and possess intrinsic optical anisotropy, the orientation of the side chains also can induce birefringence.^{12,13} Here a novel method to molecularly engineer the birefringent properties of the polymer film by controlling the rotation of the side groups is introduced. With the introduction of an ortho-methyl group into the benzene ring of the *N*-phenylmaleimide, the orientation of the benzene rings along the polymer backbone is achieved and the polymer film exhibits a large negative birefringence (~ 0.02) which is very difficult to obtain solely by mechanical orientation .

VI.2 Experimental Section

N-phenylmaleimide and *trans*-stilbene are commercially available from Aldrich and used as received. *N*-(*o*-tolyl)maleimide and *N*-dodecylmaleimide were prepared from the reaction of maleic anhydride with *O*-toluidine and dodecylamine according to the methods described in the literature,¹⁷ purified by column chromatography (hexane/ethyl acetate). The synthesis of the maleimide – stilbene alternating copolymer is described as follows. The monomers (stilbene and maleimide, 1:1 mixing ratio, ~10 wt%) and 1,2-dichloroethane were added together with an initiator [2,2'-azobisisobutyronitrile (AIBN)] in a 50-mL, septum sealed glass bottle equipped with a magnetic stirrer. The initiator concentration was 0.2 wt%. The mixtures were degassed by purging with argon for 20 min and polymerized at 60 °C for 24 hours. The copolymers were then isolated by precipitation into hexane. The collected crude products were re-dissolved into chloroform and precipitated in hexane. The cycle was repeated for three times to remove unreacted monomers. All polymers were dried under vacuum at 60°C overnight before characterization.

Molecular weights of synthesized polymers were determined using size exclusion chromatography (SEC) using a Waters 717 Autosampler equipped with three in-line PLgel 5 mm Mixed-C columns, Waters 410 RI detector, Viscotek 270 dual detector, and in-line Wyatt Technology miniDAWN multiple angle laser light scattering (MALLS) detector. SEC measurements were performed at 40 °C in chloroform at a flow rate of 1.0 mL/min. Glass transition temperatures were determined using a TA Q1000 DSC at a heating rate of 10°C/min under nitrogen.

Polymer films were prepared by solution casting from 3 wt% chloroform solution onto pre-cleaned fused silica plates at room temperature. The polymer solutions were filtered using Whatman 1 μm Teflon filters. The fused silica plates were placed on an anti-vibration air table during the solution casting process to ensure obtaining smooth polymer films. After drying at room temperature overnight, the polymer films were dried in a vacuum oven to remove any residual solvent.

The refractive index measurements were carried on HS-190 Spectroscopic Ellipsometer (J. A. Woollam Co., INC.) with a 75W light source and high speed monochromator system. The ellipsometer had EX-IR and UV-VIS detectors which can cover wavelength from 300 nm to 2100 nm. Both transmission and reflection modes have been measured. Data were acquired from 0 to 30 degree with 15 degree step under the transmission mode and from 45 to 65 degree with 10 degree step under the reflection mode. The experimental data were modeled by WVASE software for Windows which yielded polymer film thickness and birefringence values.

VI.3 Results and Discussions

For the first studies the conformations of *N*-phenylmaleimide and *N*-(*o*-tolyl)maleimide were modeled by geometry optimization at B3LYP level using Gaussian 03. The basis set employed was 6-31G*. The potential energy diagrams for internal rotation of the benzene ring in these two maleimides are shown in Figure VI.1. For *N*-phenylmaleimide, the energy barrier for the free rotation of the benzene ring is very small, about 3 kcal/mol, comparable to the activation energy for rotation about the carbon-carbon bond in ethane.¹⁴ Thermal energy available from the surroundings is

sufficient to overcome this energy barrier so the benzene ring can rotate freely. However, the activation energy for the free rotation of the benzene ring in *N*-(*o*-tolyl)maleimide is about 125.8 kcal/mol which is too high to be overcome by the thermal energy available at room temperature. The ortho methyl group significantly hinders the free rotation of the benzene ring so that it is out-of-plane of the imide ring. The torsional angle between the benzene ring and the imide ring is estimated to be 65 degrees from the optimized conformation of the *N*-(*o*-tolyl)maleimide.

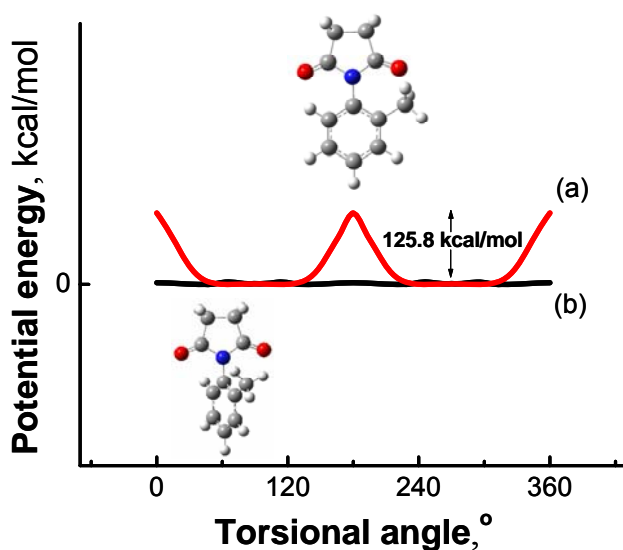
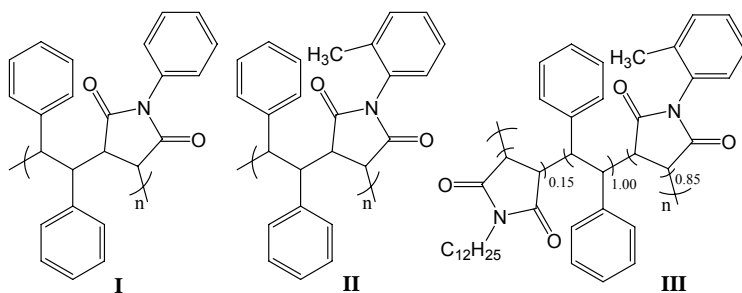


Figure VI.1 Potential energy diagram for internal rotation of benzene ring as a function of torsional angle between the benzene ring and imide ring in *N*-(*o*-tolyl)maleimide (a) and *N*-phenylmaleimide (b).

Benzene is anisotropic with different polarizabilities in different directions: the electron clouds can be more easily deformed in the plane of the ring than in the direction perpendicular to the plane of the ring (Scheme VI.2a).¹¹ If the benzene rings are aligned in a certain direction and can not rotate freely, the material will show birefringence depending on the orientation of the benzene rings. To test this hypothesis, two alternating

copolymers of *N*-(*o*-tolyl)maleimide and *N*-phenylmaleimide with stilbene (Scheme VI.1) were synthesized. Maleimide - stilbene comonomer system is a classical “donor-acceptor” system undergoing very fast free radical polymerization producing high molecular weight polymer.¹⁵ Since maleimide-stilbene copolymers are rigid with very high glass transition temperature (no T_g observed up to 270 °C), high molecular weight is required for the polymer to form films. By a solution casting method, the *N*-phenylmaleimide - stilbene copolymer (Scheme 1I, M_n = 262000, M_w/M_n = 1.92) and *N*-(*o*-tolyl)maleimide – stilbene copolymer (Scheme 1II, M_n = 148000, M_w/M_n = 1.66) form colorless optically transparent films.

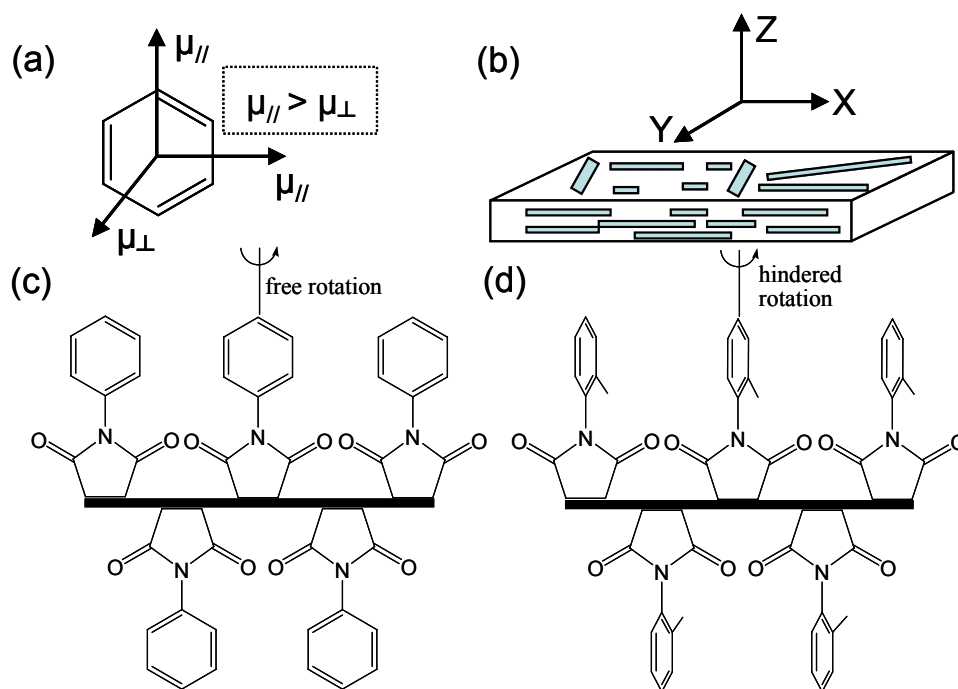
Scheme VI.1 Structures of the maleimide – stilbene alternating copolymers used in this study: *N*-phenylmaleimide - stilbene copolymer (I); *N*-(*o*-tolyl)maleimide – stilbene copolymer (II); *N*-(*o*-tolyl)maleimide – stilbene copolymer containing 15% dodecylmaleimide (III).



During the film casting process, the rigid polymer chains align parallel to the film surface (in-plane orientation) but randomly distribute within the film surface (Scheme VI.2b). For the *N*-phenylmaleimide - stilbene copolymer, all of the benzene rings can rotate freely so the alignment of the polymer backbone to the film surface would not induce

birefringence (Scheme VI.2c). This was confirmed by the measurement of the refractive indices in the X, Y (film surface or in plane direction) and Z (out-of-plane direction) which are almost identical in the visible range (Figure VI.2a).

Scheme VI.2 Large birefringence originated from the optical anisotropy (a) and ortho-methyl induced orientation of benzene ring (c,d) when polymer chains align parallel to film surface (b).



Large negative birefringence, around 0.02, was observed for the *N*-(*o*-tolyl)maleimide – stilbene copolymer film (Figure VI.2b). The ortho-methyl groups induce the benzene rings to preferentially align vertical to the film surface so the polymer film has larger polarizability as well as higher refractive index in the Z (out-of-plane) direction (Scheme VI.2d). Since the polymer chains are distributed randomly within the

film surface, the polymer film is isotropic in the in-plane direction. The birefringent property of the *N*-(*o*-tolyl)maleimide - stilbene copolymer films shows a dependence on the film thickness. The negative birefringence decreases with increased film thickness (Figure VI.3). This decrease is probably due to the reduced extent of alignment of the polymer chains parallel to the film surface with increased film thickness.⁹ Since the maleimide – stilbene copolymers are fairly rigid, the resulting polymer films are brittle. To enhance the film strength, a small fraction of *N*-dodecylmaleimide was copolymerized with *N*-(*o*-tolyl)maleimide and stilbene. The long alkyl dodecyl chains can act as the plasticizer and enable some mobility to the polymer chains when they are under stress. The *N*-(*o*-tolyl)maleimide – stilbene copolymer ($M_n = 79000$, $M_w/M_n = 1.84$) containing 15 mole% of *N*-dodecylmaleimide forms robust clear films. The incorporation of dodecyl maleimide slightly reduces the negative birefringence since the *N*-(*o*-tolyl)maleimide is “diluted”.

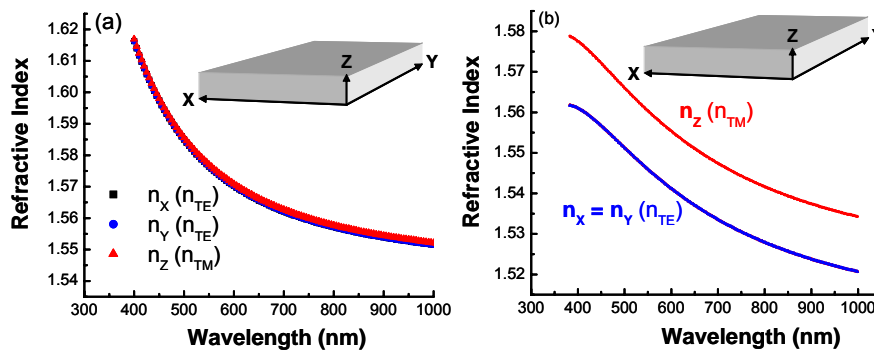


Figure VI.2 The refractive indices of films in X, Y and Z directions for *N*-phenyl maleimide-stilbene copolymer (a) and *N*-(*o*-tolyl)maleimide-stilbene copolymer (b).

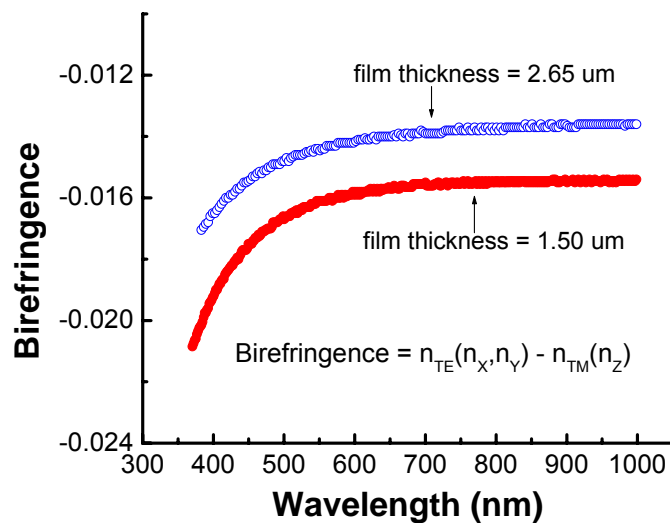


Figure VI.3 Effect of film thickness on the birefringent property of the film of *N*-(*o*-tolyl)maleimide-stilbene copolymer.

VI.4 Conclusions

To conclude, the birefringent property of the polymer film can be dramatically affected by the orientation of the pendent side groups along the polymer backbone. Using the maleimide - stilbene alternating copolymers as model systems, the orientation of the side groups can be easily achieved by hindering the free rotation of the benzene ring with an ortho-methyl group. The orientation of the benzene ring can induce large negative birefringence for the polymer film when the rigid polymer backbones align parallel to the film surface. Such large negative birefringence is difficult to obtain by mechanical drawing of polymer films. The polymer developed in this study can be conveniently synthesized from easily accessible monomers and could be used as a compensation material for LCD¹⁶ or as the dopant to produce zero-birefringence optical polymers.^{5,6}

References

- (1) Ma H.; Jen, A.K.Y.; Dalton, L.R. *Adv. Mater.* **2002**, *14*, 1339.
- (2) Marder, S.R.; Kippelen, B.; Jen A.K.Y.; Peyghambarian, N. *Nature* **1997**, *388*, 845.
- (3) Eldada, L.; Shacklette, L.W. *IEEE J. Select. Top. Quant. Electron.* **2000**, *6*, 54;
- (4) Weber, M.F.; Stover, C.A.; Gilbert, L.R. Nevitt, T.J.; Ouderkirk, A.J. *Science* **2000**, *287*, 2451.
- (5) Tagaya, A.; Ohkita, H.; Mukoh, M.; Sakaguchi, R.; Koike, Y. *Science* **2003**, *301*, 812.
- (6) Tagaya, A.; Ohkita, H.; Harada, T.; Ishibashi, K.; Koike, Y. *Macromolecules* **2006**, *39*, 3019.
- (7) Lorkowski, H.J.; Pfeiffer, K.; Biebricher, M.; Franke, H. *Polymers for Advanced Technologies* **1996**, *7*, 501.
- (8) Li, F.M.; Harris, F.W.; Cheng, S.Z.D. *Polymer* **1996**, *37*, 5321.
- (9) Li, F.M.; Kim, K.H.; Savitski, E.P.; Chen, J.C.; Harris, F.W.; Cheng, S.Z.D. *Polymer* **1997**, *38*, 3223.
- (10) Grishchenko, A.E.; Cherkasov, A.N. *Physics – Uspekhi* **1997**, *40*, 257.
- (11) Riande, E.; Saiz, E. *Dipole Moments and Birefringence of Polymers*, Prentice – Hall: Englewoods Cliffs, New Jersey, **1992**.
- (12) Natansohn, A.; Rochon, P.; Gosselin, J.; Xie, S. *Macromolecules* **1992**, *25*, 2268.
- (13) Natansohn, A.; Rochon, P. In *ACS Symposium Series: Photonic and Optoelectronic Polymers*; K. J. W. Samson A. Jenekhe, Ed.; American Chemical Society: Washington, DC, **1997**; Vol. 672, p 236.
- (14) Carey, F.A. *Organic Chemistry*, 3rd Ed.; McGraw-Hill: New York, **1996**; chapter 3.

(15) Turner, S. R.; Arcus, R. A.; Houle, C. G.; Schleigh, W. R. *Polymer Engineering and Science* **1986**, *26*, 1096.

(16) Robinson, M.G.; Chen, J.M.; Sharp, G.D. *Polarization Engineering for LCD Projection*; John Wiley & Sons: West Sussex, **2005**.

(17) Cava. M. P.; Deana. A. A.; Muth, K.; Mytchell, M. J. *Organic Syntheses*; Wiley: New York: 1973; Collect. Vol. V, p 944.

Chapter VII: Synthesis and Characterization of Poly(aryl ether sulfone) Copolymers Containing Terphenyl Groups in the Backbone

VII.1 Introduction

Poly(aryl ether sulfone)s (PAES), with high glass transition temperatures (T_g), are amorphous aromatic tough thermoplastics and have unique high performance properties as engineering materials.¹ The synthesis and characterization of PAESs have been extensively investigated and well reviewed.²⁻⁷ However, there are some undesirable features originating from their amorphous nature. They suffer from solvent sensitivity especially under stress and are subject to solvent cracking and they cannot form oriented film or fiber. The use temperature of PAES is usually about 30 °C lower than T_g . These shortcomings preclude their use when solvent resistance and high-temperature dimensional stability are required.⁸

One way to overcome the above mentioned deficiencies of PAES is to make these polymers semi-crystalline.⁹ For example, semi-crystalline thermoplastics such as poly(aryl ether ketone)s (PAEK) exhibit good solvent resistance.¹⁰ The crystalline phase also can act as physical crosslinks to enhance the high-temperature dimensional stability. Semi-crystalline engineering plastics such as polyesters have use temperatures much higher than their T_g s because they can be biaxially oriented and heat set. To achieve this goal, random or segmented copolymers poly(aryl ether ketone-co-sulfone)s (PAEKS) have been widely explored to obtain high T_g semi-crystalline engineering thermoplastics.¹¹⁻¹³ Unfortunately such efforts are not very successful due to unwanted side reactions.¹⁴

The ability of PAEKs to crystallize is generally ascribed to the close bond angles at aromatic ether (around 121°) and carbonyl groups (120-122°) leading to the linear chain geometry required for polymer crystallization.¹⁵ Because the bond angles at sulfonyl (around 106°) and aromatic ether (around 121°) groups are very different, the backbones of the PAESs have to adopt highly kinked conformations which interferes with the crystallization process.¹⁵ The incorporation of terphenyl groups into the polysulfone backbone promoted the crystallization but the polymers were highly insoluble with very high melting points and are thus non-processable.¹⁶ In this study random and segmented PAESs containing terphenyl group in the backbone were synthesized and the effect of terphenyl group on the thermal properties of the PAESs was investigated.

VII.2 Experimental Section

General considerations. All reagents were purchased from Aldrich and used as received unless otherwise noted. 4,4'-Dichlorodiphenylsulfone (DCDPS) was purchased from Aldrich and recrystallized from toluene. 4,4'-Difluorodiphenylsulfone (DFDPS, 99+%) and 4,4'-isopropylidenediphenol (BPA, 99+%) were purchased from Aldrich and used as received. 4,4'-Biphenol (BP) was obtained from Eastman Chemical and sublimed before use. 4,4'-(Hexafluoroisopropylidene)diphenol (BPAF), purchased from Aldrich, was purified by sublimation and dried under vacuum. NMR spectra were determined at 25°C at 400 MHz with a Varian Unity spectrometer. The elemental analysis was done by Atlantic Microlab, Inc. (Norcross, Georgia).

Size exclusion chromatography (SEC): Molecular weights of synthesized polymers were determined using size exclusion chromatography (SEC) using a Waters 717 Autosampler equipped with three in-line PLgel 5 mm Mixed-C columns, Waters 410 RI detector, Viscotek 270 dual detector, and in-line Wyatt Technology miniDAWN multiple angle laser light scattering (MALLS) detector. The dn/dc values were determined on-line using the calibration constant for the RI detector and the mass of the polymer sample. SEC measurements were performed at 40 °C in tetrahydrofuran at a flow rate of 1.0 mL/min. For all samples, it was assumed that 100% of the polymer eluted from the column during the measurement.

TGA and DSC: Thermogravimetric analysis (TGA) was conducted under nitrogen, from 25 to 800 °C at a heating rate of 10 °C using a TA Instrument TGA 295. Glass transition temperatures were determined using a TA Q1000 DSC at a heating rate of 10°C/min under nitrogen.

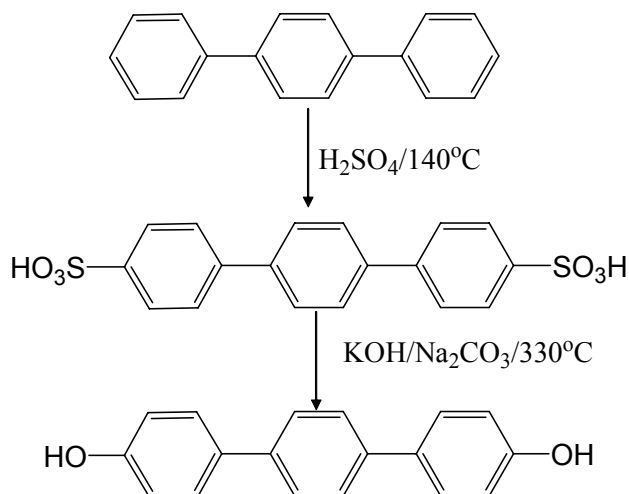
Wide angle X-ray diffraction (WAXS): Photographic flat plate WAXS studies were conducted using a Philips PW 1720 X-ray diffractometer emitting Cu-K α radiation (1.54 Å wavelength), operating at a voltage of 40 kV and tube current of 20 mA. The sample to film distance was set to 47.3 mm for all samples. Direct exposures (4 hr) were made in a Warhus camera using Kodak Biomass MS film in an evacuated sample chamber. The sample thickness was in the range of 12-14 mils.

Preparation of 4, 4'-dihydroxyterphenyl (DHTP). The synthetic procedure of 4, 4'-dihydroxyterphenyl (DHTP) is shown in Scheme VII.1.¹⁷ 130 g of concentrated sulfuric acid were heated to 110 °C, and 40 g of terphenyl were added. The temperature was raised to 140 °C and maintained for 4 hours. After cooling to 100 °C, 120 ml of water

were added drop-wise, and the mixture was allowed to cool and then filtered with suction, giving a crude product which was used directly in the next stage.

The stainless steel vessel in a Parr reactor was charged with 170 g of potassium hydroxide, 17 g of sodium carbonate and 70 g of the crude product described above. The temperature was raised to 330 °C and the mixture was stirred for 3 hours under argon. The mixture was then cooled to 100 °C and the pressure was released by opening the valve. The components of the reaction mixture were transferred out by the addition of 1 liter of water and the crude product precipitated and was filtered with suction. The crude product was suspended in 2 liter of water, acidified with concentrated hydrochloric acid, heated to 90 °C and filtered with suction while still hot. The crude product was dried and re-crystallized twice from N, N'-dimethylacetamide (DMAc). Yield: 85% as a white powder. ¹H NMR (d₆-DMSO, 100MHz) δ ppm: 7.56 (s, 4H, Ar-H), 7.46 (d, 4H, Ar-H), 6.80 (d, 4H, Ar-H). ¹³C NMR (d₆-DMSO, 400MHz) δ ppm: 157.10, 138.14, 130.50, 127.54, 126.31, 115.78. Elemental Analysis: Calculated C, 82.42; H, 5.38; O, 12.20. Found: C, 82.37; H, 5.52; O, 12.08.

Scheme VII.1 The synthesis of 4,4'-dihydroxyterphenyl.



Preparation of random PAESs. The copolymerization procedures were similar for all random DHTP containing PAESs (Scheme VII.2).¹⁸ A typical copolymerization for DHTP BPA random copolymer is described below. First, 1.918 g (7.31 mmol) of DHTP, 3.000 g (10.45 mmol) of DCDPS, and 0.716 g (3.13 mmol) of BPA were added to a three necked flask equipped with an overhead mechanical stirrer, an argon inlet, and a Dean–Stark trap. Potassium carbonate (13.7 mmol, 1.92 g), and sufficient DMAc (35 mL) were introduced to afford a 20% (w/v) solid concentration. Toluene (17 mL; usually, DMAc/toluene = 2/1 v/v) was used as an azeotroping agent. The reaction mixture was refluxed at 145°C for 4 h to dehydrate the system. The temperature was raised slowly to 170°C by the controlled removal of the toluene. The reaction was allowed to proceed for 24 h. The solution was cooled to room temperature and the copolymer was precipitated in acidic water. The precipitated copolymer was washed with deionized water and then vacuum dried at 120°C for 24 h.

Preparation of segmented PAESs. The copolymerization procedure was similar for all the segmented terphenyl containing PAESs. A typical copolymerization for the segmented copolymers is described below. First, 1.418 g (7.62 mmol) of BP and 2.114 g (8.32 mmol) of DFDPS were added to a three necked flask equipped with an overhead mechanical stirrer, an argon inlet, and a Dean–Stark trap. Potassium carbonate (1.263 g, 3.13 mmol), and 20 g of diphenylsulfone were introduced to afford a 20% (w/v) solid concentration. Toluene (15 mL) was used as an azeotroping agent. The reaction mixture was refluxed at 145 °C for 4 h to dehydrate the system. The temperature was raised slowly to 175 °C by the controlled removal of the toluene. The reaction was allowed to proceed for 24 h. To the same reaction flask described previously, 2.000 g (7.62 mmol) of 4,4'-dihydroxyterphenyl, 1.762 g (6.93 mmol) of DFDPS, and 1.263 g (3.13 mmol) of potassium carbonate, and 15 g of diphenylsulfone were introduced. Toluene (20 mL) was used as an azeotroping agent. The reaction mixture was refluxed at 145 °C for 4 h to dehydrate the system. The temperature was raised slowly to 170 °C by the controlled removal of the toluene. The reaction was allowed to proceed at 175 °C for 1 h, 200 °C for 1 h, 250 °C for 1 h, 300 °C for 2 h. At the final stage of the polymerization, the polymerization solution would climb up the stirring rod indicating the high molecular weight of the polymer. The solution was cooled to room temperature and the copolymer was taken out by breaking the reaction flask. The solid was heated and swelled in boiling DMAc three times to remove the diphenylsulfone. After that the solid was successively rinsed with hot acetone, hot water and hot ethanol to clean the polymer and then vacuum dried at 120 °C for 24 h.

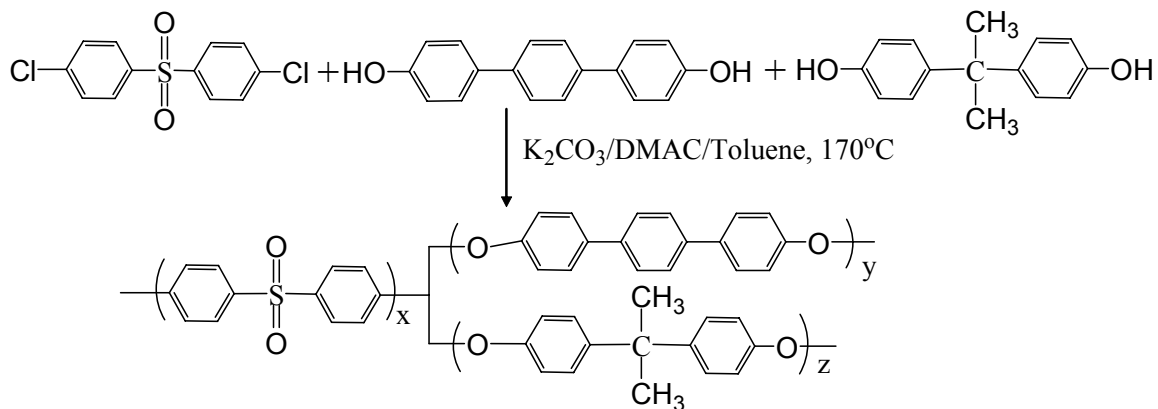
VII. 3 Results and Discussions

Synthesis of polymers. Polycondensations of bisphenols with stoichiometric amounts of DCDPS or DFDPS were carried out in the presence of excess potassium carbonate as a base in aprotic polar solvents such as DMAc, sulfolane or diphenylsulfone depending on the solubility of the polymers (see the experimental section for details). A representative example of the synthesis of random polysulfone copolymers using BPA, DHTP and DCDPS is shown in scheme VII.2. For the synthesis of random polysulfone copolymers, only DCDPS was used. Very good conversions and high molecular weights were obtained as indicated by the SEC data shown in Table VII.1. The percentages of the DHTP in the copolymer were verified by the ¹H-NMR and very close to the monomer feed ratios. When the copolymerization contained 70% DHTP (since the mole ratio of phenol to DCDPS was always kept to 1:1, the percentage mentioned here is the mole percentage of DHTP to the total amount of bisphenols), sulfolane was used as the solvent to keep the polymers soluble during the polymerization.

For the synthesis of segmented copolymers, the BPA or BP containing fluorine terminated oligomers ($M_n = 5K$) were synthesized first. Because the oligmer synthesized from DHTP and DCDPS or DFDPS is insoluble in organic solvents, we could not synthesize the segmented copolymers by connecting the two different oligmers directly.¹⁹ To overcome the solubility problem, the BPA or BP containing fluorine terminated oligmers were mixed with the DHTP and DFDPS for the second polycondensation step. The BPA or BP containing fluorine terminated oligmers were enchaind by the DHTP DFDPS oligmers formed in-situ. A representative example of the synthesis of random polysulfone copolymers using BP, DHTP and DFDPS is shown in scheme VII.3. The

BPA or BP containing chlorine terminated oligmers were not reactive enough to form high molecular weight segmented polymer. So only DFDPS was used for the synthesis of segmented polysulfone copolymers. The segmented PAES copolymers show big differences in solubility and appearance from the random ones with the same composition. Although we cannot exclude the occurrence of trans-etherification during the polymerization to make segmented PAES copolymers, such possible trans-etherification can be reduced greatly by using the much more reactive DFDPS instead of the DCDPS.²⁰

Scheme VII.2 The synthesis of DHTP-BPA random PAES copolymer.



Scheme VII.3 The synthesis of DHTP - BP segmented PAES copolymer.

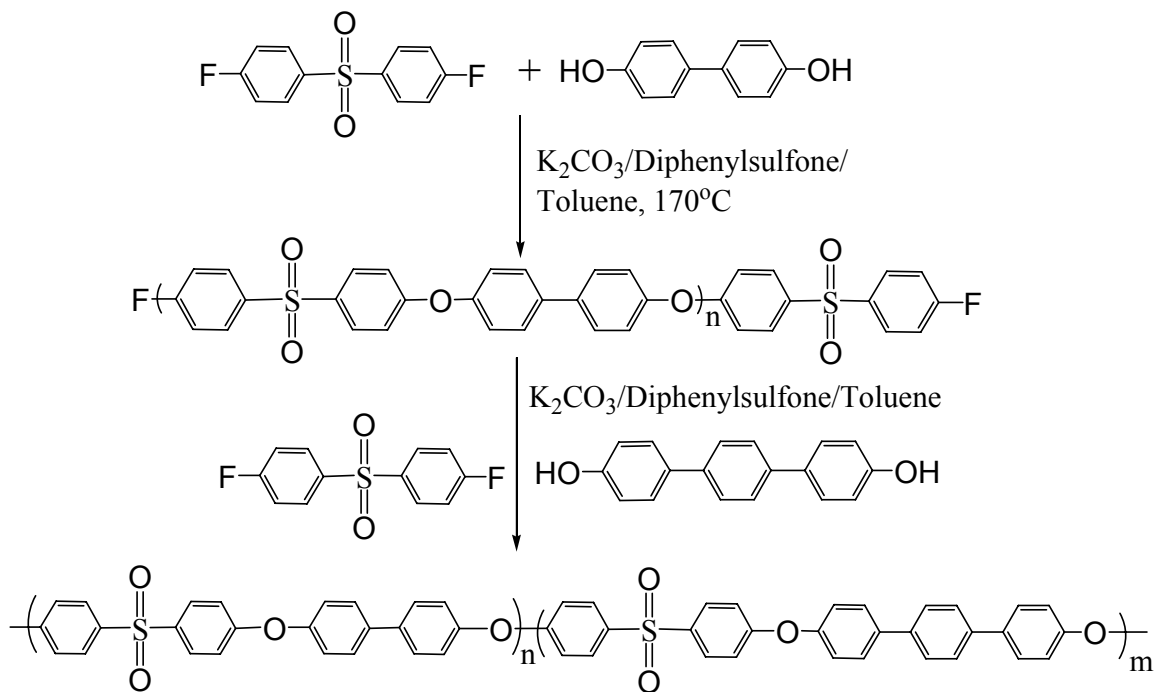


Table VII.1 Compositions, molecular weights and molecular weight distributions of the random polysulfone copolymers.

Compositions			M_n (g/mole)	M_w/M_n
BPA, 100%	DHTP, 0%	DCDPS, 100%	28200	2.90
BPA, 90%	DHTP, 10%	DCDPS, 100%	49500	2.61
BPA, 70%	DHTP, 30%	DCDPS, 100%	29200	1.94
BPA, 50%	DHTP, 50%	DCDPS, 100%	48100	2.23
BPAF, 100%	DHTP, 0%	DCDPS, 100%	29200	2.82
BPAF, 90%	DHTP, 10%	DCDPS, 100%	36500	2.92
BPAF, 70%	DHTP, 30%	DCDPS, 100%	22600	2.33
BPAF, 50%	DHTP, 50%	DCDPS, 100%	26900	2.14

Solubility of polymers. The incorporation of DHTP decreased the solubility of the polysulfone copolymers. The polysulfone copolymer synthesized only from DHTP and DCDPS is insoluble in any organic solvents. During the polymerization the polymer precipitated out quickly from sulfolane in the powder form. This is likely just low molecular weight oligomer. For random copolymers synthesized from BPA or BPAF with DHTP, the polymers are soluble in THF, chloroform and DMAc at room temperature when the molar percentage of DHTP is lower than 70%. For random copolymers synthesized from BP and DHTP, the polymers are soluble in hot DMAc or NMP when the molar percentage of DHTP is lower than 70%. The solubility of the segmented copolymers is significantly lower than that of the random copolymers. The segmented copolymer from BPA and DHTP is only soluble in hot DMAc. The segmented copolymer containing BP is only slightly swelled in boiling DMAc.

Polymer Crystallization. These polysulfone copolymers demonstrated excellent thermal stability with a 5% weight loss between 490 and 500 °C in nitrogen. For the DHTP-DCDPS polysulfone copolymers, glass transition temperature T_g and melting temperature T_m were 250°C and 370°C respectively, close to the reported values.¹⁶ This indicates that the terphenyl group does straighten the polymer chain and facilitate the packing of the polymer chains to form crystallites. Since this polymer is non-processable, BPA, BPAF and BP were incorporated to lower the glass transition temperature and the melting temperature.

However, even containing 70% DHTP, the synthesized random copolymers are non-crystalline and exhibit no crystallization or melt transition in DSC measurements. The glass transition temperatures increase with the increased amount of incorporated

DHTP in a BPA copolymer and are summarized in Figure VII.1. Similar results were obtained when incorporating BPAF or BP. These random copolymers exhibit considerably higher T_g values than the corresponding PAESs without terphenyl groups. This is attributed to the more rigid polymer backbone of these polymers because of the presence of the terphenyl groups.²¹ It seems that the terphenyl groups have to be concentrated to induce chain crystallization.

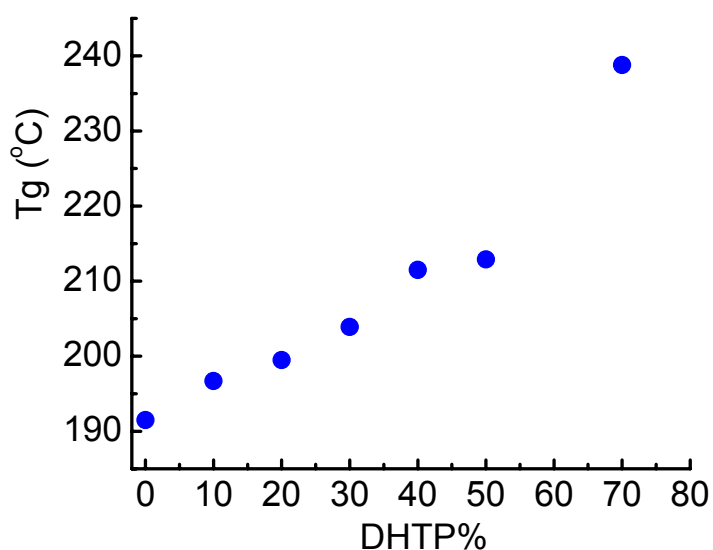


Figure VII.1 Glass transition temperatures of the random BPA-DHTP polysulfone copolymers containing different amounts of DHTP.

For the segmented PAES containing 50% BPA and 50% DHTP, no well-defined crystallization or melt transition was observed in DSC measurements. Crystallization was clearly shown in the first heating cycle of the DSC measurement of segmented PAES containing 50% BP and 50% DHTP (Figure VII.2). The formation of crystallites was also confirmed by the wide angle X-ray diffraction (Figure VII.3). The melting temperature is

320°C which is low enough for processing. However, no crystallization or melt transition was observed in the second heating cycle (Figure VII.2), even when the sample was annealed at 300°C for 30 minutes. Although re-equilibration of the segmented copolymer in the DSC measurement cannot be totally ruled out, such crystallization behavior is very similar to polycarbonate which undergoes solvent-induced crystallization and shows very slow crystallization rate in the melt state.²²

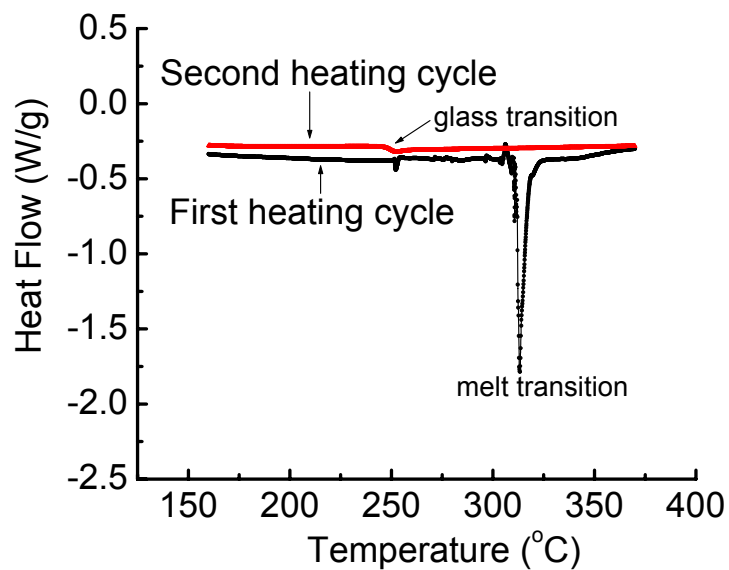


Figure VII.2 DSC curves (first and second heating cycles) of the segmented PAES containing 50% BP and 50% DHTP, obtained at a heating rate of 10 °C/min.



Figure VII.3 WAXS pattern of the segmented PAES containing 50% BP and 50% DHTP.

VII.4 Conclusions

In this study 4,4'-dihydroxyterphenyl has been incorporated into the backbone of conventional PAESs to make them semi-crystalline. The more linear and rigid terphenyl groups can induce the formation of crystallites for the segmented PAES containing 50% BP and 50% DHTP. The semi-crystalline segmented PAES copolymer showed a melting temperature 320°C in the first heating cycle of DSC measurement. The formation of crystallites was confirmed by the WAXS. No crystallization was observed in the second heating cycle of the DSC measurements indicating a very slow crystallization rate of the copolymer in the melt state.

References:

- (1) Cotter, R.J. *Engineering Plastics: A Handbook of Polyarylethers*. McGraw-Hill Companies, Inc., 1995.
- (2) Johnson, R.N.; Farnham, A.G. *Journal of Polymer Science, Part A*, **1967**, 5, 2415.
- (3) Gatham K. V.; Turner S. *Polymer*, **1974**, 15, 665.
- (4) Attwood, T.E.; King, T.; Leslie, V.J.; Bose, J.B. *Polymer*, **1977**, 18, 369.
- (5) Viswanathan, R.; Johnson, B.C.; McGrath, J.E. *Polymer*, **1984**, 25, 1827.
- (6) Lakshmana, R.V. *Polymer Reviews*, **1999**, 39, 655.
- (7) Harrison, W.L.; Hickner, M.A.; Kim, Y.S.; McGrath, J.E. *Fuel Cells*, **2005**, 5, 201.
- (8) Friedman, M.; Walsh, G. *Polymer Engineering and Science*, **2002**, 42, 1756.
- (9) Galeski, A. *Prog. Polym. Sci.*, **2003**, 28, 1643.
- (10) Lakshmana, R.V. *Polymer Reviews*, **1995**, 35, 661
- (11) Jones, M.E.B. (ICI, Ltd.). U.S. Patent 4,052,365, 1977.
- (12) Botkin, J.H.; Cotter, R.J.; Matzner, M.; Kwiatkowski, G.T. *Macromolecules*, **1993**, 26, 2372.
- (13) Carlier, V.; Devaux, J.; Legras, R.; Bunn, A.; McGrail, P.T. *Polymer*, **1994**, 35, 415.
- (14) Devaux, J.; Carlier, V.; Bourgeois, Y. In *Handbook of Thermoplastics*; Olabisi, O., Ed.; Marcel Dekker, Inc.: New York, 1997; p951.
- (15) Colquhoun, H.M.; Williams, D.J. *Acc. Chem. Res.* **2000**, 33, 189.
- (16) Staniland, P. A. *Bull. Soc. Chim. Belg.* **1989**, 98, 667.
- (17) Ulrich, E. (BASF), U.S. Patent 5,008,472, 1991

- (18) Harrison, W.L.; Wang, F.; Mecham, J.B.; Bhanu, V.A.; Hill, M.; Kim, Y.S.; McGrath, J.E.; *J. Polym. Sci. Part A: Polymer Chemistry*, **2003**, *41*, 2264.
- (19) Ghassemi, H.; McGrath, J.E.; Zawodzinski, T.A. *Polymer*, **2006**, *47*, 4132.
- (20) Johnson, R.N.F.; Alford, G. *J. Polym. Sci. Part A-1*, **1967**, *5*, 2415.
- (21) Banerjee, S.; Maier, G. *Chem. Mater.* **1999**, *11*, 2179.
- (22) Mercier, J. P. *J. Polym. Sci., Polym. Symp.* 1967, *16*, 2059.

Chapter VIII: Final Conclusions and Future Work

VIII.1 Final Conclusions

Alternating copolymerization of substituted stilbenes and maleic anhydride or substituted maleimide is a convenient and powerful tool to synthesize highly functional polymers with spatially arranged functional groups. The polymers can be obtained with high yields and high molecular weights. The rigidity of the polymer backbone has been investigated by light scattering, DSC, SEC and ^2H solid state NMR techniques. The copolymers have a rigid backbone with a persistence length around 10 nm. The result of the solid state NMR torsional angle measurement of the TDAS-MA copolymer has shown that the H- ^{13}C - ^{13}C -H linkages in the maleic anhydride units are enchained in a predominately *cis* configuration.

Various functional groups can be easily attached onto the polymers and enable some unusual and fundamentally interesting properties. By carefully selecting the functional groups and facile chemical modifications, the copolymers can be converted into highly charged polyelectrolytes or alternating polyampholytes. Novel rod-coil block copolymers containing rigid polyampholyte segments were also synthesized and investigated. The chain rigidity has a dramatic effect on the electrostatic interactions between polyelectrolytes. The PIC aggregates formed from these rod-coil block copolymers were found to be responsive to pH changes and added salt. The unique solution properties of the rigid polyampholytes are induced by the like-charge attractions imparted by the rigid chains.

The spatial arrangement of the pendant groups can be utilized to tune the optical properties of the polymer film. The birefringent property of the polymer film can be

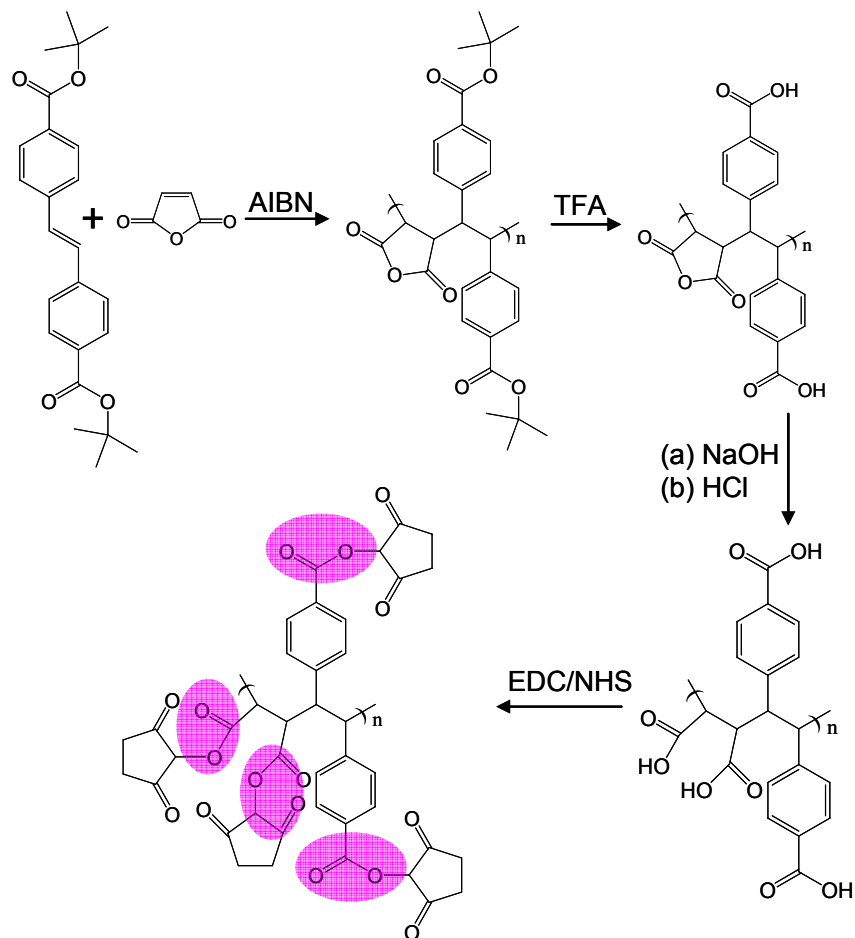
dramatically affected by the orientation of the pendent side groups along the polymer backbone. Using the maleimide - stilbene alternating copolymers as model systems, the orientation of the side groups can be easily achieved by hindering the free rotation of the benzene ring with an ortho-methyl group. The orientation of the benzene ring can induce big negative birefringence for the polymer film when the rigid polymer backbones align parallel to the film surface. Such large negative birefringence is difficult to obtain by mechanical drawing of polymer films. The polymer developed in this study can be conveniently synthesized from easily accessible monomers and could be used as compensation material for LCD or as the dopant to produce zero-birefringence optical polymers.

4,4'-Dihydroxyterphenyl has been incorporated into the backbone of conventional poly(aryl ether sulfone)s (PAES) to make them semi-crystalline. The more linear and rigid terphenyl groups can induce the formation of crystallites for the segmented PAES containing 50% BP and 50% DHTP. The semi-crystalline segmented PAES copolymer showed a melting temperature 320°C in the first heating cycle of DSC measurement. The formation of crystallites was confirmed by the WAXS. No crystallization was observed in the second heating cycle of the DSC measurement likely due to the slow crystallization rate of the copolymer in the melt state.

VIII.2 Future Work

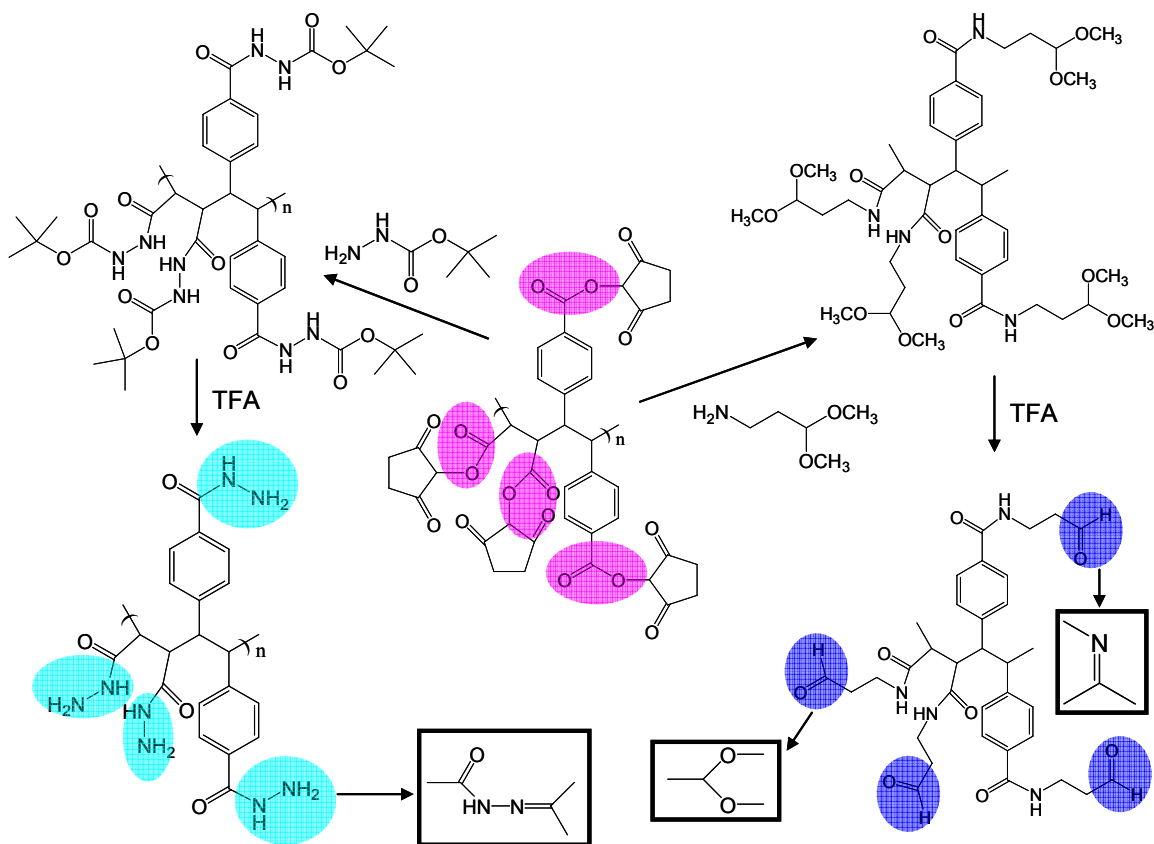
Functionalization of di-*t*-butyl-trans-4,4'-stilbenedicarboxylate – maleic anhydride copolymer. The di-*t*-butyl-trans-4,4'-stilbenedicarboxylate – maleic anhydride copolymer carries many reactive *t*-butyl ester and succinic anhydride groups so have the potential to be used as a versatile carrier for drugs. Scheme VIII.1 shows a possible strategy to introduce active *N*-hydroxysuccinimide (NHS) ester groups with a well-established method. Such polymer can act as the precursor to load drug molecules and biocompatible PEO chains.

Scheme VIII.1 A possible strategy to introduce active *N*-hydroxysuccinimide (NHS) ester groups to the di-*t*-butyl ester stilbene – maleic anhydride copolymer.



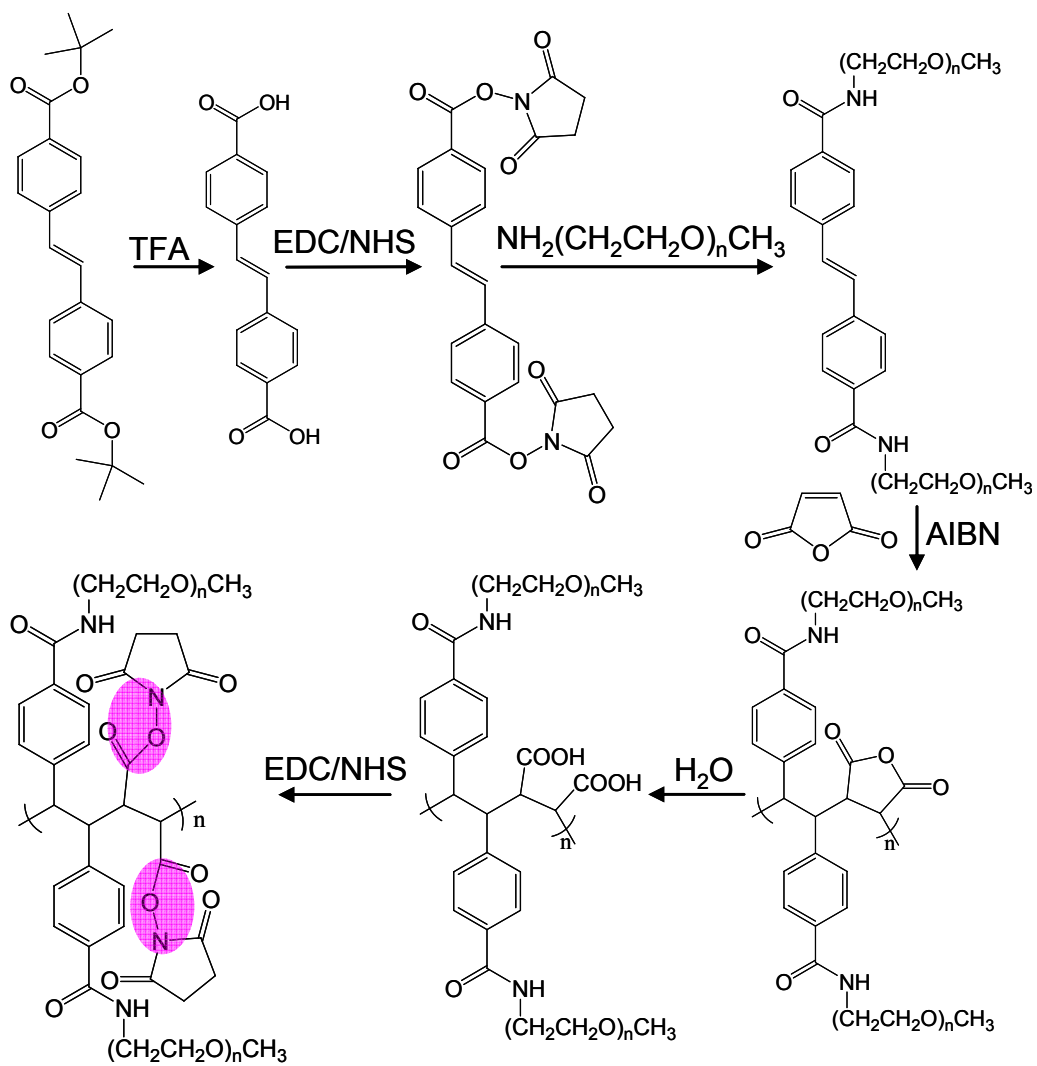
The possible functionalization methods to introduce functional groups which can form acid-labile linkages with some potential drugs such as DOX are shown in the following scheme.

Scheme VIII.2 Possible strategies to introduce acid-labile linkages for the drug delivery.



Besides the drugs, other functional groups such as PEG and receptors for molecular recognition can be easily incorporated into the polymer-drug conjugate. The following scheme shows the introduction of PEG chains.

Scheme VIII.3 Possible strategy to incorporate PEG chains into the polymer-drug conjugates.



Structure of the polymeric aggregates formed by rod-coil block copolymers containing rigid polyampholyte blocks based on N, N, N', N'-tetraalkyl-4, 4'-diaminostilbene and maleic anhydride. The morphological changes of the aggregates formed by rod-coil block copolymers containing rigid polyampholyte blocks based on N, N, N', N'-tetraalkyl-4, 4'-diaminostilbene and maleic anhydride upon pH variation or salt addition is an area that is of considerable interest. Vesicle-like structures for OEGMA₂₆-*b*-TDASMA₃₁ at pH 7 with 0.3M NaCl were observed from preliminary TEM (transmission electron microscopy) studies (Figure VIII.1). However the polymeric aggregates are sensitive to salt and pH therefore sample preparation for conventional TEM measurement leads to significant structural change. To properly investigate the morphological changes of these aggregates requires the use of cryo-TEM which is not available at Virginia Tech.

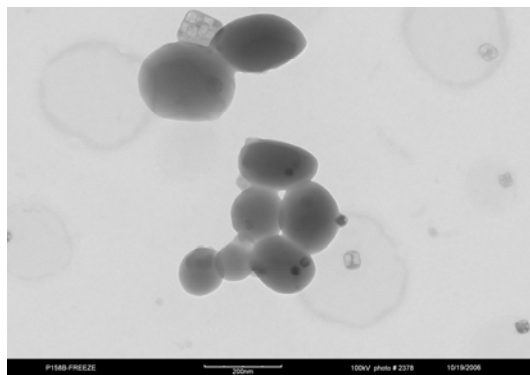


Figure VIII.1 TEM picture of the polymeric aggregates for OEGMA₂₆-*b*-TDASMA₃₁ at pH 7 with 0.3M NaCl.

Chain rigidity of the stilbene – maleic anhydride or maleimide alternating copolymers. Generally large pendant groups such as a benzene ring will hinder the free rotation of the carbon-carbon backbone bonds and increase the stiffness of the polymer

backbone. Persistence length is a direct measure of the intrinsic chain stiffness for a linear polymer chain. The persistence lengths for polymers with varying concentration of pendant benzene groups could serve as a good measure of the impact of large pendant groups on polymer backbone stiffness.

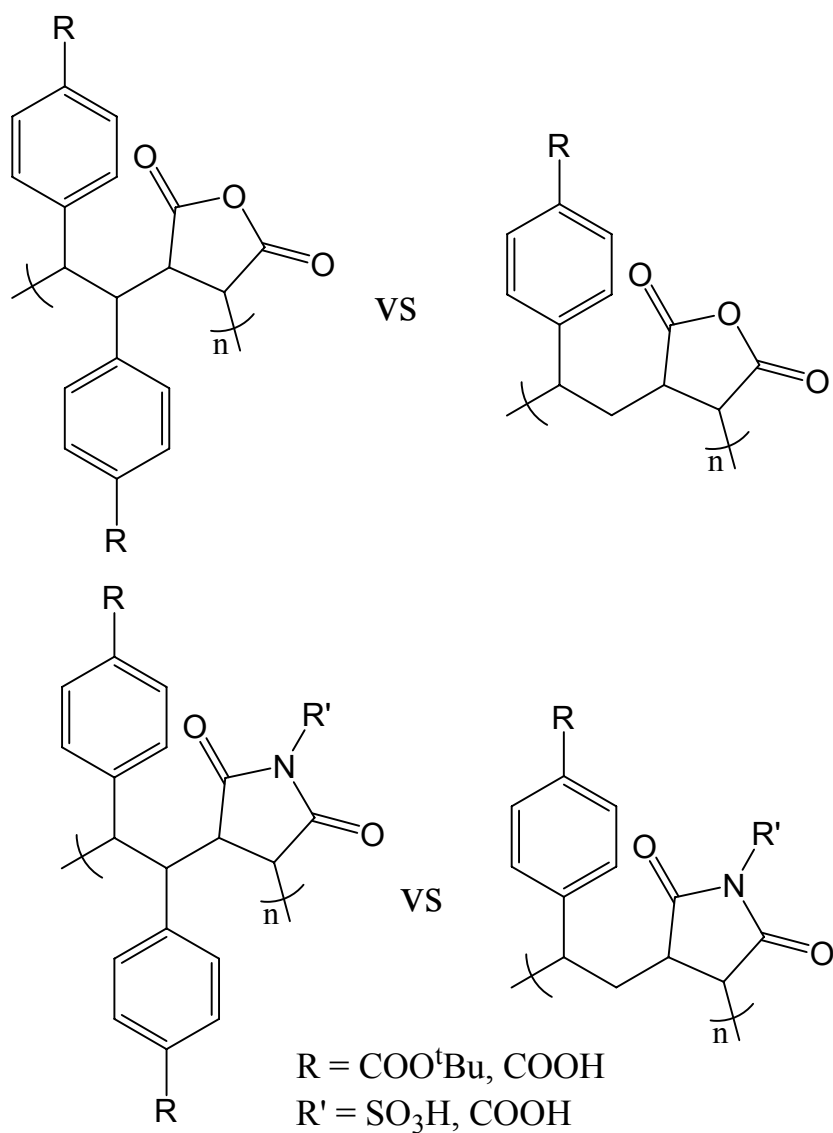
The alternating copolymerizations of stilbene and styrene with maleic anhydride or maleimide are well explored in the literature. We have recently studied the polymerization of 4,4'-substituted stilbenes with these strong electron acceptors. Our studies indicated that these alternating copolymers have backbones that have semi-flexible or rod-like characteristics. The difference between the persistence lengths of stilbene based copolymer and styrene based copolymer will show how one extra pendant benzene group per repeat unit can influence the stiffness of the polymer backbone. The following are the general structures of the copolymers that can be the basis for such a study.

Synchrotron small angle X-ray scattering (SAXS) is the best technique to measure the persistence length of the polymer backbone in solution. When R is dibutylamino group the alternating copolymer is very soluble in THF and the persistence length of the polymers in neutral form can be measured and compared.

Water is another good solvent for the SAXS measurement. To make the polymers soluble in water, the R group in the Scheme 1 can be carboxylate acid or *t*-Bu ester group which can be converted into carboxylate group easily. For charged polymers, highly salt concentration will be needed to screen the electrostatic repulsion between the charged groups. For maleic anhydride copolymers the anhydride rings will be opened with the hydrolysis in water. The torsional angle measurement by 2Q-HLF Solid State NMR

shows a 60° rotation of the polymer backbone after the hydrolysis. To avoid this complication, substituted maleimide with sulfonic acid or carboxylic acid groups can be incorporated into the copolymer along with carboxylic acid substituted stilbene and styrene.

Scheme VIII.4 General structures of the copolymers with different amounts of benzene groups.



Appendix

^1H NMR Spectra of the Substituted Stilbene Maleic Anhydride Alternating Copolymers

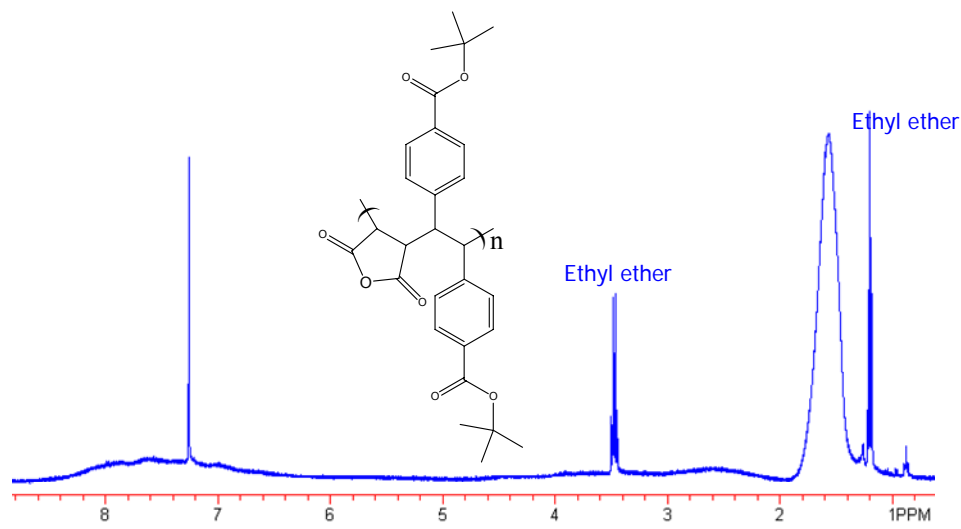


Figure 1 ^1H NMR Spectra of di-*t*-butyl-*trans*-4,4'-stilbenedicarboxylate - maleic anhydride copolymer in CDCl_3 .

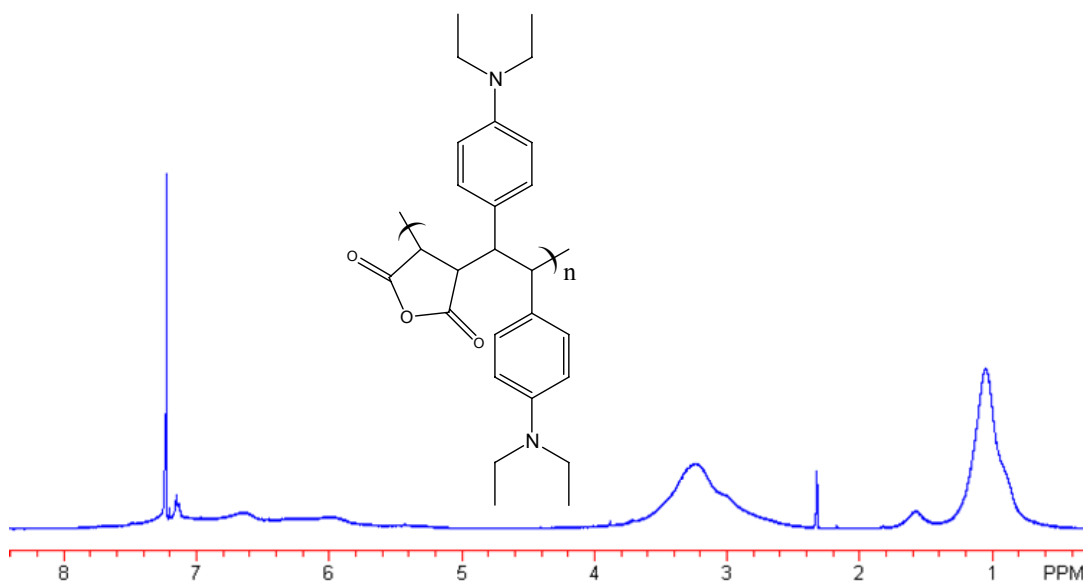


Figure 2 ^1H NMR Spectra of *N,N,N',N'*-tetraethyl-4,4'-diaminostilbene - maleic anhydride copolymer in CDCl_3 .